

MATHEMATICAL MODELLING IN
BATCH EMULSION POLYMERIZATION

Cao Tungyu

This thesis is submitted in
partial fulfillment of the
requirements for the degree
of Master of Philosophy.

The University of Aston in
Birmingham, U.K.

June, 1981.

Mathematical Modelling in Batch Emulsion PolymerisationSUMMARY

Emulsion polymerisation, suspension polymerisation and the dispersion processes of styrene in water have been carried out at 50°C in a stainless steel, stirred batch reactor of 3.6 dm³ capacity. The reactor was fitted with a temperature control facility and could be operated with or without internal baffles.

A mathematical model covering stages I, II and III of emulsion polymerisation has been proposed and its predictions have been compared with experimental data.

Classical models do not present satisfactory predictions for the case of low soap concentrations or for the case of high impeller speed at low or intermediate soap concentrations. The model presented here overcomes this problem by taking into account the amount of soap adsorbed onto the dispersed monomer droplet interface. An existing relationship between monomer droplet size, impeller speed and impeller diameter for an unbaffled vessel and a new relationship for a baffled vessel were incorporated into the model.

During stage III the increase in monomer particle viscosity reduces the translational mobility of the radicals with the result that the reaction rate increases dramatically (the gel-effect). Analogous behaviour in suspension polymerisation of styrene has been investigated and a relationship between the termination rate constant and the level of monomer conversion has been developed. This relationship is incorporated into the model for emulsion polymerisation.

The predictions of the current model incorporating the soap adsorption and the gel effect amendments are in good agreement with experimental data for emulsion polymerisation of styrene at 50°C across the whole of the conversion.

KEY WORDS: Emulsion polymerisation, styrene, dispersion, modelling, gel-effect.

To
My Motherland

ACKNOWLEDGEMENTS

- The author wishes to thank:

Dr. M.P. Wilson who suggested and personally supervised this research project.

Dr. A.J. Merry for providing the test rig and for his helpful advice.

Dr. M.C. Jones for valuable discussions on the model.

Dr. A.P.H. Jordan for his assistance in computing.

The staff and technicians of the Department of Chemical Engineering of the University of Aston in Birmingham, U.K. for their invaluable assistance.

Vera, Jean and Sharon for their typing and their patience.

SECTION I

INTRODUCTION	1
--------------	---

SECTION II

THE LITERATURE SURVEY	9
-----------------------	---

2.1	The Qualitative Theory of Emulsion Polymerization	10
2.2	Mathematical Model	13
2.2.1	Smith-Ewart Model	13
2.2.2	Gardon Model	15
2.2.3	Harada Model	19
2.2.4	Min and Ray Model	21
2.3	Gel-Effect	22
2.4	Dispersion	25
2.5	Determination of Particle Size	

SECTION III

EXPERIMENTAL EQUIPMENT AND TECHNIQUES	32
---------------------------------------	----

3.1	Flow Chart and Equipment	33
3.2	Experiment of Emulsion Polymerization	39
3.3	Experiment of Suspension Polymerization	40
3.4	Dispersion Tests	41

SECTION IV

INTRODUCTION AND DEVELOPMENT OF ANALYTICAL TECHNIQUE	42
4.1 Droplet Size Analysis	43
4.1.1 Photomicrographic	43
4.1.2 Coulter Counter	44
4.2 Determination of Monomer Conversion	51
4.2.1 Precipitation with Methanol	53
4.2.2 Precipitation with Aluminium Chloride	53
4.2.3 Direct Drying	54
4.2.4 Comparison of Techniques	54
4.3 Development of the Technique for the Measurement of Particle Size Using Light Transmission	55
4.3.1 General Description	55
4.3.2 Setting up the Technique for Measuring Particle Size in Emulsion Latex	56
4.3.3 Determination of Particle Size Using Extinction Method	61
4.3.3.1 Collecting Basic Data	61
4.3.3.2 Diluting	62
4.3.3.3 Estimating the Mass Concentration of the Particles in the Diluted Latex	63
4.3.3.4 Finding the Density of Particles in the Diluted Latex	64
4.3.3.5 Estimating the Refractive Index	65
4.3.3.6 Measuring the Extinction Coefficient	65
4.3.3.7 Evaluating the Parameter K/α and the Average Radius of Particles	65
4.3.3.8 Correcting the size of Particles	66
4.3.4 Comparison between the Results from this Technique and the Electron Microscopic Method	67

SECTION V

	THE MATHEMATICAL MODEL	69
5.1	Setting up the Model for Stage I	70
5.1.1	General Description	71
5.1.2	Setting up the Differential Equation for Particle Nucleation	73
5.1.3	Derivation of the Equation for the Surface Area of Monomer Droplets	74
5.1.4	Estimating the Parameters of Monomer Droplets	75
5.1.5	Derivation of the Equation for Estimating the Surface Area of Particles	76
5.1.6	Derivation of the Equation for Estimating the Volume of Polymer Particles	78
5.1.7	Derivation of the Equation for Estimating the Fractional Monomer Conversion	79
5.1.8	Derivation of the Equation for Estimating the Number of Particles	80
5.2	Setting up the Model for Stage II	80
5.3	Setting up the Model for Stage III	

SECTION VI

	THE RESULTS AND DISCUSSION	87
6.1	Determination of the Dependence of Termination Rate Constant on Monomer Conversion	88
6.2	Formulation of the Dispersion Data in Baffled Reactor	93
6.3	Capabilities of the Model	97
6.3.1	The prediction of the Model for Particle Nucleation	97
6.3.2	Conversion-versus-Time Plots for Baffled Reactor	103
6.3.3	The effect of Stirring Rate	107
6.3.4	The Gel-Effect	110
6.3.5	Baffled Reactor	117

SECTION VII

	CONCLUSIONS	121
	SUGGESTIONS FOR FURTHER WORK	130
	NOMENCLATURE	132
	REFERENCES	134
	APPENDIX	138
Appendix I	Computer Program for Determination of Particle Size Using Extinction Method	139
Appendix II	Computer Programs for the Computation of the Dependence of Termination Rate Constant on Monomer Conversion	143
	(1) DEFF1 The Computation of $\frac{dX_p}{dt}$ from $t-X_p$ Data Using Differentiation Method	144
	(2) REG3 The Formulation of K_t and X_p Using Multiple Regression Method	145
	(3) XKT The Evaluation of K_t against X_p	147
Appendix III	Computer Programs for Formulation of the Dispersion Data in Baffled Reactor	148
	(1) DISPER The Evaluation of the Average Diameter of Monomer Droplets for the Various Sample from the Dispersion Data	149
	(2) The Formulation of D_d^0 So and N Using Regression Method	150
Appendix IV	Computer Program for Smith-Ewart Model	151
Appendix V	Computer Program for Stage I and Stage II in Unbaffled Reactor	155
Appendix VI	Computer Program for Gel-Effect	161
Appendix VII	Computer Program for Baffled Reactor	165

SECTION I

INTRODUCTION

SECTION 1

INTRODUCTION

Emulsion polymerization is one of the most important methods for effecting the process of addition polymerization. It is carried out in a system which includes a monomer (or monomers) and a dispersion medium, generally water, in which the monomer is either virtually insoluble, or else sparingly soluble. A micelle-generating substance, namely the emulsifier, is usually present and a water soluble initiator is generally used. The polymerization takes place, in the main, within the monomer swollen polymer particles which according to the Harkins model for emulsion polymerisation are nucleated within the micelles.

The emulsion polymerization process offers significant advantages over bulk, solution or suspension polymerization. Although the internal viscosity of the particles is extremely high, the viscosity of the emulsion remains low during the process of emulsion polymerization. Heat transfer therefore is no real problem and good temperature control can often be achieved thus avoiding the "runaway reaction" which is often observed in bulk polymerisations. The combination of highly effective surface active agents, very mild agitation and the small size of the polymer particles minimizes the tendency of the particles to coalesce so that, in contrast to suspension polymerization, emulsion polymerization is suitable for the production of sticky, rubbery polymers. Furthermore, the

polymer is produced in latex form and this is an obvious advantage in certain industrial applications.

Emulsion polymerization polymers are characterised by a very high molecular weight. The reason for this follows from the fact that free radicals are not formed within the particles but enter into the particle from the surrounding aqueous phase in which the initiator is dissolved. When a free radical enters a non-growing particle, polymerization is initiated and continues until it is terminated by the entry of another radical into the particle. Therefore, the average life time of growing polymer radicals in emulsion polymerization is much longer than for the other polymerization processes. Thus, it is possible for a growing molecule to grow to a very high molecular weight before being terminated. This growth of the polymer chain can proceed simultaneously in a large number of particles, which are isolated from each other by the intervening water phase. A growing polymer molecule in one particle cannot terminate one in another particle. This means that the total number of radicals in unit emulsion volume is larger in emulsion polymerization than in other polymerization processes, therefore, the overall rate of polymerization is high. These two important characteristics of emulsion polymerization make it a valuable commercial process. High product molecular weight for instance is especially necessary when producing synthetic rubber with satisfactory elastomer properties. High conversion rate of course leads to

reduced production costs.

For the reasons mentioned above, the emulsion polymerization process is of increasing importance to commercial polymer production. In both batch and continuous reactor systems it has become a major processing step in the manufacture of polymer products such as paints, inks, coatings, adhesives, flocculants, synthetic rubbers, plastics, high impact strength copolymers and so on. Current latex production by emulsion polymerization throughout the world is of the order of a million tons per year. In spite of its great economic importance however and although emulsion polymerization has been carried out for at least 50 years, the detailed quantitative behaviour of these reactions is still not well understood. For this reason, it is considered of considerable benefit to develop a reliable, efficient predictive mathematical model for emulsion polymerization reactors.

The emulsion polymerization system is heterogeneous in that it consists of several phases which change in character during the polymerization process. The behaviour of an emulsion polymerization reactor also differs for the different monomers that may be polymerised by this process. In addition, the purities of the monomer and of the other ingredients, the gas space atmosphere, the geometry of the reactor and its accessories, the impeller speed and the reaction conditions all affect the progress of an emulsion polymerization.

Consequently, the modelling of emulsion polymerization is extremely complex. In spite of this, a number of workers have devoted themselves to the study of emulsion polymerization science. Since the classical work of Smith-Ewart (1) on the modelling of emulsion polymerization, a great number of papers have appeared which have either modified the classical model or have proposed their own new models.

It is apparent from the literature that none of the numerous previous models for emulsion polymerization have considered the effect on the reaction of the adsorption of emulsifier onto the surface of the monomer droplets. In many instances the amount of this adsorbed emulsifier may be ignored because it is a relatively small proportion of the total emulsifier concentration. However, if the emulsifier concentration is low, or if the impeller speed is high enough, the proportion of the adsorbed emulsifier on the monomer droplet surface will be comparable with that of the micellar soap. In this case the effect of the adsorbed soap must clearly be taken into account. Several workers have studied the effects of stirring on the process of emulsion polymerization. Shunmukham (2) noted that violent agitation would reduce the polymerization rate and increase the induction time. Schoot et al (3) suggested that the increase in induction time is associated with inhibition by trace oxygen in the nitrogen atmosphere used and the decrease in polymerization rate is due to increasing mass transfer between the gas and liquid

phases as agitation becomes more severe. Evans et al (4) Omi et al (5) and Nomura et al (6) pointed out that, under a highly purified nitrogen atmosphere, the decrease in the rate of polymerization and in the number of polymer particles with increased agitation may be due to the fact that the micelle population is a function not only of the soap concentration, but also of the amount of soap adsorbed onto the surface of the monomer droplets, i.e. a function of the degree of dispersion which is directly dependent on the agitation. In this work, a mathematical model for Stage I and Stage II of emulsion polymerization is established which takes into account the soap adsorbed on the surface of monomer droplets. The soap adsorption model is described in detail in Section VI.

In modelling Stage III of the reaction difficulties are encountered which are associated with the auto-acceleration of the conversion rate with increasing monomer conversion. This phenomenon is often known as the Trommsdoff effect, or gel-effect. Friis et al. (7-10) carried out experimental emulsion and bulk polymerizations of polymethylmethacrylate (7, 8) and polyvinyl acetate (7, 9). By using a steady state model they were able to model the gel-effect. They also compared their model (10) with the experimental data obtained by Grancio (11). They also looked at styrene polymerization and the relationship which they used to relate the termination constant to monomer conversion for polystyrene was based on Hui's work (12) on the thermal polymerization of styrene in bulk which was

carried out over the temperature range of 100-200°C. It was found, at least at 50°C, that this relationship overestimates the termination rate constant if it is used for modelling the emulsion polymerization reaction, particularly at high levels of conversion. Gardon (13,14) developed a mathematical model based on a non-steady state assumption for Stage II. Unfortunately, it does not extend to Stage III because the relationship between termination rate constant and monomer concentration in the particles was not known. In the present work, a functional dependence of monomer conversion has been generated using experimental suspension polymerization data. A non-steady state mathematical model for Stage III has been developed, which is combined with the model for Stage I and Stage II mentioned above to construct a general model over the whole conversion range of the emulsion polymerization. A comparison has been made between the predicted and the experimental data. It is described in Section VI.

The flow pattern of the liquid in a baffled reactor is significantly different from that in an unbaffled reactor. The velocity distribution in the former is more uniform than in the latter (15) and the extent of monomer dispersion in the baffled reactor is much greater than that in the unbaffled one. Vermeulen et al (16) presented a correlation from their work for a baffled reactor, in which the Sauter mean diameter of the droplets is directly proportional to the impeller speed to the power (-1.2). Unfortunately, their formula is

only valid for the system in the absence of emulsifier. Merry obtained an empirical formula (17) for the dispersion of styrene in an emulsifier solution in water, in which the mean diameter of droplets was shown to be proportional to the impeller speed to the power (-1.08). This formula however can only be used for the unbaffled reactor. Harada et al (32) presented a correlation for the dispersion of styrene in an emulsifier solution in water for a baffled reactor, and in this case average diameter of the dispersed monomer droplets is proportional to impeller speed to the power (-0.75) and to the emulsifier concentration to the power (-1.5) for a lower limit of the emulsifier concentration of 3.13 g/dm^3 water, which is above the emulsifier concentration range used in the current study. Therefore, in the present work, the dependence of the average droplet diameter upon emulsifier concentration and impeller speed ^{in a baffled reactor} has been investigated and it has been included in the mathematical model for emulsion polymerization mentioned above. The results predicted from the model are compared with the experimental data as described in Section VI.

Apart from setting up the mathematical model for emulsion polymerisation, a technique, with which particle sizes as small as 0.09 micron may be measured, has been developed, this technique has been based on Mie's theory (19) on the work of Bateman (20) and of Merry (17).

SECTION II

LITERATURE SURVEY

- 2.1 The Qualitative Theory of Emulsion Polymerization
- 2.2 The Mathematical Model
 - 2.2.1 The Smith-Ewart Model
 - 2.2.2 The Gardon Model
 - 2.2.3 The Harada Model
 - 2.2.4 The Min and Ray Model
- 2.3 Gel-Effect
- 2.4 Dispersion
- 2.5 Determination of Particle Size.

2.1 The Qualitative Theory of Emulsion Polymerization

In the 1940's Harkins proposed an important qualitative theory (21-24) which laid a solid foundation for the modelling of emulsion polymerization. The main features of this theory are best illustrated diagrammatically as in Figure 2.1.

Figure 2.1 (a) shows the system before initiation has occurred. The emulsifier molecules are present mainly in the form of micelles, a small amount is adsorbed onto the surface of the monomer droplets, and a further small amount is dissolved in the water in the form of free molecules whose saturated concentration is defined as the critical micelle concentration (c.m.c.). Micelles are able to concentrate monomer at their centres so that monomer can be solubilised by emulsifier. Only a very small amount of monomer is dissolved in the water as free molecules. Compared with the micelles, the monomer droplets are relatively large. Generally speaking, the diameter of the droplets is about 10 micron but the micelles about 0.01 micron. In a typical case, the number of monomer droplets would be about 10^{12} $1/\text{cm}^3$, but for micelles the number would be about 10^{18} $1/\text{cm}^3$ (25).

Figure 2.1 (b) shows the system after the initiator is charged. Free radicals are generated in the aqueous phase and these diffuse into the micelles to initiate the polymerization. The micelles in which initiation takes place become polymer particles. The monomer

droplets act as reservoirs from which the monomer migrates constantly into particles through the aqueous phase, thus supplying the growing particles.

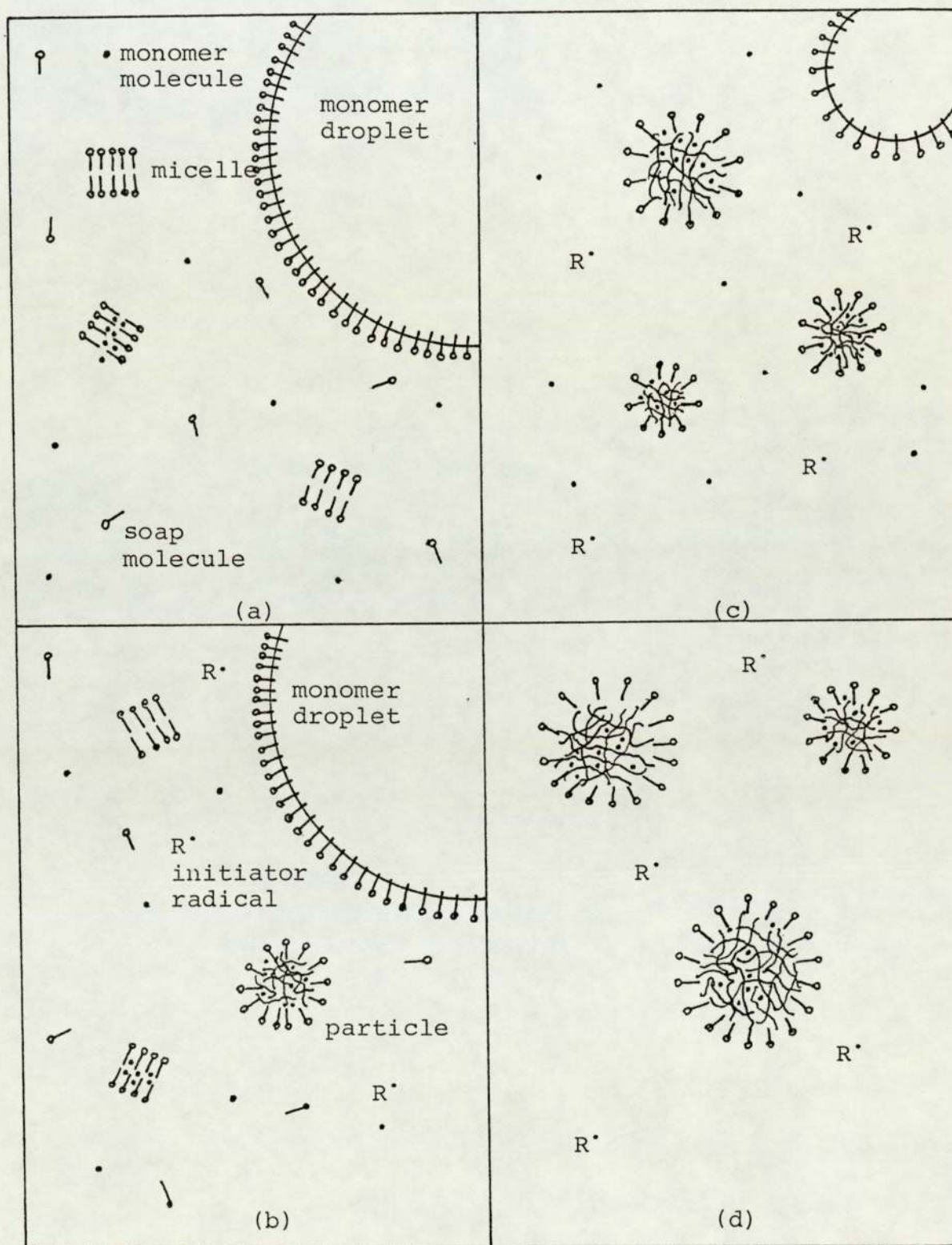


Figure 2.1 A physical picture of emulsion polymerization
 (a) dispersion stage, (b) Stage I (c) Stage II (d) Stage III

Particle nucleation and growth of the particles lead to an increase in the specific surface area of the particles. There is therefore a tendency to adsorb more free molecules of the emulsifier from the true aqueous phase onto this new surface and this in turn tends to lead to the destruction of micelles. Thus, as polymerization proceeds, the micellar emulsifier tends continuously to change into adsorbed emulsifier so that the micellar emulsifier eventually disappears. The period of the reaction from the charging of the initiator to the disappearance of the micelles is known as Stage I.

Figure 2.1 (c) shows the system after all the micelles have disappeared. The emulsifier is found in three forms, namely, adsorbed onto the particle surface, adsorbed onto the droplets surface and dissolved in the aqueous phase. Monomer is continually diffusing from the droplets to the particles through the aqueous phase to supply the particles as they increase in size. The number of particles, that is the number of reaction loci, remains constant once all the micelles have disappeared and so, therefore, as the polymerization rate is a function solely of the number of particles the rate also remains constant. As polymerization proceeds, eventually the monomer droplets also disappear. The period of the reaction from the disappearance of micelles to the disappearance of monomer droplets is known as Stage II.

Figure 2.1 (d) shows the system after the droplets have disappeared. At this stage the emulsifier exists in two forms only, namely adsorbed onto the surface of the particles and dissolved in the aqueous phase in free solution. The rate of polymerization gradually falls off due to the monomer depletion at the reaction loci. In normal cases, the final diameter of the particles is about 0.1 micron and the number of particles is about 10^{16} 1/cm³.

2.2 Mathematical Model

2.2.1 The Smith-Ewart Model

Smith and Ewart (1, 26, 27) treated Harkins' physical model quantitatively for Stage I and Stage II of emulsion polymerization. They provided two experimentally verifiable equations for Stage I and predicted that the final particle number should be proportional to the 0.4 power of the initiator concentration and to the 0.6 power of the emulsifier concentration. In addition, they also provided recurrence equations based on the steady-state assumption for Stage II. Most of the models presented after Smith and Ewart modified or extended this classical model. The model may be summarized as follows:

For Stage I, it was assumed that all free radicals are generated in the aqueous phase and then migrate into micelles and particles. Smith and Ewart assumed the two following possible cases:

- (1) When all radicals enter only into micelles and generate new particles there. In this case, the number of particles per cc of water at the end of Stage I can be described using the following equation

$$N_p = 0.53 \left(\frac{R}{\mu}\right)^{0.4} S^{0.6} \quad (2-1)$$

where N_p = number of particles per cc of water, l/cc water

R = rate of radical generation, l/cc water min.

μ = volume growth rate of particles, $\mu = (K_p/N_A) (dm/dp) \{\phi_m/(1-\phi_m)\}$, $\text{cm}^3/\text{min. particle}$

S = area provided by emulsifier, $\text{cm}^2/\text{cc water}$.

- (2) When radicals enter into both micelles and polymer particles, the ratio of entry into one or the other depending only on the ratio of the external surface area of micelles and particles. In this situation, the equation becomes:

$$N_p = 0.37 \left(\frac{R}{\mu}\right)^{0.4} S^{0.6} \quad (2-2)$$

For Stage II, Smith and Ewart made a population balance on N_i the number of particles per cc of water containing i radicals, and obtained the following non-steady state recurrence equation:

$$\frac{R}{N_p} (N_{i-1} - N_i) + \frac{K_{oa}}{\bar{V}} \{N_{i+1}(i+1) - N_i i\} + \frac{K_t}{\bar{V}N_A} \{N_{i+2}(i+2)(i+1) - N_i i(i-1)\} = 0 \quad (2-3)$$

where K_o = radical desorption rate constant, cm/min.
 a = average surface area of one particle at a given time, $\text{cm}^2/\text{particle}$
 \bar{V} = average volume of one particle at a given time, $\text{cm}^3/\text{particle}$.
 K_t = termination rate constant, $\text{cm}^3/\text{mole min}$
 N_A = Avogadro number

The first term of equation (2-3) considers the transfer of the radicals from the aqueous phase to the particles. (R/N_p) represents the rate of this transfer into a single particle.

The second term considers the transfer of radicals from particles into the aqueous phase. $(K_o a i / \bar{V})$ represents the rate of this transfer out of a single particle.

The third term considers the loss of free radicals by mutual termination of the radicals. $\{K_t i (i-1) / \bar{V}\}$ denotes the rate of this loss of radicals from a single particle.

2.2.2 The Gardon Model

The definitive exposition of the Gardon theory of emulsion polymerization was published in six papers which appeared in 1968 (13, 14, 28-31). He recalculated and extended the Smith-Ewart model. He used a different mathematical method from Smith and Ewart and he derived the equations for calculating the surface area of the particles, the reaction time, the number of particles, the

molecular weight and the monomer conversion for Stage I. He considered the case of slow termination of radicals instead of Smith and Ewart's fast termination, and he obtained an equation relating reaction time to monomer conversion. The model is described briefly below:

For Stage I. Gardon considered that each particle absorbs radicals at a rate proportional to its surface area $4\pi r_i^2$. If n_i is the number of radicals per cc of water whose radius is r_i and N_t is the number of particles per cc of water, the differential equation of particle nucleation is

$$\frac{dN_t}{dt} = \frac{R}{S} \{ S - 4\pi (\sum n_i r_i^2)_t \} \quad (2-4)$$

He derived the equation below based on equation (2-4) by using a numerical method.

$$y(x) = 0.318 x^{\frac{5}{3}} - 0.701 x^{\frac{5}{3}} y\left(\frac{x}{2}\right) \quad (2-5)$$

$$u(x) = 0.279 x \{ 1.91 - y(x) - 4y\left(\frac{x}{2}\right) \} \quad (2-6)$$

$$z(x) = 0.265x^2 - 0.047x^{3.55} \quad (2-7)$$

where y = dimensionless surface area

$$y = \frac{4}{S} \sum n_i r_i^2 \quad (2-8)$$

x = dimensionless time

$$x = \left(\frac{12\pi}{5}\right)^{\frac{3}{5}} K^{\frac{2}{5}} \left(\frac{R}{S}\right)^{\frac{3}{5}} \quad (2-9)$$

K = the relative rate of volume growth of particle.

$$K = \frac{3}{4\pi} \frac{K_p}{N_A} \frac{dm}{dp} \frac{\phi}{1-\phi_m} \quad (2-10)$$

u = dimensionless particle number

$$u = 4 \left(\frac{5}{12\pi} \right)^{\frac{2}{5}} S^{-\frac{3}{5}} \left(\frac{K}{R} \right)^{\frac{2}{5}} N_t \quad (2-11)$$

Z = dimensionless conversion

$$Z = 4 \left(\frac{12\pi}{5} \right)^{\frac{1}{5}} S^{-\frac{6}{5}} \left(\frac{R}{K} \right)^{\frac{1}{5}} (\sum n_i r_i^3) \quad (2-12)$$

K_p = propagation rate constant, cm³/mole min.

dm = density of monomer, gram/cm³

dp = density of polymer, gram/cm³

ϕ_m = volume fraction of monomer in particles.

When polymerization has proceeded to the end of Stage I equations (2-5), (2-6) and (2-7) become:

$$t_{I-II} = 0.365 \left(\frac{S}{R} \right)^{0.6} K^{-0.4} \quad (2-13)$$

$$N_p = 0.208 S^{0.6} \left(\frac{R}{K} \right)^{0.4} \quad (2-14)$$

$$Z_{I-II} = 0.3016$$

where t_{I-II} = reaction time elapsed at the end of Stage I, min.

Z_{I-II} = the value of parameter Z at the end of Stage I.

For Stage II, Gardon derived a set of differential equations based on a non-steady state assumption which is described as follows:

$$I \frac{df_0}{dz} = 3.81(-f_0) + \frac{Q_3}{Z}(zf_i)$$

$$I \frac{df_1}{dz} = 3.81(f_0 - f_1) + \frac{Q_3}{Z}(6f_3)$$

$$I \frac{df_2}{dz} = 3.81(f_1 - f_2) + \frac{Q_3}{Z}(12f_4 - 2f_2)$$

$$I \frac{df_i}{dz} = 3.81(f_{i-1} - f_i) + \frac{Q_3}{Z}\{(i+2)(i+1)f_{i+2} - i(i-1)f_i\} \quad (2-15)$$

$$\sum f_i = 1 \quad (2-16)$$

$$\sum if_i = I \quad (2-17)$$

$$\frac{dz}{dx} = 0.372I \quad (2-18)$$

where f_i = number fraction of the particles each of which contains i radicals.

I = average number of radicals in one particle

Q_3 = dimensionless termination parameter

$$Q_3 = \frac{K_t}{K_p} \cdot \frac{dp}{dm} \cdot \frac{1-\phi_m}{\phi_m} \quad (2-19)$$

Gardon fitted the numerical solution of the above equations to the following quadratic equation which is the relationship between conversion and reaction time.

$$Z = \frac{0.05464}{Q_3} x^2 + 0.186x + 0.0721 \left(1 - \frac{1.14}{Q_3^{0.94}}\right) \quad (2-20)$$

2.2.3 Harada Model

Harada et al (32) developed a model of emulsion polymerization with the assumption that there is not more than one radical in each polymer particle. In this model they considered the effect of radical transfer both to the monomer droplet and to the transfer agent and the effect of the ratio of the amount of radicals diffusing into micelles to that diffusing into the polymer particles. They obtained several differential equations as follows:

$$\frac{dN_p}{dt} = \frac{R}{1 + K_2 N_p / K_1 m_s} \quad (2-21)$$

$$\begin{aligned} \frac{dN_1^*}{dt} = & K_1 m_s R^* - K_p \{M\} N_1^* + K_2 N R^* - K_2 N_1^* R^* + K_{fm} \{M\} N^* - \\ & K_{fm} \{M\} N_1^* + K_{fT} \{T\} - K_{fT} \{T\} N_1^* \end{aligned} \quad (2-22)$$

$$\frac{dN_j^*}{dt} = K_p \{M\} N_j^{*-1} - K_p \{M\} N_j^* - K_2 N_j^* R^* - (K_{fm} \{M\} + K_{fT} \{T\}) N_j^* \quad (2-23)$$

$$\frac{dN^*}{dt} = K_1 m_s R^* + K_2 (N_p - 2N^*) R^* \quad (2-24)$$

$$\frac{dP_j}{dt} = K_2 N_j^* R^* + K_{fm} \{M\} + K_{fT} \{T\} N_j^* \quad (2-25)$$

where N_p = number of particles per cc of water, particles/cc

water $N_p = N + N^*$

N = number of inactive polymer particles per cc
of water, particles/cc water

- N^* = number of growing polymer particles per cc of water, particles/cc water
 R^* = concentration of radicals in aqueous phase, radicals/cc water
 R = rate of radical generation, radicals/cc water, min.
 m_s = number of micelles per cc of water, micelles/cc H_2O
 K_1 = radical diffusion coefficient from aqueous phase to micelles, cc water/molecule min.
 K_2 = radical diffusion coefficient from aqueous phase to particles, cc water/molecule min.
 N_j^* = number of particles containing a polymer radical with j monomer units, particles/cc water
 N^* = number of active polymer particles, particles/cc water
 $\{M\}$ = monomer concentration in particles, g.mole/cm³
 $\{T\}$ = concentration of transfer agent in particles, g.mole/cm³
 K_{fm} = transfer rate constant to monomer, cm³/g.mole.min.
 K_{fT} = transfer rate constant to transfer agent, cm³/g.mole.min.
 P_j = dead polymer containing j units, molecules/cc water

Harada et al solved the equations mentioned above for two limiting cases. One case is that for which the radicals generated in the aqueous phase preferentially enter the micelles, the other is that for which almost all the radicals generated in the aqueous phase are captured by the particles present. For these two cases, they obtained the

equation for calculating the number of particles and derived the correlation relating monomer conversion to time. Their model gives excellent agreement with the experimental results.

2.2.4 The Min and Ray Model

Recently, a more comprehensive detailed mathematical model was formulated for emulsion polymerisation reactors by Min and Ray(33,34). This model consists of complex multivariate population balance equations coupled to material and energy balances for the reactor. It includes all previous models as special cases. They also demonstrated the computer simulations of the model both for batch emulsion polymerisation reactors for the polymerisation of methyl methacrylate(35) and for semi-batch emulsion polymerisation for the polyvinyl chloride system(36). They showed that the model predictions are shown to be in good agreement with laboratory experimental data and with pilot plant data. To model emulsion polymerisation systems they made;

- 1) a particle size distribution balance
- 2) an individual particle balance
- 3) a micelle balance
- 4) a monomer droplet balance
- 5) an aqueous phase balance
- 6) a general material balance
- 7) a general energy balance

In this model they took into consideration the following factors:

- (1) water-soluble initiators will decompose

and form free radicals in the aqueous phase while monomer-soluble initiators will form free radicals in the monomer droplets, in the dissolved monomer in the aqueous phase, and in the polymer particles.

- (2) Particles can be formed both from micelles and from oligomers in the aqueous phase.
- (3) Shorter chains and radicals can be desorbed from particles, micelles and monomer droplets.
- (4) Coalescence between polymer particles will occur.
- (5) Both homogeneous and heterogeneous particles morphology can be treated.
- (6) The gel-effect is considered
- (7) The model can describe both continuous well-stirred and batch emulsion polymerization reactors.
- (8) The particle size distribution will influence the behaviour of emulsion polymerization reactors.
- (9) The aqueous phase polymerization will contribute to the total polymerization rate.
- (10) The polymer particle may be stabilised by both emulsifier and polymer chain ends.

2.3 Gel-effect

As mentioned above, the Smith-Ewart model was based on the instantaneous termination assumption (1). This approximation seems to be reasonable for describing Stage I and Stage II but is not valid for Stage III because of the Trommsdorff effect (37), i.e. the gel-effect.

Harada claimed (18) that their model, which is based on the instantaneous termination assumption, is in excellent quantitative agreement with the experimental results except in the range where autoacceleration occurs. As Gardon (28) pointed out, in Stage III, polymer concentration in the particles increases with increasing monomer conversion. Thus as termination is known to be a diffusion-controlled process the termination rate constant must decrease with increasing conversion during Stage III, this is what is normally described as the Trommsdorff or gel-effect. It would follow that the Smith-Ewart assumption of instantaneous termination becomes very questionable for Stage III even for small particle sized latexes with low initiation rate.

Friis et al. published several papers to deal with the gel-effect in emulsion polymerization (7-10, 41). They suggested that in bulk polymerization the termination reaction becomes diffusion controlled and the termination rate constant decreases by 3 to 4 orders in the conversion interval 0-100%. This decrease in termination rate constant, which will be referred to as the gel-effect, always causes a significant increase in the rate of polymerization and can also shift the molecular distribution to higher molecular weights. They pointed out that in emulsion polymerization a single polymer particle can be regarded as a locus of bulk polymerization with intermittent initiation. A decrease in the termination rate which is observed in bulk polymerization should therefore also occur in a single polymer particle. Therefore, the increase

in rate due to ^{the} gel-effect in emulsion polymerization of various monomers can be accounted for quantitatively by means of data from bulk polymerization.

The relationships between termination rate constant and monomer conversion that they suggested for various monomers are shown as follows:

Methylmethacrylate (valid temperature range, 40-90°C)

$$\frac{K_t}{K_{t0}} = \left\{ \frac{1}{1-x_p} \exp(BX_p + C x_p^2) \right\}^2 \quad (2-26)$$

$$B = -41.54 + 0.1082 T$$

$$C = 23.46 - 0.0785 T$$

Styrene (valid temperature range, 50-200°C)

$$\frac{K_t}{K_{t0}} = \left\{ \exp\{-(BX_p + CX_p^2 + DX_p^3)\} \right\}^2 \quad (2-27)$$

$$B = 2.57 - 5.05 \cdot 10^{-3} \cdot T$$

$$C = 9.56 - 1.76 \cdot 10^{-2} \cdot T$$

$$D = -3.03 + 7.85 \cdot 10^{-3} T$$

Vinyl acetate (valid temperature, 50°C)

$$\frac{K_t}{K_{t0}} = 2 \exp(B + CX_p + DX_p^2 + EX_p^3) \quad (2-28)$$

$$B = 17.6620$$

$$C = -0.4407$$

$$D = -6.7530$$

$$E = -0.3495$$

where K_t = termination rate constant at $x_p = x_p'$,
 $\text{cm}^3/\text{mole min.}$

K_{t0} = termination rate constant at $x_p = 0$,
 $\text{cm}^3/\text{mole min.}$

X_p = fractional monomer conversion

T = absolute temperature, $^{\circ}\text{K.}$

Friis fitted the values of K_t estimated from equation (2-26) (2-27) and (2-28) to a steady state model as presented in equation (2-3) to obtain the relationship between X_p and time. They have compared the predicted results from the model with the experimental data. It seems to be in good agreement.

2.4 Dispersion

In the past twenty-five years a number of workers have studied liquid/liquid dispersions in both baffled vessels and unbaffled vessels. Vermeulen et al. (43) presented a correlation for a baffled reactor.

$$\frac{\overline{ds}}{D} = kf(\phi) - \left(\frac{N^2 D^3 \rho}{\sigma_i}\right)^{-0.6} \quad (2-29)$$

where D = impeller diameter

N = impeller speed

σ_i = surface tension

ρ = fluid density

k = constant

ϕ = phase ratio

\overline{ds} = Sauter diameter

$$\overline{ds} = \frac{\sum n_i d_i^3}{\sum n_i d_i^2} \quad (2-30)$$

Dt = Reactor diameter

f(ϕ) = a function of ϕ whose value is presented by various workers as follows:

<u>Worker</u>	<u>f(ϕ)</u>
Calderbank (44)	1+3.75 ϕ (for D/Dt = 2/3) 1+9 ϕ (for D/Dt = 1/3)
Scully (45)	1+3.3 ϕ
Brown and Pitt (46)	1+3.14 ϕ
Mylnek and Resnik (47)	1+5.4 ϕ
Coulaloglou (48)	1+4.47 ϕ

Merry (17) carried out dispersion tests on the system water, styrene in the presence of soap (Nansa) in an unbaffled reactor. The tests were carried out under different emulsifier concentrations and impeller speeds and in reactors of differing diameters. The droplet sizes were determined by use of a Coulter Counter. The power dissipated by the impeller was measured by using a pulley-balance system. He obtained the following correlations for unbaffled reactors.

$$D_d = D_d^i \left(\frac{N}{N_i}\right)^{-1.08} \left(\frac{D}{D_i}\right)^{-0.185} \quad (2-31)$$

For $Re < 8 \times 10^3$

$$N^{0.61-0.24 \ln Re} Re^{0.07-0.12 \ln Re} = \text{const} \quad (2-32)$$

For $Re > 8 \times 10^3$

$$N^{1.22-0.24 \ln Re} Re^{1.19-0.12 \ln Re} = \text{const} \quad (2-33)$$

where N = impeller speed

D = impeller diameter

N_i = reference impeller speed

D_i = reference impeller diameter

D_d = mean droplet diameter

D_d^i = reference mean droplet diameter

Re = Reynolds number

$$R = \frac{ND^2 \rho}{\mu} \quad (2-34)$$

ρ = density of fluid

μ = Dynamic viscosity

Nomura et al. (6) also developed an empirical formula for the system water, styrene and sodium lauryl sulphate though for a baffled reactor.

$$D_d = 1.05 (0.15 + 1.4S^{-3/2}) (N^3 D^2)^{-1/4} \quad (2-35)$$

where S = emulsifier concentration

This formula is only valid however in the range of emulsifier concentration $S > 3.13 \text{ g/Dm}^3$ water which is higher than the soap levels to be used in the current study.

2.5 Determination of particle size

The most important fundamental property of a latex is the particle size and the particle size distribution. In emulsion polymerization, the reaction rate, molecular weight and its distribution and the polymer properties all relate to the particle size and to the number of particles. Five methods have been used in the past for finding the value of the particle size: (i) electron microscopy (ii) soap titration (iii) light scattering (iv) centrifugation and (v) turbidity. Methods (i) and (v) can yield particle size distribution, from which the average values can be deduced. Methods (ii) (iii) and (v) give only average values.

(i) Electron microscopy:

This method can give a complete picture of the particles present in a latex. Size analysis is carried out by measuring the diameter of images of the polymer particles printed on an electron micrograph (49).

(ii) Soap titration

The soap titration method for the determination of particle sizes is based upon the concept that the soap is adsorbed on the surface of polymer particles until the surface is entirely covered by a monomolecular film of emulsifier molecules, each of which covers a definite area (for sodium lauryl sulphate $A_s = 3.5 \times 10^{-15} \text{ cm}^2$ /one molecule (18)). If the latex contains less soap than is required for saturation of the particles, then virtually no free soap is present in the true aqueous phase. When

the soap is added beyond the point of saturation then the free soap will appear. When this free soap concentration reaches the critical micelle concentration, micelles are formed and at this point sudden changes in the properties of the latex, such as surface tension, conductance ratio, adsorption of the coloured or fluorescent dye, etc., will occur. If these properties are measured the final point of the titration may be found. According to the amount of the emulsifier added up to this point, the surface area of the particles is easily calculated (50-53).

(iii) Light scattering (54)

Light scattering is based upon the measurement of the angle between a beam of incident light and the angle of maximum intensity of scattered light. The angular dependence of intensity depends upon the relative refractive indices of the particles, the medium, the wavelength of the light and the size of the particles.

(iv) Centrifugation (55)

An ordinary centrifuge can be adapted to determine the particle size of a latex. Firstly the latex is diluted to a solid content of 2% and then centrifuged at 2700 r.p.m. while the temperature is kept fairly constant by use of dry ice. Samples are removed at various times by means of a hypodermic syringe with the needle inserted to a depth of 2 cm. The concentrations of these samples are determined. A roughly quantitative particle size contribution curve can be calculated from these data.

(v) Turbidity

Measurement of light transmission is one of the most popular methods available for measuring the particle size. It is based on the dependence of the turbidity of a dilute latex upon the particle size and on the other parameters. Barns and La Mer (56-58) did much work in this area both theoretically and in the development of the technique for the determination of the size of colloidal particles using Mie's theory (19). Of more direct use to the measurement of polystyrene latex is the method developed by Bateman et al. (20). They published a table (see Table 2-1) of theoretically determined values of total Mie scattering coefficient against wavelengths and particle radii. It is valid for the case of particle diameters more than 0.2 micron. Merry (17) extended Bateman's measurement range to smaller diameters using an interpolation method. The data he obtained seems to be reasonable in the region of particle diameter greater than 0.14 micron, but it results in a significant error if the particle size is smaller than 0.14 micron.

Table 2-1 Total Mie Scattering Coefficients for Polystyrene Spheres in Water

r(A).....	800	1320	1940	2555	3300	4070	5000	5855	7000
λ_0									
		K							
3700	0.232	0.802	1.703	2.595	3.438	3.743	3.352	2.637	1.863
4300	0.144	0.526	1.185	1.945	2.792	3.450	3.723	3.458	2.710
5000 =	0.0891	0.333	0.809	1.387	2.147	2.864	3.466	3.698	3.474
5600	0.0614	0.232	0.611	1.084	1.730	2.400	3.084	3.500	3.691
6500	0.036	0.153	0.416	0.767	1.275	1.843	2.515	3.031	3.520
7500	0.0211	0.102	0.276	0.543	0.935	1.400	1.986	2.506	3.090
8500	-	0.0705	0.193	0.397	0.701	1.086	1.581	2.055	2.642
9500	-	0.0490	0.144	0.293	0.548	0.852	1.275	1.689	2.247

Dispersion equations assumed: for water, $n = 1.324_0 + 3.046 \times 10^{-11} / \lambda_0^2$; for polystyrene,

$$n_p = 1.5683 + 10.087 \times 10^{-11} / \lambda_0^2$$

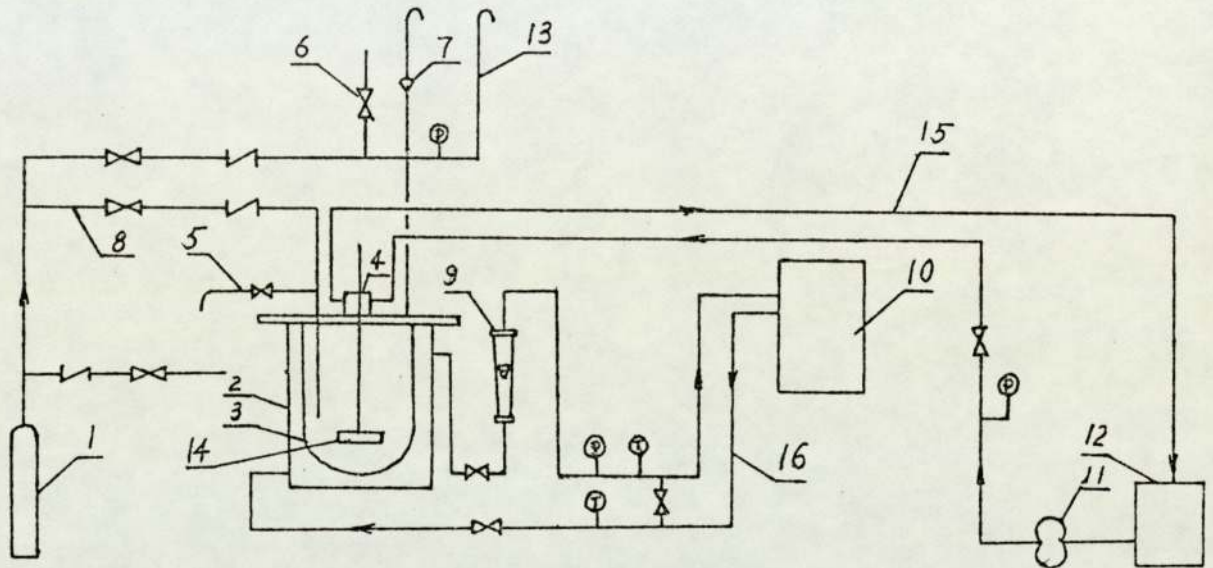
SECTION III

EXPERIMENTAL EQUIPMENT AND TECHNIQUES

- 3.1 Flow diagram and Equipment specification
- 3.2 Emulsion polymerization - Experimental technique
- 3.3 Suspension polymerisation - Experimental technique
- 3.4 Droplet dispersion tests

3.1 Flow Diagram and Equipment Specification

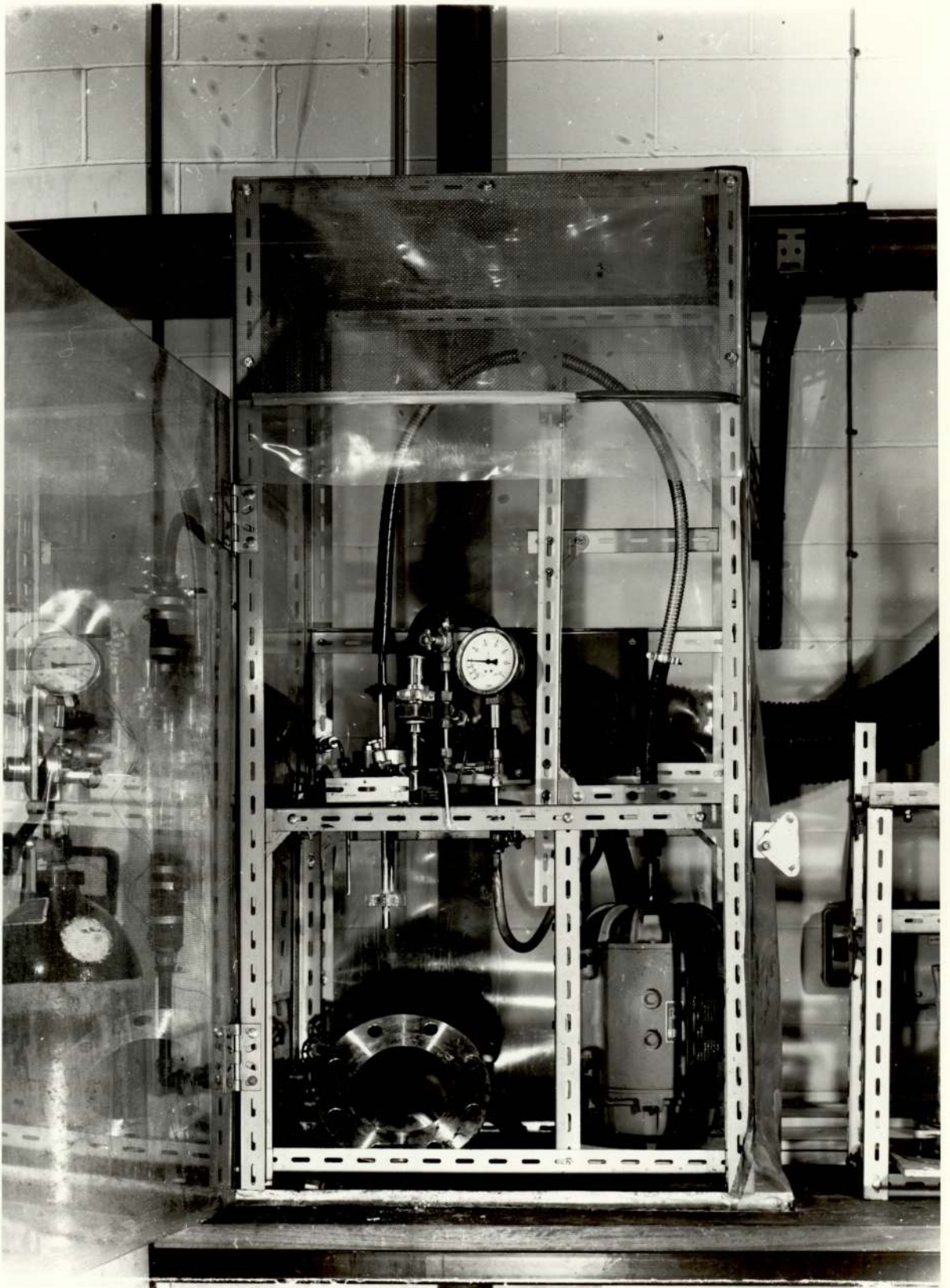
The flow chart for the emulsion polymerization, suspension polymerization and monomer dispersion runs is shown in Figure 3.1.



- | | |
|--------------------------------|--------------------------------------|
| 1. nitrogen cylinder | 2. jacketed heat exchanger |
| 3. reactor vessel | 4. axial seal |
| 5. sample line | 6. charge line |
| 7. safety valve | 8. purge pipe |
| 9. flow indicator | 10. Churchill temperature controller |
| 11. gear pump | 12. lubricant reservoir |
| 13. overpressure vent line | 14. impeller |
| 15. lubricant circulation line | 16. heat exchange fluid line |

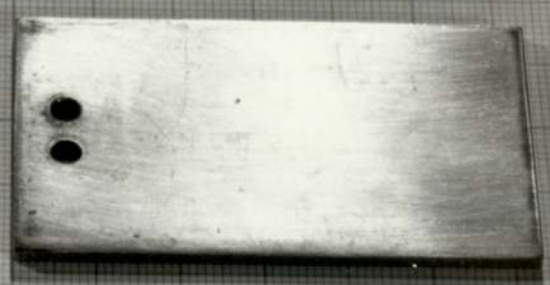
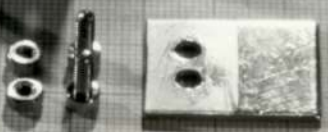
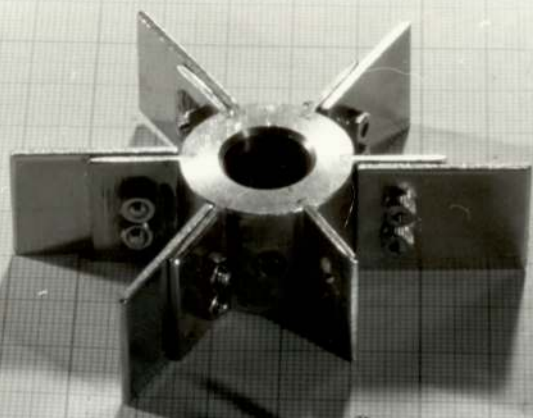
Figure 3.1 Flow Diagram

The reactor used in this work was designed and equipped by Merry(17) of this department. The reactor system is shown in figure 3.2.

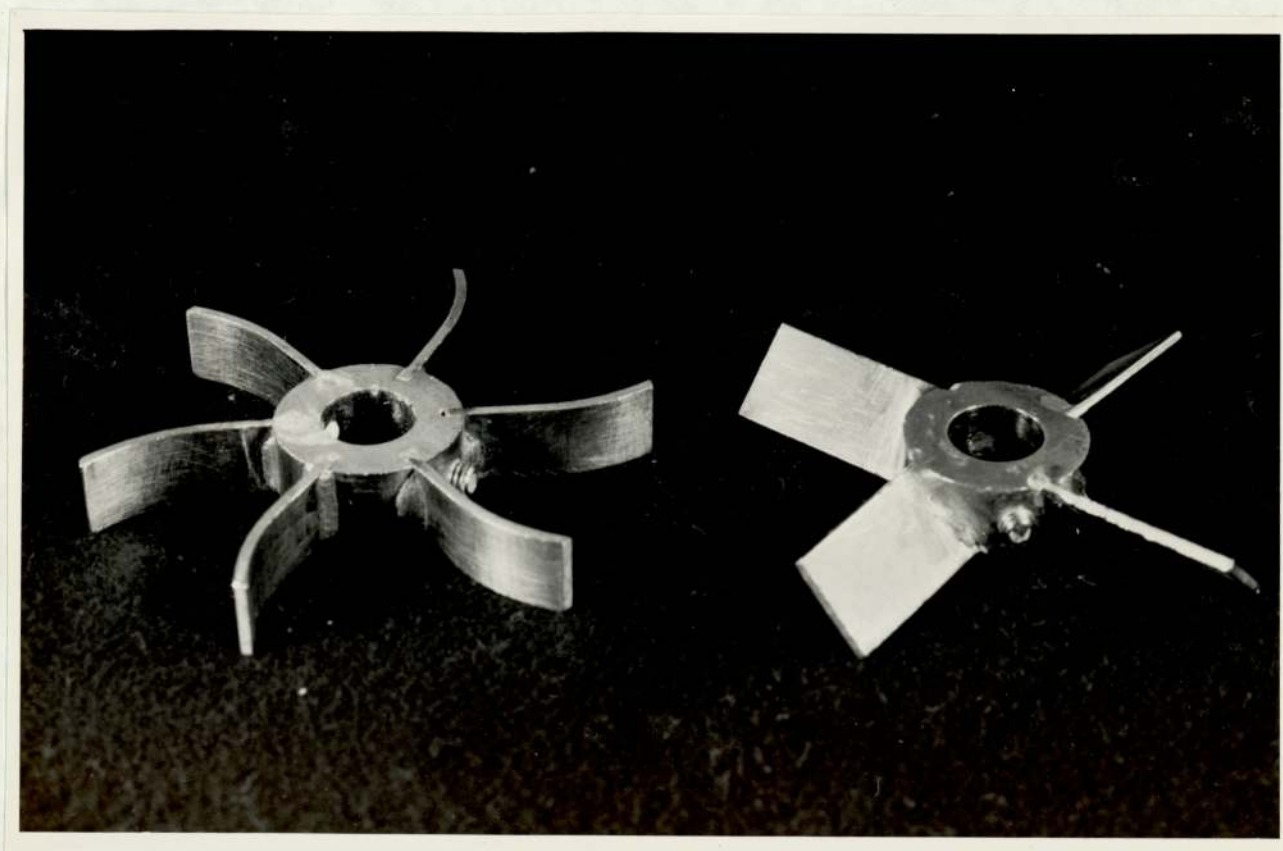


As shown in the photograph, the main body of the reactor was a cylindrical stainless steel vessel with a dished bottom. It was of 152 mm bore and had a wall thickness of 6.5 mm. The vessel was secured to its lid by means of a flange which was again made of stainless steel. The lid of this reactor was constructed from a mild steel flange lined with a sheet of stainless steel to ensure that the contents of the vessel contacted only with the stainless steel. The lid was secured to the vessel with eight 3/4 inch mild steel bolts. The lid, also carried the charge line, purge line, sample line overpressure vent line, safety valve and bearing. The maximum working pressure of the reactor was 10 bar. In order to allow temperature control, the reactor was fitted with a jacket through which water as the heat exchange medium was circulated. The temperature of the circulating water was controlled by a Churchill Captain unit, which has both a heating and cooling facility. The impeller for emulsion polymerisation was a six-bladed turbine type of 75mm. diameter as shown in Fig2.3 and a combination of impellers of 75 mm diameter for suspension polymerization as is shown in Figure 3.3. The combined impeller consisted of a 4-bladed inclined turbine and a 6-bladed swept-back turbine mounted on the same shaft, the inclined turbine being mounted 96 mm above the swept-back. They are shown in Figure 3.4.

Figure 3.3 Turbine type impeller for emulsion
polymerization



< 5cm >



(a)

(b)

Figure 3.4 The impellers for suspension polymerization

(a) 6-bladed back-swept turbine

(b) 4-bladed inclined turbine



Figure 3.5. The Baffle

Another possible adaption to the reactor were the stainless steel baffles which consisted of eight vanes running parallel to the axis of the vessel and located at 45° intervals along the vessel wall. Each of the vanes had a width of 20 mm. The baffle is shown in Figure 3.5.

3.2 Emulsion Polymerization Experiments

Prior to a polymerization run, the reactor vessel and all the accessories in the reactor were thoroughly cleaned. The cleaning involved scouring with an abrasive cloth or brushing with a wire brush, then washing thoroughly with a 1% solution of sodium lauryl sulphate and distilled water and finally rinsing with redistilled water.

The required volumes of redistilled water and styrene were measured using a graduated cylinder and the required masses of sodium lauryl sulphate and potassium persulphate were weighed accurately. The emulsifier and the initiator were then dissolved in the water and both this solution and the styrene were charged into the reactor. The vessel was then firmly bolted to its lid. To exclude the oxygen from the reactor, the contents of the reactor were purged 5 times with nitrogen by successively pressuring the reactor to approximately 3 bar and then venting to atmosphere. On the fifth venting, the pressure was dropped down to about 1.5 bar, the operating pressure.

After purging, the temperature at which the reaction was to be performed was selected on the Churchill Captain unit. Then stirring was started and heating began. When the reaction temperature was reached, timing was started. The samples for analysis were drawn off through the dip pipe the end of which was located in the middle position of the emulsion depth in the reactor. The interval between sampling was arranged to be 15 or 20 minutes depending on the run. The reaction continued until the monomer conversion was greater than 90%.

3.3 Suspension Polymerization Experiments

The reactor cleaning operation for suspension polymerization was the same as that for emulsion polymerization as detailed above.

After cleaning and bolting the vessel to the lid, the required volume of redistilled water and styrene were measured using a graduated cylinder and the required amount of polyvinyl alcohol as stabilizer and β, β' -azobisisobutyronitrile as initiator were weighed accurately. Then the stabilizer was dissolved into the water by heating and stirring while the initiator was dissolved into the styrene.

These two solutions were then charged into the reactor. The process of purging with nitrogen was the same as that for emulsion polymerization.

After purging, stirring and heating were started when the reaction temperature was reached timing was started. The samples for analysis were drawn off through the dip pipe. The intervals between sampling were arranged to be 30 minutes.

3.4 Dispersion Tests

After cleaning according to an identical procedure as above the vessel was secured to its lid. The defined volumes of distilled water and styrene were measured using a graduated cylinder such that the phase ratio of water to monomer was the same as in the emulsion polymerizations. The required mass of sodium lauryl sulphate was weighed accurately, this was then dissolved in water, thereafter both this solution and the styrene were charged into the reactor. Each batch used in the dispersion tests was subjected to five impeller speeds of 450, 550, 650, 750 and 850 r.p.m. The procedure was to start at 450 r.p.m. and to stir at this speed for one hour and then to increase to the next speed. A sample for analysis was withdrawn at the end of each hour long interval and these were analysed immediately after withdrawal. The method of analysis is described in Section 4.

SECTION IV

ANALYTICAL TECHNIQUES

- 4.1 Droplet size analysis
 - 4.1.1 Photomicrographic technique
 - 4.1.2 The Coulter Counter
 - 4.1.3 Comparison between Photomicrographic Method and Coulter Counter Method
- 4.2 Determination of degree of monomer conversion
 - 4.2.1 Precipitation with methanol
 - 4.2.2 Precipitation with aluminium chloride
 - 4.2.3 Direct drying
 - 4.2.4 Comparison of Techniques
- 4.3 Development of the technique for the measurement of particle size using light transmission
 - 4.3.1 General description
 - 4.3.2 Setting up the technique for measuring particle size in an emulsion latex
 - 4.3.3 Determination of particle size using extinction method.

In this section, the methods of both droplet size analysis and the determination of monomer conversions are introduced and the technique of the measurement of very small particle sizes is developed.

4.1 Droplet Size Analysis

Two methods of droplet size analysis, namely a photomicrographic technique and the Coulter Counter method, were employed in this study. They are described briefly below.

4.1.1 Photomicrographic

In this technique, photographs of the dispersion were taken through a microscope. The numbers of droplet images within the different size intervals on the photographs were counted. Thus the distribution and the Sauter mean droplet diameter could be calculated.

The photographs of monomer droplets using the microscope were obtained using the following procedure. Firstly, the latex sample was diluted. The bottle containing the latex sample was shaken gently, two drops of the sample were extracted from the middle position of the depth of the contents in the bottle into the syringe and then 4cc of redistilled water was also taken into the syringe. The syringe was shaken gently to mix the contents. A slide for holding the sample was made up of two glass plates and two small spacers of perspex sheet having a thickness of about 0.1mm. These two

spacers were put between the two glass plates to make a narrow slit, as is shown in Figure 4.1.

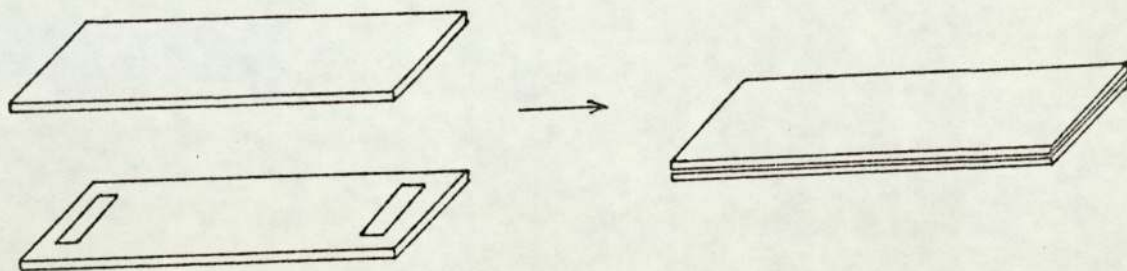


Figure 4.1 The Slide

The dilute sample in the syringe was injected slowly into the slit. It was found that in this way the droplets could be evenly distributed across the slide between the two glass plates, without observing swarming of the drops and without fear of evaporation.

The slide was placed under the microscope, three to five photographs of different parts of the slide were taken using a Miranda Sensorex 30 mm still camera. The microscope is shown in Figure 4.2 and a typical photograph of monomer droplets taken through the microscope is shown in Figure 4.3.

4.1.2 The Coulter Counter

The Coulter Counter is a widely used piece of equipment for the analysis of particle sizes of solid materials in the size range 2 to 300 micron but it is also used in the analysis of liquid droplets in dispersion. Figures 4.4 and 4.6 show the equipment



Figure 4.2 The Microscope

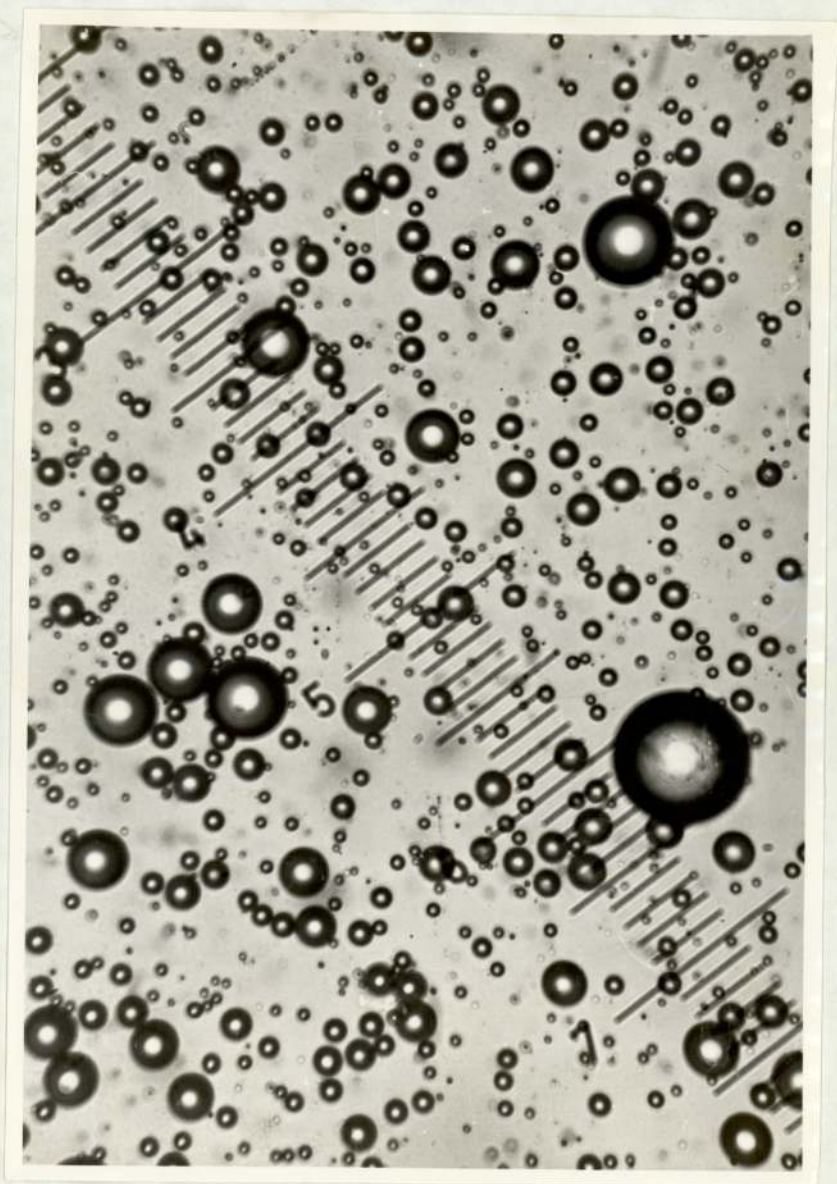


Figure 4.3 Droplets in the dispersion x 635

and Figure 4.5 shows a simplified diagram of the Coulter Counter cell. As is seen in these figures, an orifice tube (B) which is filled with the electrolyte solution in water is immersed into the same electrolyte solution in a cup (A) containing the particles or droplets. The only contact between the electrolyte solution volumes inside and outside of the tube is through an orifice of known diameter in the wall of the tube. On the horizontal section of the mercury manometers (D), two electrodes are installed. The volume of the tube between the two electrodes is fixed and known. Thus the volume of the electrolyte solution passing through the orifice in a given time may be determined. If the electric circuit is connected, then an electric current will pass between the two electrodes (C), one inside the tube and another outside the tube both placed near to the orifice. The electrolyte solution will flow through the orifice by virtue of the pressure between the outside of the tube and the inside of the tube. When the droplets dispersed in the electrolyte solution pass through the orifice the area for current to flow is reduced and thus the resistance between the electrodes changes.

The electrical signal resulting from the resistance fluctuations is fed into the analysis section of the Coulter Counter where it is decoded. A threshold setting is manually selected which relates to a certain particle size. After successively monitoring the whole range of particle sizes, the droplet size distribution and average droplet size may be obtained.

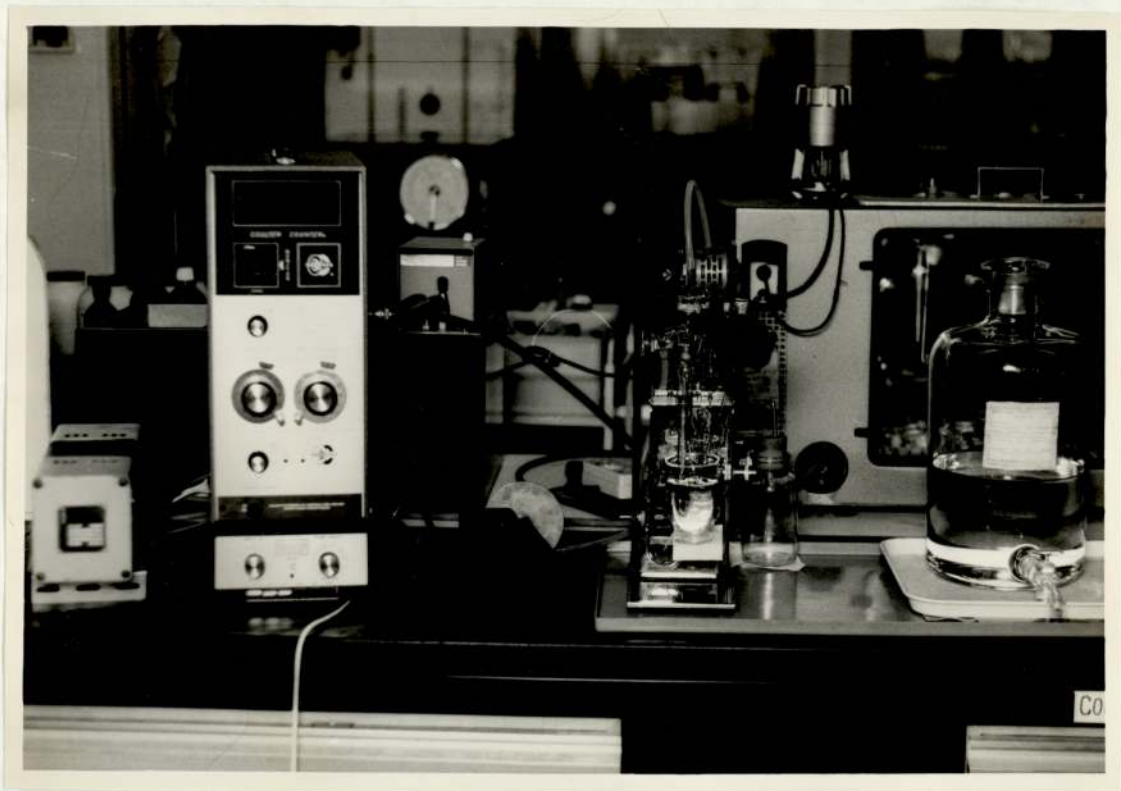


Figure 4.4 The Coulter Counter

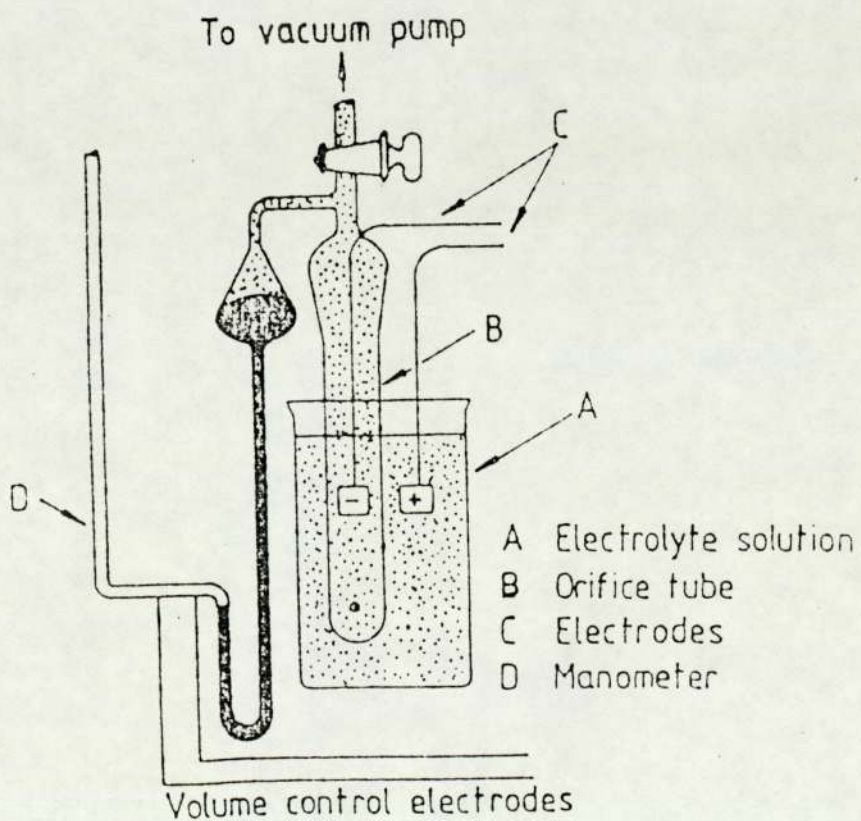


Figure 4.5 Test Cell of Coulter Counter

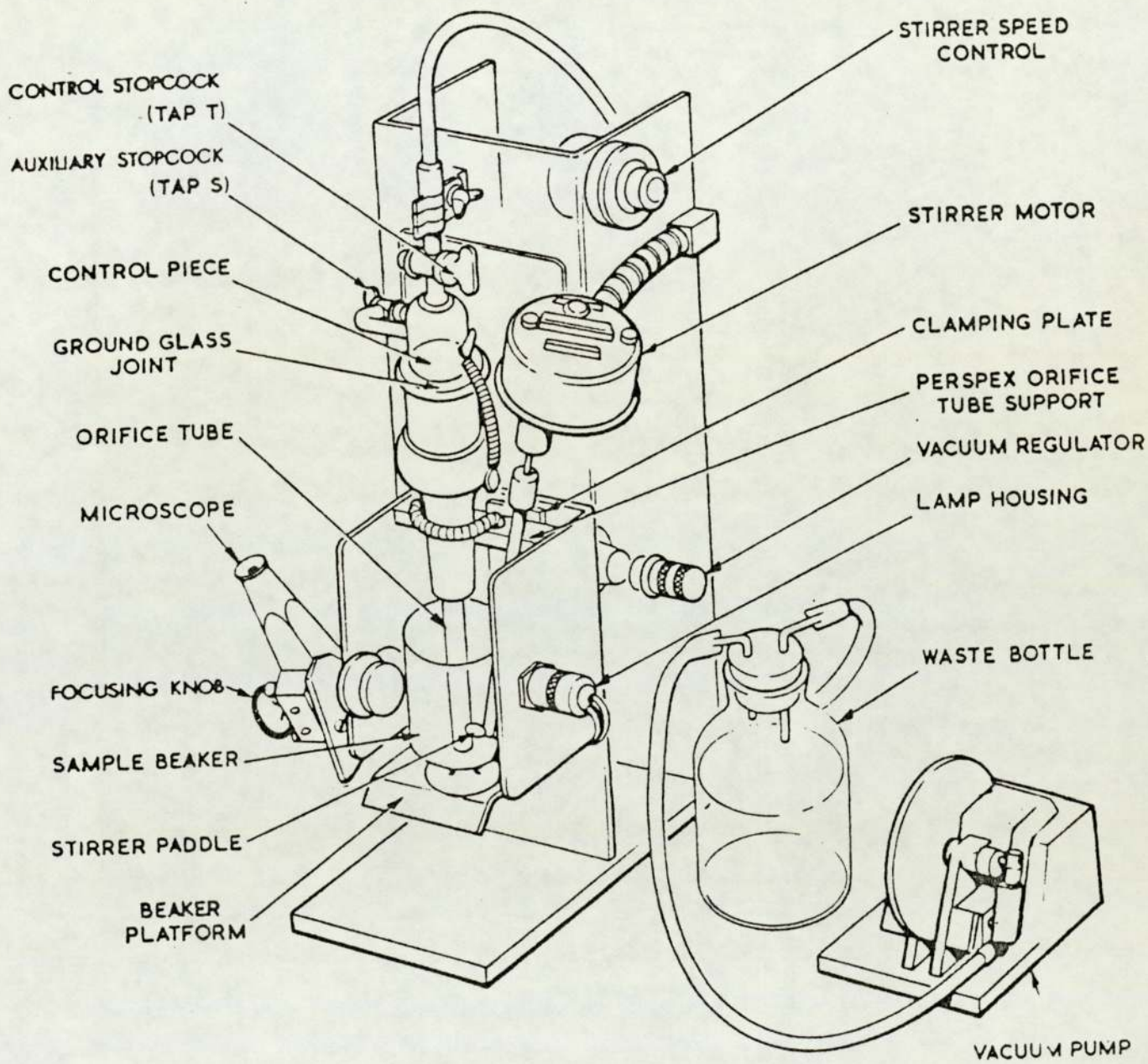


Figure 4.6 Glassware and Stand Assembly of Coulter Counter

The simplified procedure for operation of this equipment is briefly introduced below.

Prior to using the Coulter Counter for measuring the droplet size, the following preparation work should be done.

(i) Make up 0.9% of sodium chloride solution in water and filter it by passing through a 0.8 micron membrane twice.

(ii) Because the droplet sizes in the system treated in this work are less than 56 micron and the manometer volume of 2 ml is used, the tube with 140 micron orifice diameter should be selected.

After preparation, a control test is needed in order to obtain the background counts on the filtered electrolyte. Then a calibration is performed using smooth particles of known density monosized particles to obtain the calibration constant K . Finally the suspension of the samples in the filtered electrolyte solution are analysed. The whole range of the droplet diameters is divided into 16 intervals by changing the lower threshold dial setting, t_L , the upper threshold dial setting, t_U , aperture current setting, I , and the reciprocal amplification, A . For each interval, the number of droplets is counted and displayed on the oscilloscope of the Coulter Counter numerically, the average diameter of the droplets, D_d , is calculated using the following equation:

Sample - Polystyrene Source - Electrolyte - NaCl Dispersant - Date - 14/2/81
 Aperture - 100 µm Manometer - 2ml Calibration - 2.1121 Matching - Operator - Cao
 Diameter Volume Gain - Control Colincidence - 0.625 Calibration - 1.85 µm
 Aperture - Resistance Control Factor, P Data

t_L	I	A	n' (raw counts)		\bar{n}'	$n'' = \frac{n'}{1000}$	B	$n'' = \bar{n}' + n''$ -B	$V = t_L \cdot I \cdot A$	$d_L = K \cdot \sqrt{V}$	An''	\bar{V}	$An \cdot \bar{V}$	$\Sigma (An) \cdot \bar{V}$	Wt%
20	8	64	1,0	1,0	0,0	0	0	0,29	10240	45.9	0.15	5120	768	768	2.51
20	8	32	3,2	1,2	3,2	0	0	2	5120	36.4	1.7	7680	13056	13824	45.15
20	8	16	7,3	6,4	2,4	0	0	4	2560	28.9	2.0	3840	7680	21504	70.24
20	8	8	2,5	2,2	2,4	0	0	1	1280	22.9	0	1920	0	21504	70.24
20	8	4	6,2	3,4	6,1	0	0	2,6	640	18.2	1.0	960	960	22464	73.37
20	8	2	4,10	4,3	3,3	0	0	2,3	320	14.4	0	480	0	22464	73.37
20	4	2	11,10	7,11	9,10	0	0	7,0	160	11.5	4.7	240	1128	23592	77.06
20	2	2	18,15	23,21	18,12	0	0	8,3	80	9.1	1.3	120	156	23748	77.56
20	1	2	20,21	19,21	26,29	0	0	13,7	40	7.2	5.4	60	324	24072	78.62
20	1	2	49,64	44,52	67,48	0	0	41,0	20	5.7	27.3	30	819	24891	81.30
20	1	1	135,145	145,130	138,8	0	0	133,8	10	4.6	72.8	15	1092	25983	84.86
20	1	1/2	335,326	293,292	311.5	0	0	246,5	5	3.6	132.7	7.5	995	26978	88.11
20	1	1/4	586,659	628,629	625.5	0	0	506,5	2.5	2.9	260	3.75	975	27953	91.30
20	1/2	1/4	943,959	976,1013	972.8	0	0	795,8	1.725	2.5	289	2.11	610	28563	93.29
20	0.354	1/4	1419	1403	1411	1	1	1130,0	0.863	2.0	334	1.29	431	28994	94.70
20	0.354	1/8	2155	2162	21585	3	3	1682,5	0.625	1.8	553	0.744	411	29405	96.19
20	0.171	1/8	3253	3088	31705	6	6	2352,5	0.443	1.6	670	0.534	358	29763	97.21
20	1/8	1/8	7291	7892	75915	36	36	4612,5	0.313	1.4	2260	0.378	854	30617	100.00

$$D_d = K(t_{LIA})^{1/3} \quad (4-1)$$

Therefore the droplet size distribution and the average droplet diameters can be obtained. A sample table illustrating the treatment of the data is shown in Table 4.1.

4.1.3 Comparison between the Photomicrographic Method and the Coulter Counter Method

Compared with the photomicrographic method, the technique using the Coulter Counter is rapid and convenient, but it was found from experiment that the data obtained showed considerable scatter and the reproducibility was rather low for determining the droplet sizes of styrene. This is suggested to be because the droplets suspended in the electrolyte solution are not stable, some of the droplets coalesce together and the styrene can evaporate during the analysis for greater accuracy, although the photomicrographic technique is time-consuming and tedious, it was used for most of the dispersion tests in this study.

4.2 Determination of Monomer Conversion

Monomer conversion is one of the most important parameters for emulsion polymerization studies. In this work, it was measured using the following procedure.

At timed intervals from zero time (15 or 20 minute intervals) the samples were taken from the reactor and each of the samples was put into a bottle of known

weight. The bottle containing the sample was weighed. According to the weight of the sample in the bottle, a definite amount of inhibitor, namely benzoquinone, was added to the bottle to give a concentration of 0.5% in the sample. The role of benzoquinone is to prevent further polymerization of the unreacted monomer. In this work, the monomer conversion was determined by using three methods which are briefly described below.

4.2.1. Precipitation with Methanol

For each of the samples, a certain amount (3-5 gram) was taken from the bottle containing the stopped sample mentioned above. The polymer was precipitated by adding it to a bottle containing about 50 ml of methyl alcohol. The precipitate was then filtered on a weighed sintered glass filter. The precipitate was washed in turn with methanol and hot water five times then finally with methanol. The precipitate was then dried to constant weight. From the weight of the dried precipitate the weight of sample and the recipe of the run of the polymerisation, the fractional conversion based on styrene could be calculated.

4.2.2 Precipitation with Aluminium Chloride

For each of the samples a certain amount was taken (3-5 gram) from the bottle containing the stopped sample mentioned above. The bottle was placed in an ice bath to cool it for fifteen minutes. 5 ml of cool hexane was added and was shaken gently. The mixture was then diluted 60 times with cooled distilled water.

Ten drops of 27% w/w aluminium chloride solution in water was then added to the dilute sample in order to precipitate the polymer. The precipitate was filtered on a weighed sintered glass filter. The precipitate was washed with hot water five times. The precipitate was then dried to constant weight. From the weight of the dried precipitate, the weight of the sample and the recipe of the run of the polymerization the fractional monomer conversion could be calculated.

4.2.3 Direct Drying

For each of the samples, a certain amount was taken (0.5-1.0 gram) from the bottle containing the sample and it was put onto an aluminium plate of known weight which was heated for half an hour prior to use. The plate was then placed in an oven to dry at 70°C overnight to constant weight. From the weight of the remains on the plate, the content of the inhibitor, the weight of the sample and the recipe of the run of the polymerization the fractional monomer conversion could be calculated.

4.2.4 Comparison of Techniques

The results from the technique using the precipitation with methanol seem to be more accurate than the other methods, but it is too time-consuming and wastes a large amount of methanol. The technique using the precipitation with aluminium chloride solution is economical in regard to the use of the solvent and can deliver reasonable results, but it is also time-consuming and the precipitate tends to agglomerate so that it is hard to dry if the

extraction of styrene with hexane is not complete. The technique of direct drying gives the most acceptable results. A major advantage of this method is that it is very convenient and it needs no organic solvent. So in this work, the latter technique was used for most of the test runs of both emulsion polymerization and suspension polymerization.

4.3 Development of the Technique for the Measurement of Particle Size Using Light Transmission

4.3.1 General Description

An important characteristic of a latex is its particle size. In emulsion polymerization, the reaction rate, molecular weight of polymer and its distribution and the polymer properties all relate to the particle size and the number of particles. The light transmission technique is one of the methods available for measuring these parameters. This technique is based on the dependence of the turbidity of a dilute latex upon the particle size and upon the other parameters. Many previous workers have devoted themselves to the development of the light transmission technique to measure the size of colloidal particles (56-58). Of more direct use to the measurement of polystyrene latex is the light transmission method developed by Bateman et al. (20). Unfortunately, Bateman's method is only valid for the case where the diameter of the particles is greater than 0.2 micron. The latex produced by emulsion polymerization, however, contains very small particles with an average

diameter much smaller than 0.2 micron, particularly in the early stages of the reaction. Merry (17) extended Bateman's measurement range to a smaller diameter range using an interpolation method. The data he obtained seems to be reasonable in the region of particle diameters greater than 0.14 micron, but it results in a significant error if the particle size is smaller than 0.14 micron.

In the current project, a light transmission technique for measuring particle sizes whose diameters are even smaller than 0.1 micron has been developed and the results obtained are compared with those determined by electron microscopy.

4.3.2 Setting up the Technique for Measuring Particle Size in Emulsion Latex.

According to Mie's theory, the total Mie scattering coefficient, K can be evaluated using the following equation.

$$K = \frac{2.303 E}{\pi r_p^2 N_p l} \quad (4-2)$$

where E = light extinction, $E = \ln I/I_0$
 I_0 = incident light intensity
 I = transmitted light intensity
 r_p = average radius of particles, em
 l = Length of scattering cell, cm
 N_p = number of particles per cm^3

If the mass concentration of the particles is denoted by C , g/cm^3 , then $C = N_p \frac{4}{3} \pi r_p^3 D_{sw}$. So

$$K = \frac{3.0707 E r_p d_{sw}}{Cl} \quad (4-3)$$

where d_{sw} = the density of particles, g/cm^3

On the other hand, α is defined as size parameter.

$$\alpha = \frac{2 \pi n r_p}{\lambda_0} \quad (4-4)$$

where λ_0 = wavelength of the incident light in the air, cm.

n = refractive index, which is given by the equation as follows:

$$n = a + b/\lambda_0^2 \quad (4-5)$$

a and b are constants, $a = 1.3240$, $b = 3.040 \times 10^{-11}$ for water (59) and $a = 1.5683$, $b = 10.087 \times 10^{-11}$ for polystyrene (60).

From equation (4-3) and 4-4) the following formula can be obtained.

$$\frac{K}{\alpha} = \frac{0.4887 d_{sw} E \lambda_0}{ncl} \quad (4-6)$$

In this project, several samples were used in which the particle sizes and the mass concentration of the particles were known. The values of E were measured using a Pye Unicam SP1800 ultraviolet spectrophotometer see Figure 4.6 within the wavelength range from 3700 \AA to 6500 \AA . The values of n were determined by equation

(4-5). Therefore, the dependence of r , K and λ_0 could be found from equation (4-3), (4-4) and (4-6). The results computed from the original data are listed in Table 4-2, Table 4-3 and Table 4-4. Five formulae which represent the relationship between the parameter K/α and r_p were obtained as follows by using polynomial regression method:

$$r_{3700} = 0.04387 + 0.1751X + 0.9485X^2 - 1.3463X^3$$

$$r_{4300} = 0.04294 + 0.4171X - 1.2214X^2 + 11.1013X^3$$

$$r_{5000} = 0.04254 + 0.7329X - 5.6351X^2 + 45.2569X^3$$

$$r_{5600} = 0.04211 + 1.0947X - 13.7433X^2 + 122.572X^3$$

$$r_{6500} = 0.04218 + 1.6546X - 29.9384X^2 + 336.231X^3$$

where X stands for K/α

Table 4-2 The values of the size parameter for various particle radii and wavelengths.

$r(\text{\AA})$	0.046	0.055	0.0645	0.0698	0.0771	0.0821	0.0958
$\lambda_0(\text{\AA})$	α						
3700	1.0516	1.2575	1.3463	1.5960	1.6204	1.8781	2.1900
4300	0.9010	1.0774	1.1843	1.3674	1.3875	1.6091	1.8763
5000	0.7724	0.9236	1.0152	1.1722	1.1889	1.3794	1.6085
5600	0.6884	0.8231	0.9048	1.0447	1.0592	1.2293	1.4335
6500	0.6919	0.7078	0.7780	0.8983	0.9016	1.0571	1.2327

Table 4-3 - Total Mie scattering coefficients of polystyrene sphere in water for smaller particles

$r(\text{\AA})$	0.046	0.055	0.0645	0.0698	0.0771	0.0821	0.0958
$\lambda_0(\text{\AA})$	K						
3700	0.01634	0.05295	0.10380	0.16270	0.20540	0.24280	0.38200
4300	0.00827	0.02843	0.05820	0.09573	0.12480	0.14890	0.22970
5000	0.00451	0.01552	0.03244	0.05584	0.07538	0.09505	0.14500
5600	0.00301	0.00991	0.02103	0.03749	0.05347	0.06743	0.10390
6500	0.00169	0.00553	0.01185	0.02234	0.03010	0.04292	0.06527

Table 4-4 - The values of parameter k/α for various particle radii and the wavelengths

$r(\text{\AA})$	0.046	0.055	0.0645	0.0698	0.0771	0.0821	0.0958
$-\lambda_0(\text{\AA})$	K/α						
3700	0.01553	0.04210	0.07710	0.10190	0.12680	0.12930	0.17440
4300	0.00918	0.02639	0.04910	0.07000	0.09885	0.09254	0.12240
5000	0.00584	0.01680	0.03195	0.04764	0.06340	0.06891	0.09015
5600	0.00437	0.01204	0.02324	0.03589	0.05049	0.05485	0.07248
6500	0.00286	0.00781	0.01523	0.02486	0.03306	0.04060	0.05295



Figure 4.6 Pye Unicam spl800 ultraviolet spectrophotometer

4.3.3 Determination of Particle Size using Extinction Technique

This technique involves measuring the turbidity of a diluted latex and estimating the values of mass particle concentration, C , and the refractive index, n . Then the parameter K/α can be calculated by means of equation (4-6). The average radius of the particles in the latex can, therefore, be found according to equation (4-7). The computer programme for this calculation is shown in Appendix I. The procedure below can be followed.

4.3.3.1 Collecting Basic Data

In order to perform this calculation, the recipe for the emulsion polymerization needed to be known. Then based on the recipe the following parameters may be estimated.

$$\text{MAXT} = \frac{W_{\text{mono}} + W_{\text{soap}} + W_{\text{I}}}{W_{\text{total}}} \quad (4-8)$$

$$\text{MAXP} = \frac{W_{\text{mono}}}{W_{\text{total}}} \quad (4-9)$$

where W_{mono} , W_{soap} , and W_{I} denote the weight of monomer, soap and initiator charged, respectively. W_{total} stands for the total weight of the contents in the reactor, and MAXT and MAXP are the maximum theoretical solid contents and the maximum theoretical polymer content, respectively.

Another important parameter TSC, the total solid content, can be determined gravimetrically.

4.3.3.2 Diluting

Because the original latex contains so many particles, the turbidity goes beyond the scope of the spectrophotometer. Therefore it had to be diluted twice to reduce the concentration of the particles in the latex.

For the first dilution, an amount of emulsion sample in a bottle (say, about 0.5 gram) was accurately weighed. The weight of this sample is denoted by g_1 . Distilled water was then added to this bottle (say 100 gram) and it was again weighed. The weight of the sample after the first dilution is called G_1 . Thus the following parameters after the first dilution may be easily calculated:

$$TSC_1 = TSC \frac{g_1}{G_1} \quad (4-10)$$

$$MAXT_1 = MAXT \frac{g_1}{G_1} \quad (4-11)$$

$$MAXP_1 = MAXP \frac{g_1}{G_1} \quad (4-12)$$

where TSC_1 , $MAXT_1$, and $MAXP_1$ are the solid content, maximum theoretical solid content and the maximum theoretical polymer content after the first dilution.

In the second dilution, a sample of first dilution (say , about 10 gram) was weighed accurately. The weight of this sample is denoted by g_2 . It was diluted again (say, till about 100gram). The weight of the second diluted latex is known as G_2 . Thus, the following formulae can be used for finding the parameters after the second

dilution:

$$TSC_2 = TSC_1 \frac{g_2}{G_2} \quad (4-13)$$

$$MAXT_2 = MAXT_1 \frac{g_2}{G_2} \quad (4-14)$$

$$MAXP_2 = MAXP_1 \frac{g_2}{G_2} \quad (4-15)$$

4.3.3.3 Estimating the Mass Concentration of the Particles in the Diluted Latex

Firstly, the monomer conversion, X_p , may be found using the equation as follows:

$$X_p = \frac{MAXP - (MAXT - TSC)}{MAXP} \quad (4-16)$$

Therefore, the weight fraction of polymer in the diluted latex, FPL, can be found.

$$FPL = MAXP_2 X_p \quad (4-17)$$

The weight of polymer in the diluted latex, W_p , should be

$$W_p = G_2 FPL \quad (4-18)$$

and the weight of monomer in the diluted latex, W_s , should be

$$W_s = (MAXT_2 - TSC_2) G_2 \quad (4-19)$$

The weight of water in the diluted latex, W_A , should be

$$W_A = (1 - MAXT_2) G_2 \quad (4-20)$$

It may be imagined that the monomer would exist

both in the aqueous phase and in the particle phase according to the partition law. If W_{SA} denotes the weight of monomer in the aqueous phase and M the partition coefficient, then:

$$M = \frac{\frac{W_{SA}}{W_A}}{\frac{W_S - W_{SA}}{W_P}}$$

or
$$W_{SA} = \frac{MW_A W_S}{W_P + MW_A} \quad (4-21)$$

For a system made up of polystyrene, styrene and water, $M = 2.2393 \times 10^{-4}$.

Consequently, the weight of monomer in the particle phase, W_{sp} , can be obtained.

$$W_{sp} = W_S - W_{SA} \quad (4-22)$$

Therefore, the mass particle concentration, C , can be written as

$$C = \frac{W_p + W_{sp}}{G_2} \quad (4-23)$$

4.3.3.4 Finding the Density of Particles in the Diluted Latex, d'_{sw}

Because the particles are swollen by monomer, the density of the particles should have a value between the density of polymer, d_p , and the density of monomer, d_m . Thus, the following equation may be used for finding the value of d'_{sw} approximately,

$$d'_{sW} = \left(\frac{W_p}{W_p + W_{sp}} \right) d_p + \left(\frac{W_{sp}}{W_p + W_{sp}} \right) d_m \quad (4-24)$$

4.3.3.5 Estimating the Refractive Index, n.

The value of the refractive index of water, n_A , and the refractive index of polymer, n_p , are first found using equation (4-5), under the different wavelength conditions (say, 3700Å, 4300Å, 5000Å, 5600Å, and 6500Å). Then the equation below is used to evaluate the average refractive index approximately.

$$n = Cn_p + (1-C)n_A \quad (4-25)$$

4.3.3.6 Measuring the Extinction Coefficient, E.

The values of E are measured by the spectrophotometer for predetermined wavelengths. To be accurate, the zero point should be adjusted each time because zero drift affects the results.

4.3.3.7 Evaluating the Parameter K/α and the Average Radius of Particles

In accordance with the parameters computed or measured above, the values of K/α may be determined by means of equation (4-6) for the predetermined wavelengths. Then from the value of K/α obtained above, the average radius of particles for each wavelength can be obtained according to equation (4-7). If we take these radii on average, the average radius of the particles in the diluted latex is finally determined.

4.3.3.8 Correcting the Size of Particles

As is mentioned above, the monomer in the latex is partitioned between the aqueous phase and the polymer phase according to the partition law. In this case, equilibrium between the two phases is actually achieved. After diluting, the equilibrium is upset and some monomer will be transferred from the polymer phase to the aqueous phase. A new equilibrium will be achieved. Because the samples adopted for measuring the particle size here are much more dilute than the latex in the reactor, the content of the monomer in the polymer phase in the diluted sample is less than that in the reactor, in other words, the size of the particle measured in this case is smaller than the actual particle size in the reactor. So the particle size measured above should be corrected to return the particle size to that under the reaction conditions. The following equation is used for this correction:

$$D_p = D'_p \left\{ \frac{d'_{sw}}{d_{sw}} \left(1 + \frac{W_{SA}}{W_p + W_{sp}} \right) \right\}^{1/3} \quad (4-26)$$

where D'_p = the average diameter of particles measured above

D_p = the average diameter of particles in the reactor

d'_{sw} = the density of the particles in the latex after the second dilution

d_{sw} = the density of the particles in the reactor

For Stage I and Stage II of emulsion polymerization,

$$d_{sw} = d_p x_{p,II-III} + d_m (1 - x_{p,II-III}) \quad (4-27)$$

For Stage III

$$d_{sw} = d_p x_p + d_m (1 - X_p) \quad (4-28)$$

where $x_{p,II-III}$ is the monomer conversion at the end of stage II.

4.3.4 Comparison between the Results from This Technique and the Electron Microscopic Method.

This technique has extended Bateman's data to a smaller particle diameter range than Merry achieved previously (17). It seems that the technique is valid for measuring the particle diameter down to 0.09 micron. The data determined with this technique are similar to those measured using an electron microphotographic method. Some results analysed by these two techniques are compared in Table 4-5. Further evidence for the validity of this method is that the results under the various wavelengths for the same sample are quite close to each other, as shown in Table 4-6.

Sample	average particle radius, micron	
	electron microscope	light extinction
N5	0.043	0.0443
N7	0.0502	0.0450
N16	0.070	0.0633
N11	0.075	0.0701

Table 4.5. Comparison of the results from the light transmission technique with those from electron microscopy.

Table 4-6 Change in radius of particles with wavelength

Sample	N5	N7	N16	N11
λ_0 (Å)	r, micron			
3700	0.0448	0.0453	0.0650	0.0671
4300	0.0447	0.0452	0.0631	0.0676
5000	0.0444	0.0451	0.0621	0.0678
5600	0.0437	0.0450	0.0638	0.0688
6500	0.0440	0.0447	0.0629	0.0735

SECTION V

THE MATHEMATICAL MODEL

- 5.1 Setting up the Model for Stage I.
 - 5.1.1 General description of the model.
 - 5.1.2 Setting up the differential equation for particle nucleation
 - 5.1.3 Derivation of the equation for the surface area of monomer droplets
 - 5.1.4 Estimating the parameters of monomer droplets
 - 5.1.5 Derivation of the equation for estimating the surface area of particles
 - 5.1.6 Derivation of equation for estimating the volume of polymer particles
 - 5.1.7 Derivation of the equation for estimating the fractional monomer conversion
 - 5.1.8 Derivation of the equation for estimating the number of particles

- 5.2 Setting up the model for Stage II

- 5.3 Setting up the model for Stage III

5.1 Setting up the Model for Stage I

Since the classical work of Smith-Ewart⁽¹⁾ on modelling emulsion polymerization, a great number of papers have appeared which either modified the classical model or proposed new models. None of these papers considered the effect of the adsorption of emulsifier onto the surface of monomer droplets. In the normal case, the amount of this adsorbed soap may be ignored because it is relatively small compared with the total soap concentration. However, if the soap concentration is low or if the impeller speed is high enough, then the proportion of the adsorbed soap on the monomer droplet surface will be comparable with that of the micellar soap. In this case, the effect of the adsorbed soap must be taken into account.

Several workers have studied the effects of stirring on the process of emulsion polymerization. Shunmukham⁽²⁾ noted that violent agitation would reduce the polymerization rate and increase the induction time. Schoot et al⁽³⁾ suggested that the increase in induction time is associated with inhibition by trace oxygen in the nitrogen atmosphere used and the decrease in polymerization rate is due to increasing mass transfer between the gas and liquid phases as agitation becomes more severe. Evans et al⁽⁴⁾, Omi et al⁽⁵⁾ and Nomura et al⁽⁶⁾ pointed out that, under a highly purified nitrogen atmosphere, the decrease in the rate of polymerization and in the number of polymer particles with increased agitation may be due to the fact that the micelle population is a function not only of the soap concentration, but also of the amount of soap adsorbed onto the surface of the monomer droplets, i.e. a function of the degree of dispersion which is directly dependent on the agitation.

In this project, a mathematical model for emulsion polymerization is established which takes into account the soap adsorbed on the surface of monomer droplets. The computed results are compared with experimental data.

5.1.1 General Description.

For a batch emulsion polymerization, definite amounts of water, monomer and soap are first charged into the reactor before charging the initiator. The soap charged will, in the main, dissolve in the water. The limiting concentration of soap up to which value the soap is in solution as single free molecules at a given reaction temperature is known as the critical micelle concentration, $[S]_{CMC}$ and any soap added above this value goes into solution but forms into aggregates known as micelles which play a significant part in the mechanism of emulsion polymerization. A proportion of the initial soap will of course be adsorbed onto the surface of the monomer droplets. The proportions of the soap distributed amongst these various forms may be easily computed. If S stands for the total area provided by soap, $[S]$ the initial soap concentration, A_d^0 the initial surface area of monomer droplets, A_m^0 the initial area of micelles and A_s the surface area occupied by one soap molecule, then

$$S = ([S] - [S]_{CMC}) N_A A_s \quad (5.1)$$

$$A_m^0 = S - A_d^0 \quad (5.2)$$

As the degree of dispersion increases it is clear that as A_d^0 becomes larger, then A_m^0 becomes proportionately smaller for a definite total amount of soap.

When the initiator is charged and the contents of the reactor reach the reaction temperature, the initiator starts to dissociate into radicals

and the reaction begins after a short induction period. The rate of radical generation, R , may be calculated from the following equation

$$R = 2k_i f [I] N_A \quad (5.3)$$

where k_i = the decomposition rate constant of initiator.

f = the efficiency of initiator decomposition.

$[I]$ = the initial initiator concentration.

The classical mechanism for emulsion polymerization^(21,23) assumes that the soap micelles, which have the ability to solubilise monomer by concentrating it in solution at their centres, are the loci for the initiation and polymerization. A radical is assumed to migrate into the centre of a micelle and to initiate polymerization there. As polymerization proceeds, the micelle becomes a monomer swollen polymer particle. More monomer migrates from the droplets to the particle to sustain the reaction. As more and more particles are formed and increase in size, more soap is adsorbed onto the particle surface, thus depleting the number of micelles. When the micellar soap is completely depleted, generally speaking, particle nucleation stops. At this point, the final number of particles is fixed. The period from the beginning of the reaction to micelle depletion is often referred to as Stage I. In this period, if the surface area of particles is denoted by A_p and the area of micelles by A_m at a given time, then

$$A_m = S - A_p - A_d \quad (5.4)$$

After Stage I, the reaction proceeds into Stage II, during which the soap can be found in three loci, namely, free soap in solution, the soap on the surface of particles and that on the surface of monomer droplets. As polymerization proceeds, the particle size will become larger, whilst

that of the monomer droplets becomes smaller and smaller. So some soap will be set free from the droplets and move to the polymer particle surface. When the monomer droplets disappear, Stage II finishes and enters into Stage III.

In Stage III, because of the disappearance of micelles and monomer droplets, the soap is present either in free solution at a concentration at or below $[S]_{CMC}$ or is adsorbed onto the surface of the polymer particles which are thus rendered stable.

5.1.2 Setting up the Differential Equation for Particle Nucleation.

Gardon⁽²⁸⁾ recalculated and extended successfully the Smith-Ewart model for emulsion polymerization by using a different mathematical approach. Neither Smith and Ewart nor Gardon considered the effect of both the critical micellar soap and the soap adsorbed on monomer droplet surface on the progress of the reaction. In the present paper, a mathematical model is set up using the same mathematical method as Gardon with the critical micellar soap and the soap adsorbed on the monomer droplet surface being allowed for.

Suppose during Stage I, the process of emulsion polymerization proceeds from time 0 to time t . To derive the differential equation, we may subdivide the time t into m very small intervals, $1, 2, 3, \dots, i-1, i, i+1, \dots, m-1, m$. At the beginning of the subinterval i , the time is τ and at the end of it, the time is $(\tau+d\tau)$. If $N_p(\tau)$ denotes the number of particles which have been nucleated during period from time 0 to time τ , $A_p(\tau)$ the surface area of polymer particles at time τ and $A_d(\tau)$ the surface area of monomer droplets at time τ , then the differential equation of particle nucleation can be set up as

follows :

$$\frac{dN_p(\tau)}{d\tau} = \frac{R}{S} [s - A_p(\tau) - A_d(\tau)] \quad (5.5)$$

5.1.3 Derivation of the Equation for the Surface Area of Monomer Droplets.

Two simplifying assumptions are adopted for this purpose:

(1) The Sauter Mean diameter of monomer droplets is taken for calculating their surface area at any given moment.

$$\bar{d}_s = \frac{\sum n_i d_i^3}{\sum n_i d_i^2} \quad (5.6)$$

(2) The number of monomer droplets, N_d , remains constant throughout Stage I and Stage II.

Based on these assumptions and defining V_d^0 as the initial volume of monomer droplets per cc of water, $r_d(\tau)$ as the radius of monomer droplets at time τ , $V_p(\tau)$ as the volume of particles per cc of water at time τ , d_{sw} as the density of particles swollen by monomer and d_m as the density of monomer, the mass balance over the monomer at time τ can be expressed as

$$V_d^0 d_m = \frac{4\pi}{3} (r_d(\tau))^3 N_d d_m + V_p(\tau) d_{sw} \quad (5.7)$$

$$r_d(\tau) = \left(\frac{3}{4\pi N_d} \right)^{1/3} \left(V_d^0 - \frac{d_{sw}}{d_m} V_p(\tau) \right)^{1/3}$$

$$A_d(\tau) = 4\pi (r_d(\tau))^2 N_d =$$

$$[3(4\pi N_d)^{1/2} V_d^0 - 3(4\pi N_d)^{1/2} \frac{d_{sw}}{d_m} V_p(\tau)]^{2/3}$$

$$\text{Let } B_2 = 3(4\pi N_d)^{1/2} V_d^0$$

$$B_3 = 3(4\pi N_d)^{1/2} (d_{sw}/d_m)$$

$$\text{So } A_d(\tau) = (B_2 - B_3 V_p(\tau))^{2/3} \quad (5.8)$$

Substituting equation(5.8) into equation (5.5), we obtain:

$$\frac{dN_p(\tau)}{d\tau} = \frac{R}{S} \{s - A_p(\tau) - (B_2 - B_3 V_p(\tau))^{2/3}\} \quad (5.9)$$

5.1.4 Estimating the Parameters of Monomer Droplets.

If A_d^0 and D_d^0 are the initial surface area per cubic centimeter of water and the initial Sauter diameter of monomer droplets, respectively, then

$$A_d^0 = 6V_d^0/D_d^0 \quad (5.10)$$

$$N_d = (6/\pi) \{V_d^0/(D_d^0)^3\} \quad (5.11)$$

The initial volume of monomer droplets, V_d^0 , can be obtained from the initial charge. The initial droplet diameter, D_d^0 , can be calculated by using Merry's empirical formula (17) for an unbaffled reactor:

$$D_d^0 = D_d^i (N/N_i)^{-1.08} (H/H_i)^{-0.185} \quad (5.12)$$

where N and H are the impeller speed and impeller diameter used in the experiment, respectively, and N_i and H_i are the impeller speed and impeller diameter used in the dispersion test, respectively. D_d^i is the Sauter mean diameter of monomer droplets which had been measured by use of a Coulter Counter in the dispersion test.

Use of this formula assumes linearity between Sauter mean droplet diameter and the term $N^{1.08} H^{0.185}$ for the system under study. Preliminary dispersion tests in the presence of sodium lauryl sulphate in concentrations in excess of the c.m.c. were seen to display such linearity.

For a baffled reactor, the empirical formula, the derivation for which is presented in Section VI, can be used.

$$D_d^0 = 2.42 S_o^{0.013} N^{-1.86} \quad (5.13)$$

Where S_0 is the total soap concentration gram /dm³ of water.

5.1.5 Derivation of the Equation for Estimating the Surface Area of Particles.

Firstly, it is necessary to find the relationship between the time and the radius of the particles. For a single growing particle, the rate of volume increase can be described by the following equation:

$$\frac{4\pi}{3} \frac{dr_p^3}{dt} = \frac{K_p}{N_A} \frac{d_m}{d_p} \frac{\phi_m}{1-\phi_m}$$

where K_p is the rate constant for polymer propagation

d_p is the density of the polymer

ϕ_m is the monomer volume fraction in the particles.

$$\text{Let } K = \frac{3}{4\pi} \cdot \frac{K_p}{N_A} \cdot \frac{d_m}{d_p} \cdot \frac{\phi_m}{1-\phi_m} \quad (5.14)$$

$$\text{So } \frac{dr_p^3}{dt} = K \quad (5.15)$$

If this particle is formed at time τ , then $r_p=0$ at time τ and $r_p = r_p$ at time t . Hence, the following integration can be obtained.

$$\int_0^{r_p} dr_p^3 = K \int_{\tau}^t dt$$

$$r_p^3 = K(t-\tau) \quad (5.16)$$

$$r_p^2 = K^{2/3}(t-\tau)^{2/3} \quad (5.17)$$

Where $(t-\tau)$ is the lifetime of the growing particle from its generation to time t .

The number of polymer particles which are formed during the interval from τ to $(\tau+d\tau)$ is denoted by $dN_p(\tau)$. Each of these particles at time t will be of the radius of r_p and surface area of $4\pi r_p^2 = 4\pi K^{2/3}(t-\tau)^{2/3}$. So at time t , the surface area of all the particles which have been formed in the interval from τ to $(\tau+d\tau)$ in one cc of water can be written as:

$$dA_p(t) = 4\pi K^{2/3}(t-\tau)^{2/3}dN_p(\tau) \quad (5.18)$$

where the $dA_p(t)$ is the increment of total surface area of the particles per cc of water at time t owing to the nucleation of $dN_p(\tau)$ particles from time τ to $(\tau+d\tau)$.

Based on equation (5.9) and (5.18), we obtain:

$$dA_p(t) = 4\pi K^{2/3} \frac{R}{S} (t-\tau)^{2/3} [S-A_p(\tau) - (B_2 - B_3 V_p(\tau))^{2/3}] d\tau \quad (5.19)$$

Let $B_1 = 4\pi K^{2/3} (R/S)$ and integrate equation (5.19) over the range from time $\tau=0$ to $\tau=t$, we obtain

$$A_p(t) = B_1 \int_0^t (t-\tau)^{2/3} [S-A_p(\tau) - (B_2 - B_3 V_p(\tau))^{2/3}] d\tau \quad (5.20)$$

According to Simpson's rule

$$F(a) - F(b) = \int_b^a f(x) dx = \frac{a-b}{6} [f(a) + 4f(\frac{a+b}{2}) + f(b)] \quad (5.21)$$

To use equation 5.21 to estimating equation 5.20 we set $a=t$, $b=0$, $x=\tau$, $F(a)=A_p(t)$, $F(b)=0$, $f(x)=f(\tau)=B_1(t-\tau)^{2/3} [S-A_p(\tau) - (B_2 - B_3 V_p(\tau))^{2/3}]$, $f(a)=f(t)=0$, $f(b)=f(0)=B_1(S-A_0)^{2/3}$, $f(\frac{a+b}{2})=$

$$f\left(\frac{t}{2}\right) = B_1 \left[S - A_p\left(\frac{t}{2}\right) - (B_2 - B_3 V_p\left(\frac{t}{2}\right))^{2/3} \right] \left(\frac{t}{2}\right)^{2/3}.$$

Substituting these into equations (5.21), the following formula can be obtained:

$$A_p(t) = \frac{B_1}{6} t^{5/3} \left[3.52S - A_d^0 - 2.52A_p\left(\frac{t}{2}\right) - 2.52(B_2 - B_3 V_p\left(\frac{t}{2}\right))^{2/3} \right]$$

Let $B_4 = 3.52S - A_d^0$, the above equation becomes

$$A_p(t) = \frac{B_1}{6} t^{5/3} \left[B_4 - 2.52A_p\left(\frac{t}{2}\right) - 2.52(B_2 - B_3 V_p\left(\frac{t}{2}\right))^{2/3} \right] \quad (5.22)$$

When time t tends to zero, the following equation is used for calculating the surface area of polymer particles approximately.

$$A_p(t) = 0.587B_1(S - A_d^0)t^{5/3} \quad (5.23)$$

5.1.6 Derivation of Equation for Estimating the Volume of Polymer Particles.

For one single particle generated at time τ , in terms of equation (5.16), the volume at time t should be $(4\pi/3)r_p^3 = (4\pi/3)K(t-\tau)$.

For $dN_p(\tau)$ particles generated during the interval from τ to $(\tau+d\tau)$, the volume at time t should be

$$dV_p(t) = \frac{4\pi}{3} K(t-\tau) dN_p(\tau)$$

From equation (5.9), it becomes

$$dV_p(t) = \frac{4\pi}{3} K \frac{R}{S} (t-\tau) \left[S - A_p(\tau) - (B_2 - B_3 V_p(\tau))^{2/3} \right] d\tau \quad (5.24)$$

Let $C_1 = (4\pi/3)K(R/s)$ and Integrate equation (5.24) over the range from $\tau=0$ to $\tau=t$, then

$$V_p(t) = C_1 \int_0^t (t-\tau) [S-A_p(\tau) - (B_2-B_3 V_p(\tau))^{2/3}] d\tau \quad (5.25)$$

Using the same method as that mentioned above, from equation (5.21) and (5.25), the following equation can be obtained

$$V_p(t) = \frac{C_1}{6} t^2 [3S-A_d^0 - 2A_p(\frac{t}{2}) - (B_2-B_3 V_p(\frac{t}{2}))^{2/3}]$$

Let $C_2 = 3S-A_d^0$, then the above equation becomes

$$V_p(t) = \frac{C_1}{6} t^2 [C_2 - 2A_p(\frac{t}{2}) - 2(B_2-B_3 V_p(\frac{t}{2}))^{2/3}] \quad (5.26)$$

When the time t tends to zero, the following equation is used for calculating the particle volume, $V_p(t)$, approximately

$$V_p(t) = \frac{C_1}{2} t^2 (S-A_d^0) \quad (5.27)$$

5.1.7 Derivation of the Equation for Estimating the Fractional Monomer Conversion.

The relationship between fractional monomer conversion, $X_p(t)$, and the volume of particles per cc of water, $V_p(t)$, at a time t can be written as

$$X_p(t) = V_p(t) (1-\phi_m) \frac{d_p}{M_0} \quad (5.28)$$

Where M_0 is the amount of monomer charged initially.

Substituting equation (5.26) into equation (5.28), we get

$$X_p(t) = \frac{C_1 d_p (1 - \phi_m)}{6M_0} t^2 [C_2 - 2A_p(\frac{t}{2}) - 2(B_2 - B_3 V_p(\frac{t}{2}))^{2/3}]$$

Let $D_1 = C_1 d_p (1 - \phi_m) / 6M_0$, then above equation becomes

$$X_p(t) = D_1 t^2 [C_2 - 2A_p(\frac{t}{2}) - 2(B_2 - B_3 V_p(\frac{t}{2}))^{2/3}] \quad (5.29)$$

5.1.8 Derivation of the Equation for Estimating the Number of Particles

Integrating equation 5.9 over the range from time $\tau=0$ to $\tau=t$

$$N_p(t) = \frac{R}{S} \int_0^t [S - A_p(\tau) - (B_2 - B_3 V_p(\tau))^{2/3}] d\tau \quad (5.30)$$

According to equation (5.21) and (5.30), we obtain the formula as follows

$$N_p(t) = \frac{R}{6S} t [6S - A_d^0 - A_p(t) - (B_2 - B_3 V_p(t))^{2/3} - 4A_p(\frac{t}{2}) - 4(B_2 - B_3 V_p(\frac{t}{2}))^{2/3}]$$

Let $Z_1 = R/6S$ and $Z_2 = 6S - A_d^0$, then

$$N_p(t) = Z_1 t [Z_2 - A_p(t) - (B_2 - B_3 V_p(t))^{2/3} - 4A_p(\frac{t}{2}) - 4(B_2 - B_3 V_p(\frac{t}{2}))^{2/3}] \quad (5.31)$$

5.2 Setting up the Model for Stage II.

The following equation is used for calculating the conversion rate in Stage II

$$\frac{dx_p}{dt} = \frac{K_p}{N_A} d_m N_p \phi_m I \frac{1}{M_0} \quad (5.32)$$

where I is the average number of radicals in one particle.

In Stage II, there is good evidence that the ratio of monomer to polymer in the particle, ϕ_m , remain constant. The number of particles per cc water, N_p , also remains a constant as particle nucleation has

stopped by the end of Stage I and the value may be calculated using the model proposed above.

In the Smith-Ewart model, the average number of radicals in one particle, I , is considered equal to $1/2$. This may be true if the particles are infinitely small. In that case, the diffusion path for radicals is so short that on entry of a second radical into an active particle termination is instantaneous. However, as is well known, the concentration of macromolecules is very high in the monomer swollen particles and the viscosity inside is relatively large. Consequently, the termination process is controlled by diffusion. When a radical enters into an active particle if the particle is large as in the latter half of Stage II, then the collision between two radicals is not instantaneous. In this case, two or more radicals may co-exist in the same particle for some time. As a result, the parameter I is greater than $1/2$ and the larger the particles, the greater the value of I will be. In our case, we are dealing with rather low soap concentrations, thus the particle size is much larger than in the normal case and therefore we must take this 'volumetric' effect into account.

Now the question is how to find the parameter I at a given conversion. Gardon^[11,12] has established a mathematical model for this purpose based on the non-steady state assumption. Here we use a similar method for solving this problem.

To simplify, an assumption of all the particles having the same size at a given time during Stage II is used.

If i denotes the number of radicals in a particle, f_i the number fraction of the particles each of which contains i radicals, \bar{V} the average

volume of a particle, a the average surface area of a particle and K_0 the radical desorption rate constant, thus the non-steady state population balance of particles in one cc of water can be described as follows

$$\frac{df_i}{dt} = \frac{R}{N_p} (f_{i-1} - f_i) + \frac{K_0 a}{\bar{V}} [f_{i+1}(i+1) - f_i i] + \frac{K_t}{N_A \bar{V}} [f_{i+2}(i+2)(i+1) - f_i i(i-1)] \quad (5.33)$$

Divide equation (5.33) by equation (5.32) and let

$$G_1 = \frac{R M_0 N_A}{k_p N_p^2 d_m \phi_m}$$

$$G_2 = \left(\frac{K_0}{K_p}\right) \pi^{1/3} N_A (6 M_0 / N_p)^{2/3} (d_p^{1/3} / d_m) (1 - \phi_m)^{1/3} / \phi_m$$

$$G_3 = (K_t / K_p) (d_p / d_m) (1 - \phi_m) / \phi_m$$

the following set of equations can be obtained

$$\frac{df_i}{dx_p} = \frac{G_1}{I} (f_{i-1} - f_i) + \frac{G_2}{x_p^{1/3} I} [f_{i+1}(i+1) - f_i i]$$

$$+ \frac{G_3}{x_p I} [f_{i+2}(i+2)(i+1) - f_i i(i-1)] \quad (5.34)$$

$$\sum f_i = 1 \quad (5.35)$$

$$I = \sum i f_i \quad (5.36)$$

Fortunately, the ratio of polymer to monomer in particles is a constant during Stage II and thus the diffusional resistance does not change with conversion, i.e. both the termination rate constant, K_t , and the value of G_3 are conversion independent throughout Stage II. The value of K_t in Stage II should be equal to that in bulk polymerization at the same conversion as at the end of Stage II, $X_{p,I-II}$, in emulsion

polymerization. It is to be calculated using the following empirical formula which is formulated in Section VI.

$$K_t = \exp(A_1 + A_2 X_{p,II-III} + A_3 X_{p,II-III}^2 + A_4 X_{p,II-III}^3 + A_5 X_{p,II-III}^4) \quad (5.37)$$

where $X_{p,II-III}$ is the functional monomer conversion at the end of Stage II. A_1, A_2, A_3, A_4 and A_5 are constants.

K_{t0} = the termination rate constant in pure styrene.

T = the absolute temperature.

Thus, a set of the simultaneous equations (5.34), (5.35) and (5.36) which consists of $(i+2)$ equations has been set up. As we know, the duration of Stage I is rather short. Therefore, the particle size is relatively small at the end of Stage I and at this point the termination process might be considered as virtually instantaneous. Thus all of f_i in which $i \geq 2$ would be zero and the value of I tends to $\frac{1}{2}$. So we would choose the threshold between Stage I and Stage II as a starting point. In this case, the initial conditions for solving the above set of equations would be $x_p = X_{p,I-II}, f_0 = 0.5, f_1 = 0.5, I = 0.5, f_2 = f_3 = f_4 = \dots = 0$. The value of I is determined by solving this set of equations at various conversions and the relationship between t and X_p can be found using equation (5.32).

5.3 Setting up the Model for Stage III

In Stage III, it is found that the autoacceleration effect of the conversion rate becomes important. This phenomenon is known as the Trommsdoff effect or gel-effect, and is extremely significant in emulsion polymerization modelling. If it is not taken into account, a significant deviation of the predicted results from the experimental results will be encountered in Stage III of the reaction. Friis et al carried out experimental emulsion and bulk polymerizations of polymethylmethacrylate (7, 9) and polyvinyl acetate (7, 10) and by using a steady state model they were able to model the gel-effect. They also compared their model with experimental data for the emulsion polymerization of styrene. The relationship which they used to relate the termination constant to monomer conversion for polystyrene was based on Hui's work (12) on the thermal polymerization of styrene in bulk which was carried out over the temperature range of 100 - 200°C. It was found, at least at 50°C, that this relationship overestimated the termination rate constant when it is used for calculating the emulsion polymerization particularly at high levels of conversion.

Gardon (13,14) developed a mathematical model based on a non-steady state assumption for Stage II. Unfortunately, it was not extended to Stage III because the relationship between the termination rate constant and the monomer concentration in the particles was not known.

In this project, the dependence of the termination rate constant upon monomer conversion has been generated using experimental suspension polymerization data (see Section VI), a non-steady state mathematical model for Stage III has been developed. When it is combined with the model developed for Stages I and II above, a mathematical model covering the whole conversion range of an emulsion polymerization is the result.

In Stage III, the ratio of monomer to polymer in the particles is no longer a constant. As polymerization proceeds, the volume fraction of monomer, $\phi(X_p)$, will increase gradually with the monomer conversion, X_p .

$$\phi(X_p) = \frac{1-X_p}{(1-X_p) + (d_m/d_p)X_p} \quad (5-38)$$

and thus the value of K_t will also decrease with X_p . This may be described by the following equation which is developed in section VI.

$$K_t = \exp (A_1 + A_2X_p + A_3X_p^2 + A_4X_p^3 + A_5X_p^4) \quad (5.39)$$

The model for Stage III can be presented as follows:

$$I \frac{df_i}{dX_p} = H_1 J_1(X_p) (f_{i-1} - f_i) + H_2 J_2(X_p) \{f_{i+1}(i+1) - f_i i\} + H_3 J_3(X_p) \{f_{i+2}(i+2)(i+1) - f_i i(i-1)\} \quad (5-40)$$

$$\Sigma f_i = 1 \quad (5-41)$$

$$\Sigma f_i i = I \quad (5-42)$$

where

$$H_1 = RN_{A O}^M / (K_p N_p^2 d_m)$$

$$H_2 = (K_O / K_p) (\pi^{1/3} N_A) (6M_O / N_p)^{2/3} (d_p^{1/3} / d_m)$$

$$H_3 = 1/K_p$$

$$J_1(X_p) = 1 - d_m X_p / d_p (1 - X_p)$$

$$J_2(X_p) = (d_m / d_p)^{1/3} \{ (1 - X_p) + d_m X_p / d_p \}^{2/3} / (1 - X_p)$$

$$J_3(X_p) = \frac{1}{1 - X_p} \exp(A_1 + A_2 X_p + A_3 X_p^2 + A_4 X_p^3 + A_5 X_p^4)$$

The initial condition is

$$X_p = X_{p, II-III}, \quad I = I_{II-III},$$

$$f_i = f_{i, II-III}, \quad (i=0, 1, 2, 3, \dots)$$

$$\text{at } t = t_{II-III}$$

In the computation, the values of f_i and I can be found by solving equations (5-40), (5-41) and (5-42) at various conversions and the corresponding dependence of X_p upon t may be determined by solving the following equation:

$$\frac{dX_p}{dt} = \frac{K_p d_m}{N_A M_O} N_p I \phi(X_p)$$

SECTION VI

RESULTS AND DISCUSSION

- 6.1 Determination of the Dependence of Termination
 Rate Constant on Monomer Conversion
- 6.2 Formulation of Dispersion Data for the Baffled
 Reactor
- 6.3 Scope of the Model
 - 6.3.1 Predictions of the model for Particle
 nucleation
 - 6.3.2 Conversion-versus-time plots for the unbaffled
 reactor
 - 6.3.3 The effect of stirring rate
 - 6.3.4 The gel-effect
 - 6.3.5 The Baffled reactor

6.1 Determination of the Dependence of Termination Rate Constant on Monomer Conversion

There is clear evidence⁽³⁸⁾ that the termination rate constant, K_t , for styrene polymerization is extremely large, and is about 5 orders larger than the propagation rate constant, K_p . The termination rate is therefore diffusion controlled even for the smallest radicals even in the early stage of reaction. As polymerization proceeds, the polymer chains entangle with each other and this causes the monomer-polymer solution to increase in viscosity and therefore the translational mobility of the radical chains will be decreased. Thus, K_t decreases dramatically with monomer conversion. Furthermore the reduction of K_t depends only upon the extent of this entanglement of the polymer chains and upon the environmental conditions in the polymerization loci regardless of whether the reaction is occurring in bulk, in the droplets of suspension polymerization or in the polymer particles of emulsion polymerization. As Friis pointed out⁽¹⁰⁾, in emulsion polymerization a single polymer particle can be regarded as a tiny locus of bulk polymerisation with intermittent initiation. A decrease in the termination rate which is observed in bulk(or suspension) polymerisation should therefore also be observed in a single polymer particle in emulsion polymerisation. Thus it seems reasonable that the relationship between K_t and monomer conversion obtained from either bulk or suspension polymerisation may be used for the emulsion polymerisation model.

According to Hui's theory, the dependence of K_t upon monomer conversion may be described by the following formula.

$$\frac{K_t}{K_p^2} = \frac{K_{t0}}{K_{p0}^2} \exp (A_2 X_p + A_3 X_p^2 + A_4 X_p^3 + A_5 X_p^4) \quad (6-1)$$

In the case of the reaction temperature being above the glass transition point, T_g , monomer molecules or chain segments can move so freely that the propagation reaction is not controlled by diffusion. Therefore, the value of K_p always maintains a fixed value as long as the temperature is not less than T_g . For polymerization of styrene if the monomer concentration is more than 2.6%, T_g will be lower than 50°C . In other words, K_p remains a constant at 50°C within the range of monomer conversion from zero to 97.4%. Consequently for the normal case, equation (6-1) becomes:

$$K_t = \exp(A_1 + A_2 X_p + A_3 X_p^2 + A_4 X_p^3 + A_5 X_p^4) \quad (6-2)$$

For bulk and suspension polymerization, the propagation rate may be described as follows⁽⁴⁰⁾:

$$\frac{dX_p}{dt} = K_p (1 - X_p) \left(\frac{K_i f\{I\}}{K_t} \right)^{\frac{1}{2}} \quad (6-3)$$

where $K_i f\{I\}$ is the decomposition rate of the initiator, which can be regarded as a constant during the reaction. This approach has been made by a number of authors previously⁽¹³⁾.

Figure 6.1 shows the interdependence between conversion and time obtained from the experimental suspension polymerization of styrene at 50°C.

For polymerization of styrene K_p is set at $1.27 \times 10^7 \text{ cm}^3/\text{mole} \cdot \text{min}^{(32)}$, and $K_i f$ at $1.782 \times 10^{-4} \text{ l/min}^{(39)}$. From fig 6.1 a series of values of (dX_p/dt) may be found using numerical differentiation, then the value of A_1 , A_2 , A_3 , A_4 and A_5 may be estimated by means of multiple regression. The computer programmes for this calculation^{ion} are shown in Appendix II.

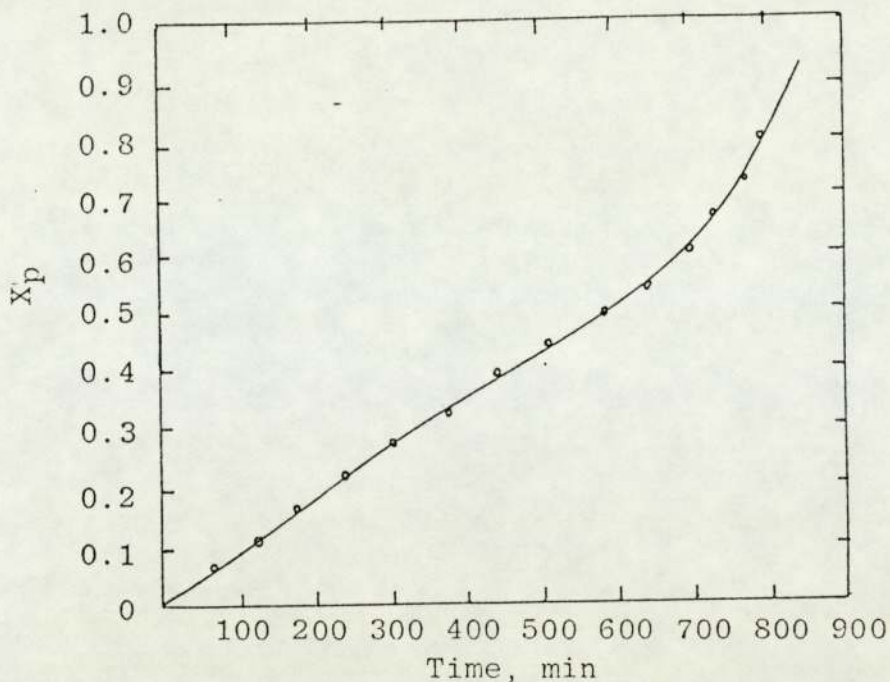


Fig. 6.1 Dependence of conversion upon the time for suspension polymerization of styrene at 50°C:
 {AlBN} = 0.216 mole/dm³ monomer, the phase ratio:
 water/monomer = 6 (volume), stabiliser (polyvinyl alcohol)
 concentration: 2.6% (in water)

The values obtained are presented below:

$$A_1 = 29.5873$$

$$A_2 = -7.4332$$

$$A_3 = 45.8577$$

$$A_4 = -95.9184$$

$$A_5 = 47.4095$$

When $X_p = 0$, $K_t = 7.073 \times 10^{12} \text{ cm}^3/\text{mole} \cdot \text{min}$. This value agrees with that in the literature (Olive⁽⁴²⁾, $6.9 \times 10^{12} \text{ cm}^3/\text{mole} \cdot \text{min}$).

Figure 6.2 shows the dependence of K_t upon conversion for suspension polymerization of styrene at 50°C. It may be seen that in the early stages K_t changes only slightly, but in the later stages, the decrease in K_t with increasing conversion is dramatic.

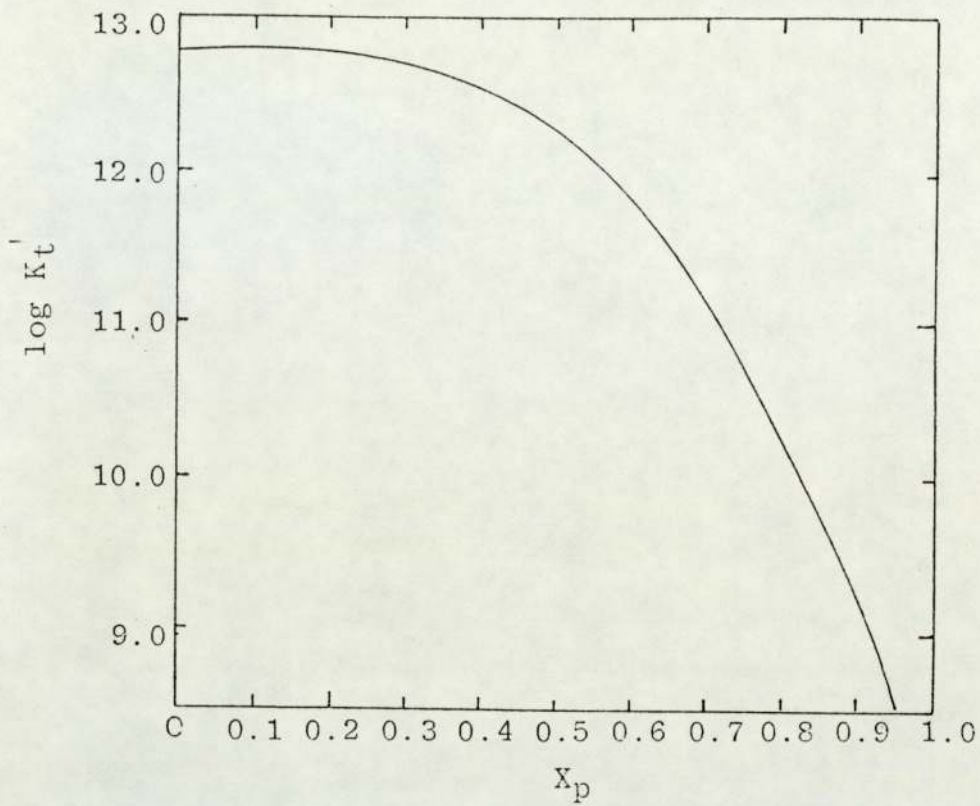


Figure 6.2 Dependence of termination rate constant upon conversion for suspension polymerization of styrene at 50°C.

6.2 Formulation of Dispersion Data for the Baffled Reactor.

To prove the validity of the model proposed above, for baffled reactors, the interdependence of the average initial diameter of monomer droplets, D_d^0 (micron), total soap concentration, S_0 (gram/Dm³ water), and impeller speed (r.p.m.) is needed in the computation. In this section it is shown how this relationship was derived.

The flow pattern of the liquid in a baffled reactor is far different from that in unbaffled reactors; the velocity distribution in the former is more homogeneous than in the latter⁽¹⁵⁾. Differences in the dispersion characteristics between baffled and unbaffled reactors would be expected and, in fact, experiment has shown that the extent of monomer dispersion in the baffled reactor is much greater than that in the unbaffled one. Vermeulen et al⁽¹⁶⁾ presented a correlation from their experimental data for baffled reactors, in which the Sauter mean diameter of the droplets is shown to be directly proportional to impeller speed raised to a power of -1.2. Unfortunately, their formula is only valid for a system in the absence of an emulsifier. Merry⁽¹⁷⁾ obtained an empirical formula for the dispersion of styrene in an emulsifier solution in water, in which the mean diameter of monomer droplets is shown to be proportional to the impeller speed raised to the power of -1.08. This formula, however, was developed for unbaffled reactors. Harada et al⁽³²⁾ proposed a

correlation for baffled reactors in which the average diameter of the dispersed monomer droplets was shown to be proportional to the impeller speed raised to the power of -0.75 and to the emulsifier concentration raised to the power -1.5. In this formula, however the lower limit of the emulsifier concentration is 3.13 gram/dm^3 water, which is beyond the emulsifier concentration range that was dealt with in this project. Therefore, to model emulsion polymerization in a baffled reactor for the case of low soap concentration a correlation is needed relating the average initial monomer droplet diameter to the impeller speed and to soap concentration.

To obtain this relationship three batches of styrene/water/sodium lauryl sulphate were tested. The emulsifier concentrations for the three batches were assigned 3.75, 2.75 and $1.75 \text{ gram per cm}^3$ of water. Five impeller speeds were set for each batch, namely, 450, 550, 650, 750 and 850 r.p.m. The average droplet diameter was obtained using the microphotographic technique described in Section IV. The results for each sample are listed in Table 6-1. The computed results from that data in Table 6-1 are listed in Table 6-2. The computer programme for this computation is shown in Appendix III (1).

Table 6.1 The experimental data of dispersion test.

diameter of particle cm	number of droplets														
	S.= 3.75					S.= 2.75					S.= 1.75				
	• Impeller Speed														
	450	550	650	750	850	450	550	650	750	850	450	550	650	750	850
2	99	93	51	-	66	29	61	25	42	14	125	20	60	41	56
3	111	114	37	78	45	23	53	37	52	58	91	36	61	33	39
4	103	91	33	27	21	11	27	21	18	22	26	9	77	24	33
5	112	70	22	22	23	7	27	23	20	26	19	5	29	12	29
6	64	42	25	10	10	7	16	11	11	17	17	10	24	23	15
7	50	28	23	12	6	9	13	8	12	17	10	3	16	11	14
8	48	26	9	7	5	6	3	9	15	9	5	4	12	5	6
9	19	17	7	2	3	2	5	5	3	4	8	4	3	7	2
10	24	7	11	2	3	2	7	4	3	-	6	1	4	1	-
11	15	11	5	3	-	3	5	2	1	-	5	-	3	1	-
12	16	11	4	-	-	2	2	2	-	-	-	-	3	1	-
13	9	3	3	1	-	1	2	-	-	-	3	-	-	1	-
14	6	2	1	-	-	1	-	-	-	-	1	3	2	-	-
15	3	3	2	-	-	1	1	1	-	-	1	2	2	-	-
16	4	4	3	-	-	-	-	-	-	-	3	1	-	-	-
17	3	-	-	-	-	2	2	-	-	-	1	1	-	-	-
18	3	3	-	-	-	-	-	-	-	-	-	2	-	-	-
19	4	2	-	-	-	2	-	-	-	-	-	-	-	-	-
20	3	-	-	-	-	2	1	-	-	-	2	-	-	-	-
21	1	-	-	-	-	-	-	-	-	-	-	-	-	-	-
22	1	-	-	-	-	1	-	-	-	-	-	-	-	-	-
23	2	-	-	-	-	1	-	-	-	-	1	-	-	-	-
24	-	-	-	-	-	1	-	-	-	-	1	1	-	-	-
25	-	-	-	-	-	2	-	-	-	-	3	-	-	-	-
26	1	-	-	-	-	-	-	-	-	-	1	-	-	-	-
27	1	-	-	-	-	1	-	-	-	-	-	-	-	-	-
28	-	1	-	-	-	-	-	-	-	-	1	-	-	-	-
30	-	-	-	-	-	-	-	-	-	-	1	-	-	-	-
31	1	-	-	-	-	-	-	-	-	-	-	-	-	-	-
32	-	1	-	-	-	-	-	-	-	-	-	-	-	-	-
38	1	-	-	-	-	-	-	-	-	-	-	-	-	-	-
40	1	-	-	-	-	-	-	-	-	-	-	-	-	-	-
41	1	-	-	-	-	-	-	-	-	-	-	-	-	-	-
50	-	-	-	-	-	-	-	-	-	-	1	-	-	-	-
56	-	-	-	-	-	-	-	-	-	-	-	-	-	-	-

Table 6-2 Average diameter of monomer droplets computed from the data in Table 6-1 for the various emulsifier concentration and impeller speed.

S_o , g/cm ³ water	3.75	2.75	1.75
N, r.p.m.	D_d^o , micron		
450	29.63	27.83	34.64
550	18.35	14.92	21.07
650	17.94	12.20	11.94
750	10.59	10.43	11.04
850	9.34	9.60	8.88

In accordance with the data obtained above, the following empirical exponential correlation was fitted using a multiple regression method.

$$D_d^o = 2.42 S_o^{0.013} N^{-1.86} \quad (6-4)$$

The computer programme for this formulation is shown in Appendix III (2).

It may be seen from formula (6-4) that in a baffled reactor, impeller speed affects the values of the average diameter of the dispersed monomer droplets more seriously than in an unbaffled reactor.

6.3 Capabilities of the Model

To illustrate the capabilities of the model proposed above, more than 30 test runs were performed under various emulsifier concentrations, initiator concentrations and impeller speeds both in the baffled reactor and in the unbaffled reactor. The experimental results are shown in figures 6.3 to 6.12, in Table 6.3 to 6.6 and in Appendix IV and V.

In the computation, the following values of the constants for emulsion polymerization of styrene are used $K_p = 1.27 \times 10^7 \text{ cm}^3/\text{mole}\cdot\text{min}^{(32)}$, $K_{if} = 5.7 \times 10^{-5} \text{ l/min}^{(61)}$, $d_m = 0.879 \text{ g/cm}^3$, $d_p = 1.049 \text{ g/cm}^3$, $d_{sw} = 0.934 \text{ g/cm}^3$, $\phi_m = 0.605$, $A_s = 3.5 \times 10^{-15} \text{ cm}^2/\text{one molecule}^{(32)}$ and $\{S\}_{\text{cmc}} = 1.8382 \times 10^{-3} \text{ mole/Dm}^3 \text{ water}^{(6)}$.

The desorption of radicals from particles to the aqueous phase for emulsion polymerization of styrene is ignored because the solubility of styrene is relatively low so that their escape from the particles is insignificant. Thus K_0 is set equal to zero and so is the value of G_2 .

6.3.1 Predictions of the Model for Particle Nucleation

The accepted mechanism for emulsion polymerization assumes that the particles are initiated in micelles, thus the number of particles and the reaction rate at a given time are functions of the amount of micellar soap. Because some soap is adsorbed onto the surface of the

monomer droplets, the micellar soap will be reduced, accordingly the number of particles, the conversion rate, the size of particles and the duration and final conversion of Stage I vary with the degree of dispersion which in turn depends on the soap concentration and the impeller speed.

Figures 6.3 and 6.4 show the computed results of the conversion and the number of particles versus time in Stage I for polystyrene.

It can be found that the conversion rate, the particle nucleation rate, final conversion at the end of stage I and the number of particles decrease with decreasing soap concentration and increasing impeller speed along the conversion history of Stage I. It can also be seen that the duration of Stage I increases with soap concentration but is affected little by the impeller speed. This is perhaps because as the reaction proceeds, the monomer droplets would shrink slightly and some soap would be set free from the droplets, therefore the duration of particle nucleation is slightly postponed especially in the case of a high degree of dispersion.

Table 6.3 shows a comparison of the results obtained by experiment and the predictions both from the classical model and from the present model. It is found that under the various soap concentrations and impeller speeds, the

present model is in acceptable agreement with experimental data. Most importantly, under low soap conditions, the classical model deviates significantly from the experimental results owing to the fact that it does not allow for the soap adsorbed onto the surface of the monomer droplets and the critical micellar soap and the advantage of the present model is thus clearly demonstrated.

The computer programme for Smith-Ewart model is shown in Appendix IV. And the program simulating the present model for the unbaffled reactor is shown in Appendix V.

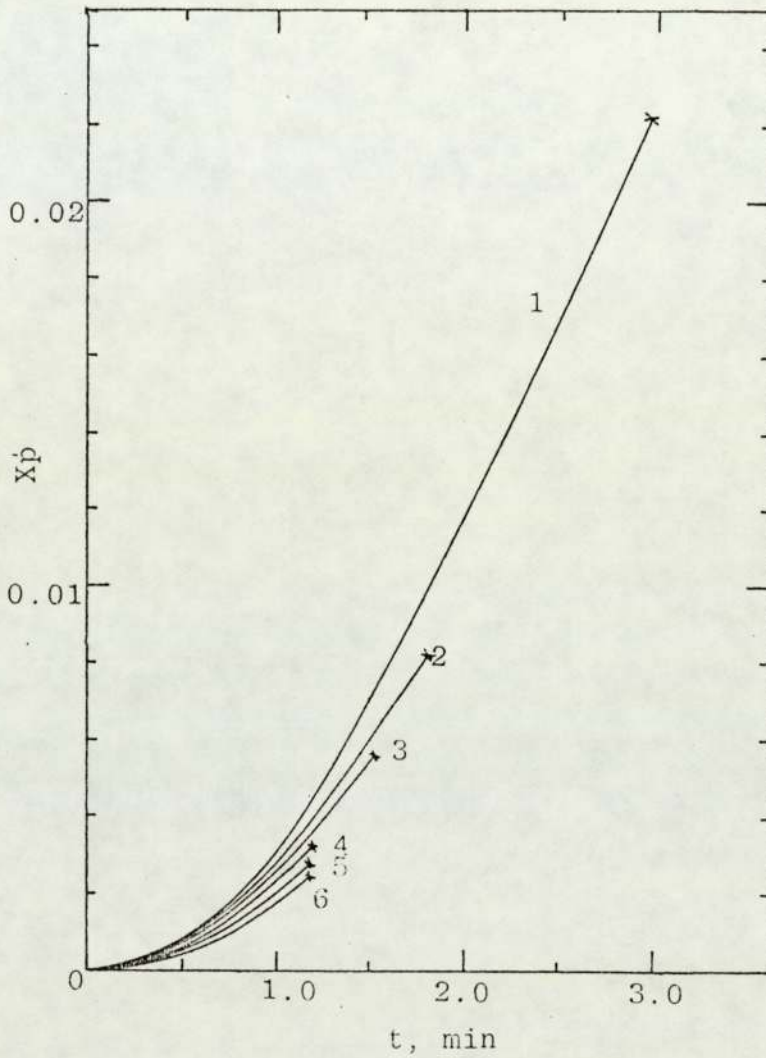


Figure 6.3 Conversion-vs-time plots computed according to the present model: $[I]=0.00463\text{mole/dm}^3\text{.water,}$

- (1) $S_0=5\text{g/dm}^3\text{,water, } N=410\text{ r.p.m.,}$
- (2) $S_0=2.5\text{g/dm}^3\text{.water, } N=410\text{ r.p.m.,}$
- (3) $S_0=2, I\text{g/dm}^3\text{.water, } N=410\text{ r.p.m.,}$
- (4) $S_0=1.5\text{g/dm}^3\text{.water, } N=410\text{ r.p.m.,}$
- (5) $S_0=1.5\text{g/dm}^3\text{.water, } N=600\text{ r.p.m.,}$
- (6) $S_0=1.5\text{g/dm}^3\text{.water, } N=800\text{ r.p.m.}$

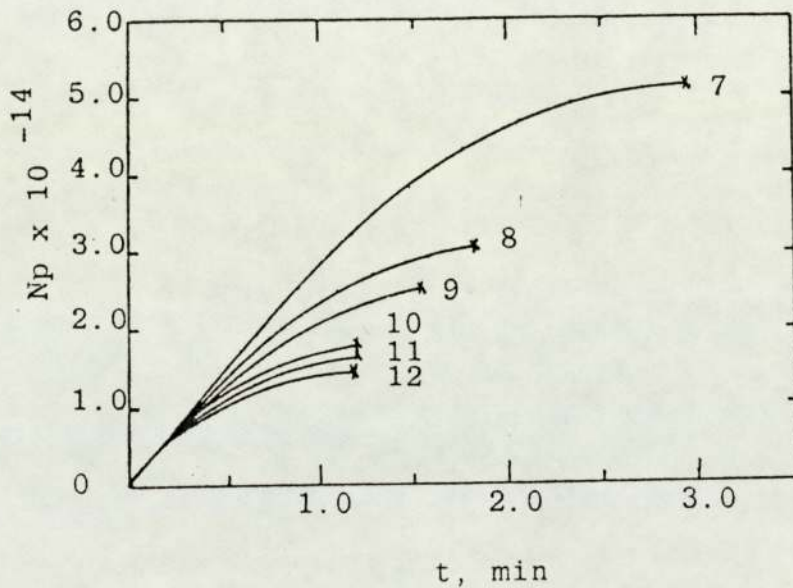


Figure 6.4 Number of particles-vs time plots computed according to the present model:

$[I] = 0.00463 \text{ mole/dm}^3$, water,

- (7) $S_o = 5.0 \text{ g/dm}^3$.water, $N = 410$ r.p.m.,
- (8) $S_o = 2.5 \text{ g/dm}^3$.water, $N = 410$ r.p.m.,
- (9) $S_o = 2.0 \text{ g/dm}^3$.water, $N = 410$ r.p.m.,
- (10) $S_o = 1.5 \text{ g/dm}^3$.water, $N = 410$ r.p.m.,
- (11) $S_o = 1.5 \text{ g/dm}^3$.water, $N = 600$ r.p.m.,
- (12) $S_o = 1.5 \text{ g/dm}^3$.water, $N = 800$ r.p.m.

Table 6.3 Final number and diameter of particles obtained by experiment and theory.

Total amount of soap g/dm^3 H_2O	Concen. of initiator g/dm^3 H_2O	Impeller speed rmp	Present Model		Experimental		Smith-Ewart Model	
			Number of particles $\times 10^{-14}$ parti. / cH_2O	Final diameter of parti. micron	Number of particles $\times 10^{-14}$ parti. / cH_2O	Final diameter of parti. micron	Number of particles $\times 10^{-14}$ parti. / cH_2O	Final diameter of parti. micron
* 7.50	2.50	410	8.085	0.1046	6.5313	0.1130	9.371	0.1023
* 3.75	2.50	410	5.552	0.1216	5.2070	0.1227	6.259	0.1169
* 2.25	2.50	410	3.607	0.1403	3.6040	0.1384	4.562	0.1298
5.00	1.25	500	5.031	0.1255	5.1834	0.1216	5.583	0.1204
2.50	1.25	410	3.034	0.1487	3.1218	0.1438	3.746	0.1386
2.00	1.25	410	2.483	0.1585	2.4514	0.1559	3.289	0.1446
1.50	1.25	410	1.809	0.1764	1.9514	0.1679	2.756	0.1532
1.50	1.25	600	1.647	0.1819	1.7215	0.1775	2.756	0.1532
1.50	1.25	800	1.484	0.1883	1.5312	0.1846	2.756	0.1532

* Raffled reactor

6.3.2 Conversion-versus-time plots for unbaffled reactor

Figures 6.5, 6.6, 6.7 and 6.8 show a comparison between the classical model, the present model and the experimental results of conversion against time and the effect of emulsifier concentration on the behaviour of emulsion polymerization reactors. If the soap level is high (Figure 6.5), the present model (Curve 14), the classical model (Curve 13) and experimental conversion-versus-time data are closer to each other compared with the case of low soap concentration. The difference between the classical model and the experimental data at this high soap level is well within the experimental error encountered and consequently, many authors simply neglected the effect of the emulsifier adsorbed on the surface of the monomer droplets. If the soap concentration is reduced, however, the fraction of the soap adsorbed on the monomer droplets increases and its effect is enhanced. As is shown in Figures 6.6, 6.7 and 6.8 the classical model deviates significantly from the experimental results but they are in good agreement with the present model which takes into account the soap adsorbed on the surface of monomer droplets.

The computer program for the classical model is shown in Appendix IV and the program simulating the present model is shown in Appendix V.

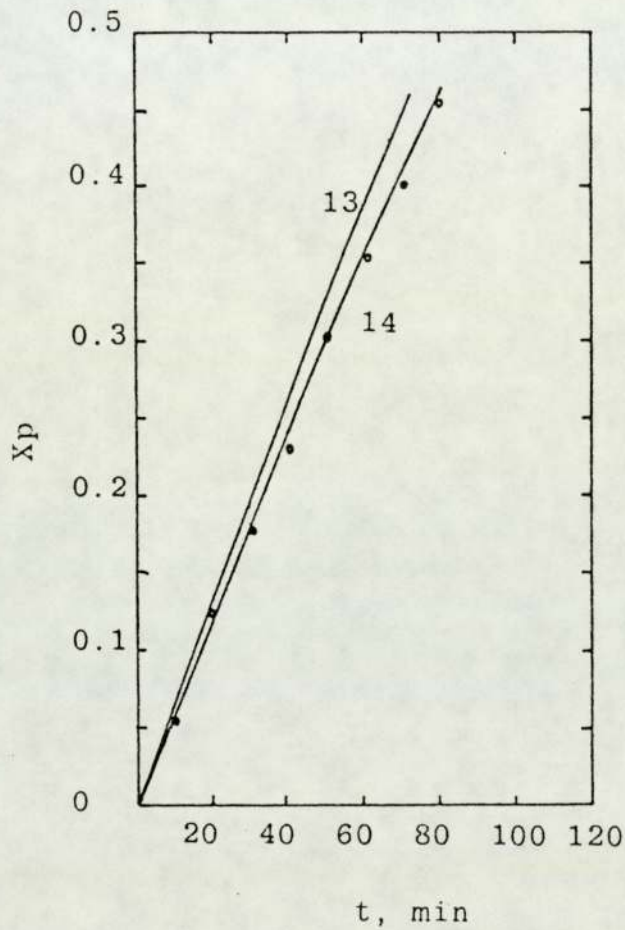


Figure 6.5 Comparison between theoretical and experimental conversion versus time plots : $S_0 = 5.0 \text{ g/dm}^3 \cdot \text{water}$, $\{I\} = 0.00463 \text{ mol/dm}^3 \cdot \text{water}$, $N = 410 \text{ r.p.m.}$ (13) Smith and Ewart model (14) present model, (.) experimental points.

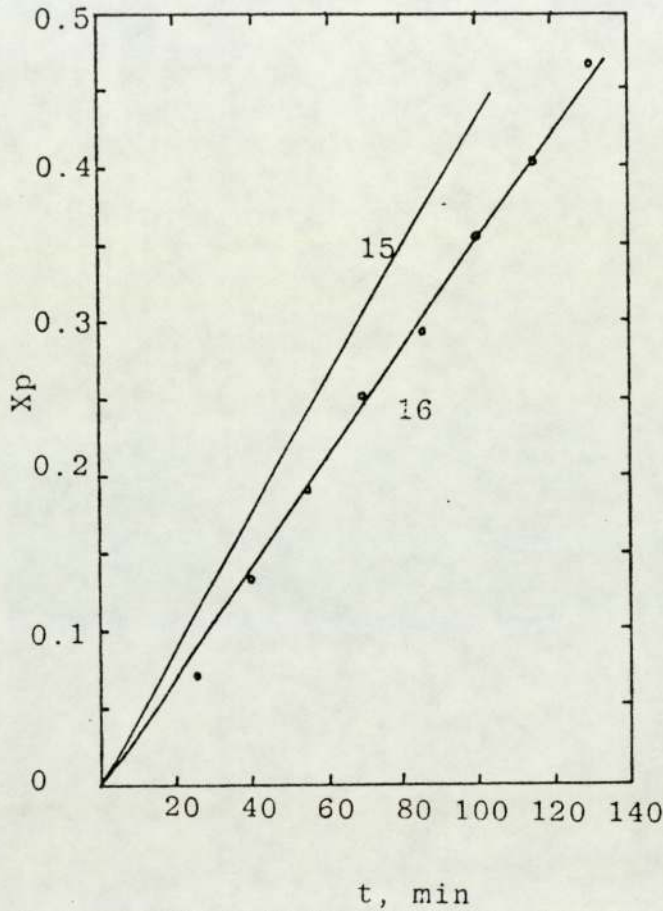


Figure 6.6 comparison between theoretical and experimental conversion versus time plots : $S_o = 2.5 \text{ g/dm}^3 \text{ water}$, $N=410 \text{ r.p.m.}$ $\{I\} = 0.00463 \text{ mol/dm}^3 \text{ water.}$; (15) Smith and Ewart model, (16) present model, (.) experimental points.

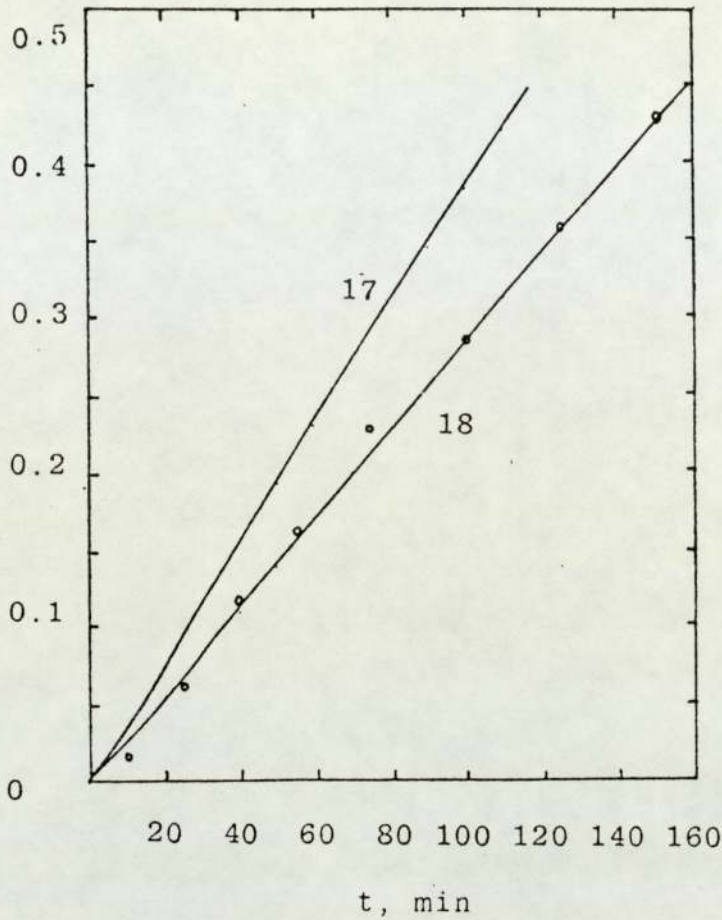


Figure 6.7 Comparison between theoretical and experimental conversion-vs-time plots: $N=410$ r.p.m., $S_0=2.0\text{g}/\text{dm}^3$.water, $[I]=0.00463$ mol/ dm^3 .water, (17) Smith Ewart model, (18) present model, experimental points

6.3.3 The effect of stirring rate

As has already been pointed out, violent agitation will result in a high degree of dispersion with the consequence that more soap will be adsorbed onto the monomer droplets and more micelles will be destroyed so that the final number of particles will be reduced, the size of particles will be increased and the conversion rate will be reduced. Figure 6.8 shows that under low soap concentrations the present model reflects dependence on impeller speeds and the predictions are in reasonable agreement with experimental results. It can be seen from Table 6.3 that under the same emulsifier and initiator concentration conditions, if the impeller speed increases from 410 r.p.m. to 800 r.p.m., then the number of particles will decrease from 1.809×10^{14} to 1.484×10^{14} while the final particle diameters will increase from 0.1764 micron to 0.1883 micron. These predictions of the present model are in excellent agreement with the experimental results.

It can be seen in Table 6.3 that the Smith-Ewart theory predicts that impeller speed has no effect on the number of particles and on the final particle diameter. If this were true for the system indicated, the number of particles should be 2.756×10^{14} and the final particle diameter should be 0.1532 micron. These values are in fact far from the true experimental values which are seen to be dependent on impeller speed. This dependence is clearly reflected in the computer predictions of the present model.

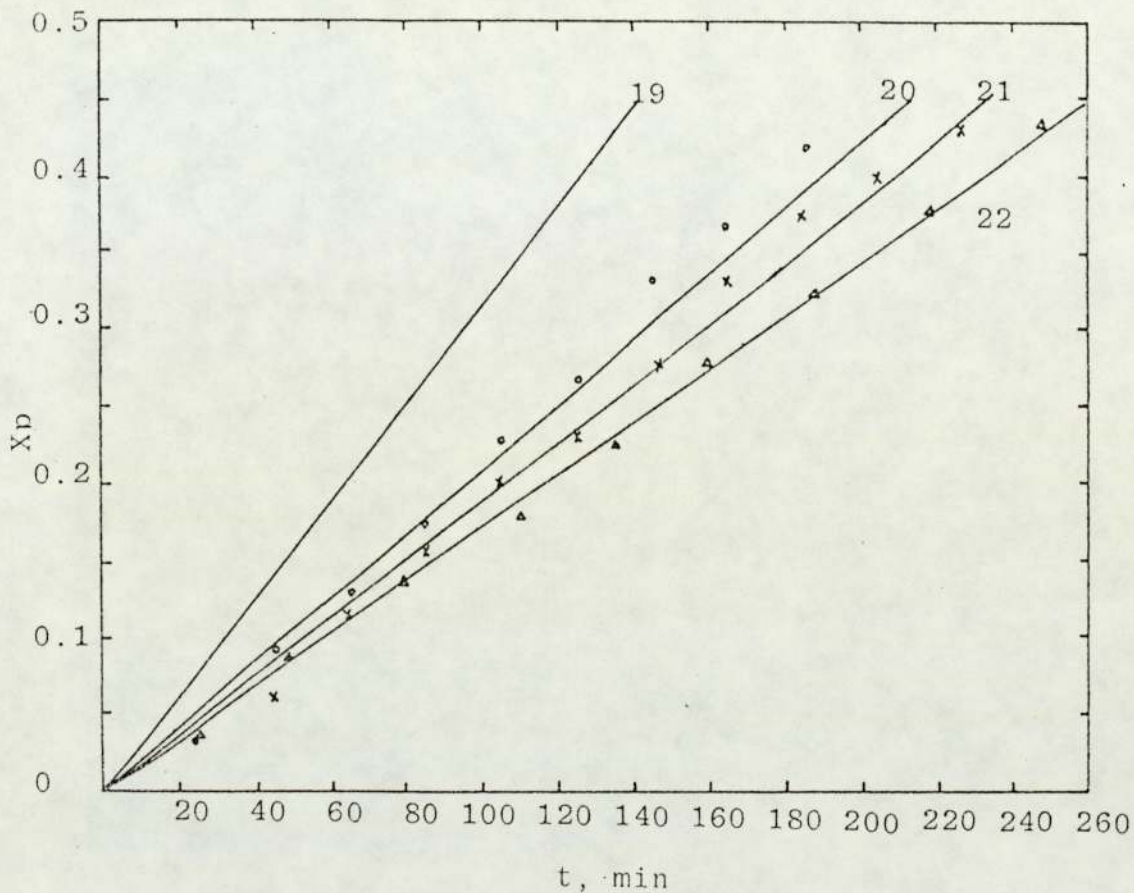


Figure 6.8 Comparison between theoretical and experimental conversion-vs-time plots: $S_0=1.5\text{g}/\text{dm}^3\text{.water}$, $[I]=0.00463\text{ mol}/\text{dm}^3\text{.water}$, (19) Smith-Ewart model, (20) present model, $N=410\text{ r.p.m.}$, (21) present model, $N=600\text{ r.p.m.}$, (22) present model, $N=800\text{ r.p.m.}$, "o" experimental, $N=410\text{ r.p.m.}$, "x" experimental, $N=600\text{ r.p.m.}$, "Δ" experimental, $N=800\text{ r.p.m.}$

6.3.4 The Gel-Effect

The predicted results from the classical model and the present model over the whole range of the monomer conversion and the corresponding experimental data are shown in Table 6.3 and Figure 6.9 to 6.11. The computer program for this calculation is shown in Appendix IV.

Table 6.3 shows predicted results from the present model for a typical case. It is clear that K_t will maintain a constant value when $X_p \leq 0.43$ because up to this point, which represents the end of Stage II, the ratio of monomer to polymer in the particles maintains a fixed value. During Stage II, however, the average number of radicals in one particle, I , slightly increases due to the particles increasing in size. When the conversion is beyond 0.43 i.e. Stage III, the value of K_t increases dramatically and the rate of increase in the value of I will accelerate owing to the gel-effect.

Figure 6.9 shows the distribution of radicals among particles at different monomer conversions for a single case. It indicates clearly that the distribution is broadened and the average number of radicals is increased along with increasing monomer conversion.

Figures 6.10 to 6.11 show conversion-versus-time plots computed by both the present model and the classical model and the experimental results. It may be seen that the

theoretical simulation is a far better prediction than the classical model in Stage I and Stage II. This is particularly evident at low initial soap concentrations. This improvement over the classical model comes from the fact that the present model has taken into consideration the emulsifier adsorbed onto the surface of monomer droplets. In Stage III, it is found that the present model (the solid lines) which allow for the gel-effect is in much better agreement with the experimental results (symbols) than the case which neglects this effect (the dashed lines). The validity of the present model is clearly demonstrated.

From Figure 6.10 and Figure 6.11, it can be seen that in Stage I and Stage II, the deviation of the experimental data and the present model from the classical model becomes more serious if the initial soap concentration is decreased. This is because the fraction of the emulsifier that is adsorbed onto the surface of monomer droplets increases with the reduction of emulsifier concentration at a given impeller speed. In other words, in these low initial soap conditions the adsorbed emulsifier will play a significant role in decreasing the number of particles and consequently in the polymerization rate.

From Figures 6.10 and 6.11 it may also be seen that the severity of the gel-effect increases as initial soap concentration decreases for a given impeller speed. There is no easily tested explanation for this but it might be

proposed that it may be associated with the observation that the radicals in the surface layer of the particles are terminated more readily than those in the body of the particles because the diffusion paths for radicals in the surface layer are short. When the initial soap concentration is low, fewer particles will be generated and thus the surface area of particles per cc of water will be smaller, and therefore fewer radicals will be able to take advantage of the fast termination zone.

Table 6.4 Interdependence between the conversion, the termination rate constant and the average number of radicals in one particle:

$S_0=2.25 \text{ g/dm}^3$ water, $R_0=2.5 \text{ g/dm}^3$ water, $N=410 \text{ r.p.m.}$

Reaction temperature: 50°C.

X	I	$K_t, \text{cm}^3/\text{mol min}$
0.10	0.500101	3.4340×10^{12}
0.20	0.500203	2.4340×10^{12}
0.30	0.500305	3.4340×10^{12}
0.40	0.500407	3.4340×10^{12}
0.43	0.500448	3.4340×10^{12}
0.50	0.500749	1.9687×10^{12}
0.60	0.502582	5.6610×10^{11}
0.70	0.514133	1.0089×10^{11}
0.80	0.599936	1.3133×10^{10}
0.85	0.758931	4.5729×10^9
0.90	1.081800	1.6483×10^9
0.95	1.608270	6.4814×10^8
0.97	1.871540	4.6323×10^8

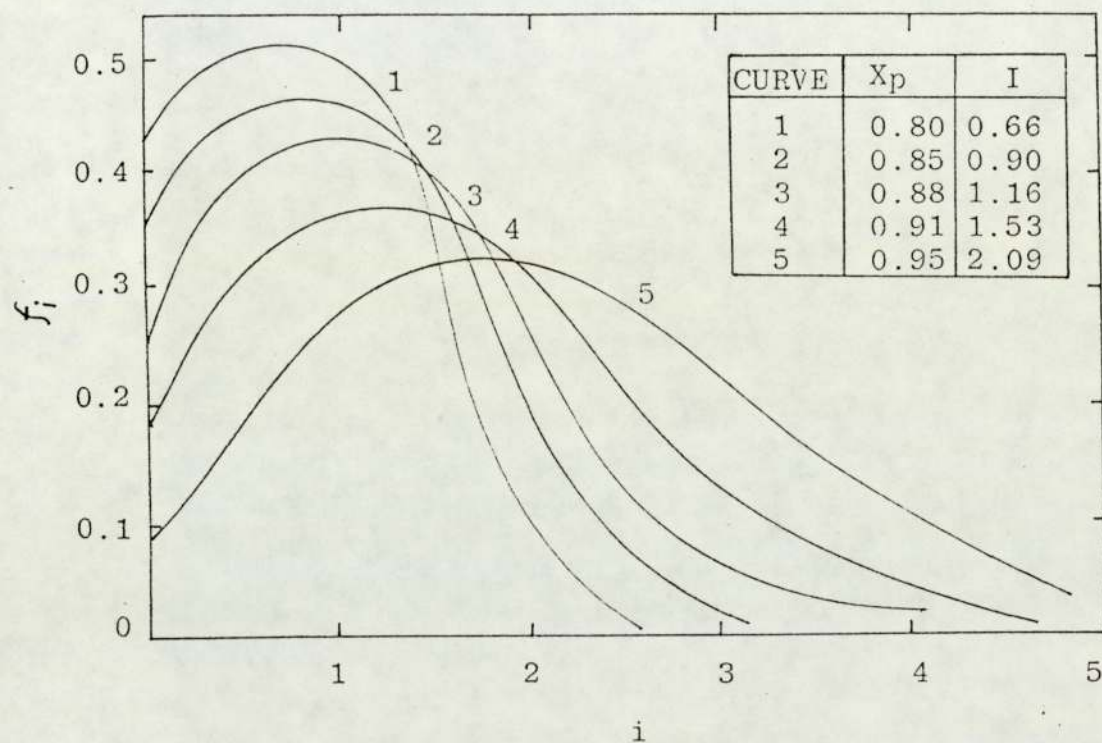


Figure 6.9 Distribution of radicals among the particles at different monomer conversions: $S_0=2.25 \text{ g/dm}^3$ water, $R_0=2.5 \text{ g/dm}^3$ water, $N=410 \text{ r.p.m.}$, reaction temperature: 50°C .

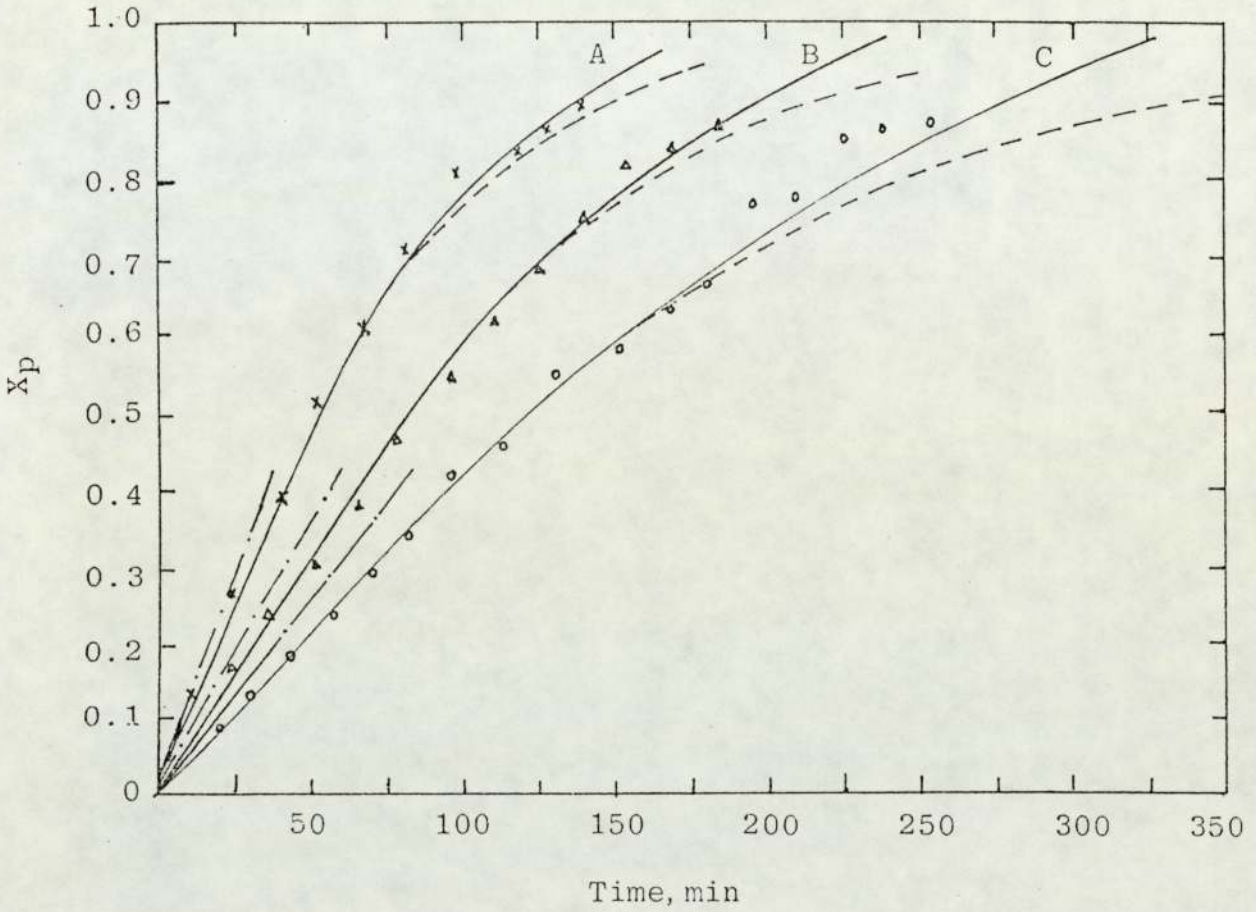


Figure 6.10 Comparison between theory and experimental data: " ____ " present, " ----" the model without considering gel-effect, " ___ . ___ " the Smith-Ewart model, $M_0=0.5$ g/g water, $R_0=2.5$ g/dm³ water, "A" $S_0=7.5$ g/dm³ water, "C" $S_0=2.25$ g/dm³ water.

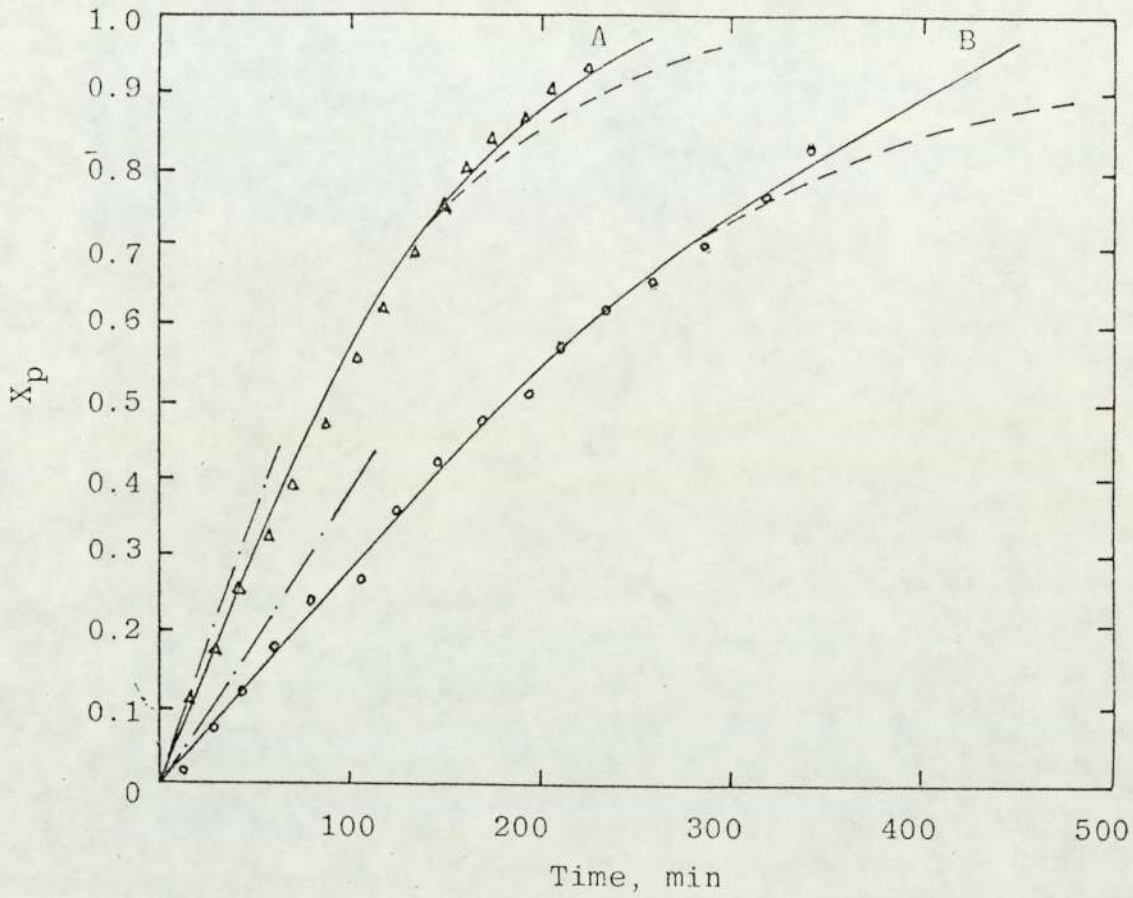


Figure 6.11 Comparison between theory and experimental data:
 "___" present model, "---" the model without
 considering gel-effect, "-.-.-" Smith-Ewart
 model, $M_0=0.5$ g/g water, $R_0=1.25$ g/dm³ water,
 "A" $S_0=5$ g/dm³ water, $N=500$ r.p.m., "B" $S_0=2.0$ g/dm³
 water, $N=410$ r.p.m.

6.3.5 The Baffled Reactor

To test the validity of the model for the baffled reactors, further test runs of emulsion polymerization were carried out in the reactor fitted with baffles as described in Section 3.1. In the computation, the dispersion formula derived above (equation 6.4) was used instead of Merry's empirical dispersion formula (equation 5.12). The results are shown in Figure 6.12 and 6.13. The computer program for this calculation is shown in Appendix VII.

Figure 6.12 and 6.13 show comparisons of conversion-versus-time plots computed by both the present model and the classical model with the experimental results across the whole range of the conversion. It indicates that the present model comes far closer to predicting the experimental data than the classical model. This is due to the fact that the present model has considered both the emulsifier adsorbed onto the surface of the monomer droplets and the gel-effect, both of which factors are ignored in the classical model. Therefore, the validity of the present model for the baffled reactor is also clearly demonstrated.

It is seen again from Figure 6.13 how impeller speed affects the behaviour of emulsion polymerization reactors. As discussed above, for the baffled reactor the extent of monomer dispersion is much more severe than that in the unbaffled reactor so that a much greater effect on the number of particles and on the polymerization rate by the level of agitation can be expected. It is clear from Figure 6.13

that the slope of the conversion-versus-time curve for the case of high impeller speed (Curve C) is much lower than that for the case of low impeller speed (Curve B). If Curve B in Figure 6.12 is compared with Curve 21 in Figure 6.8 for the unbaffled reactor of the same impeller and soap concentration it is clearly seen that the baffled reactor gives rise to a much reduced reaction rate and particle number as may be expected from the higher specific monomer surface area available for soap adsorption in baffled systems.

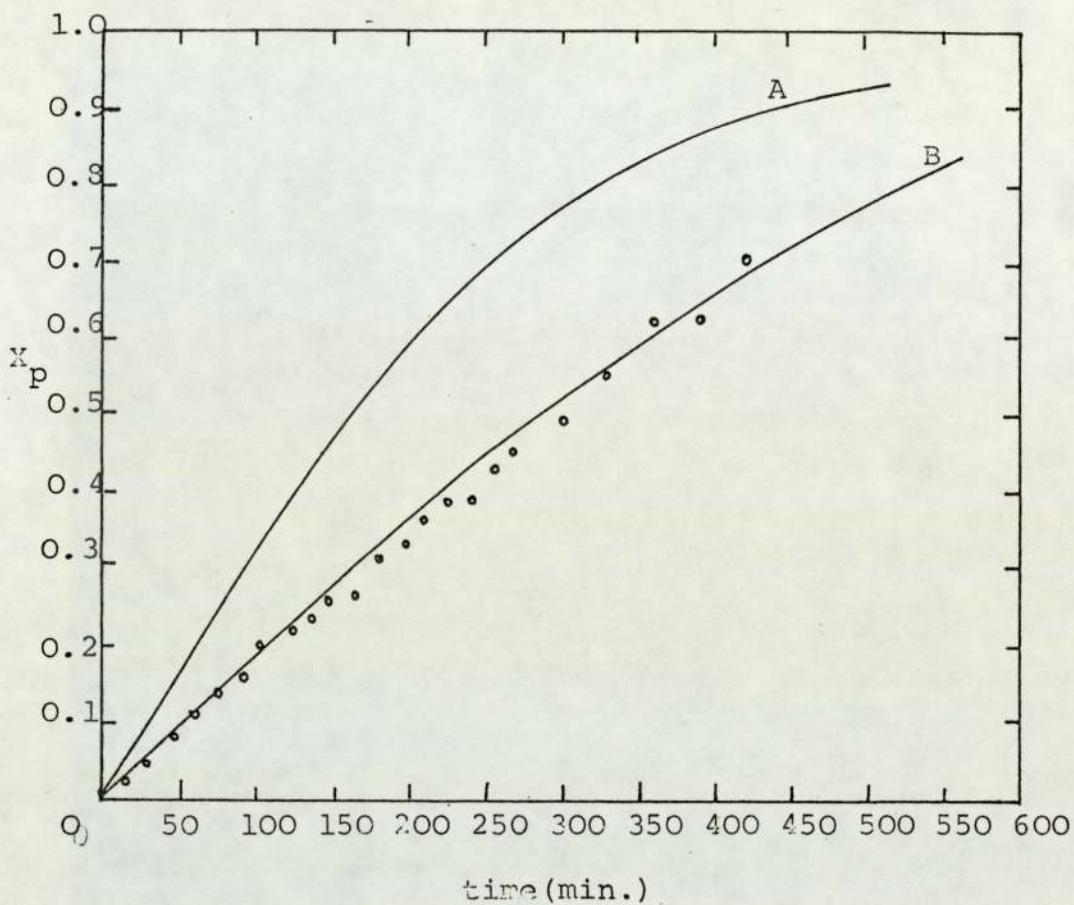


Figure 6.12 Comparison between theory and experimental data for baffled reactor $S_0 = 1.5 \text{ g/dm}^3$ water, $R_0 = 1.25 \text{ g/dm}^3$ water. $M_0 = 0.5 \text{ g/g}$ water, $N = 600 \text{ r.p.m.}$ "A" Smith-Ewart model, "B" present model. Reaction temperature 50°C.

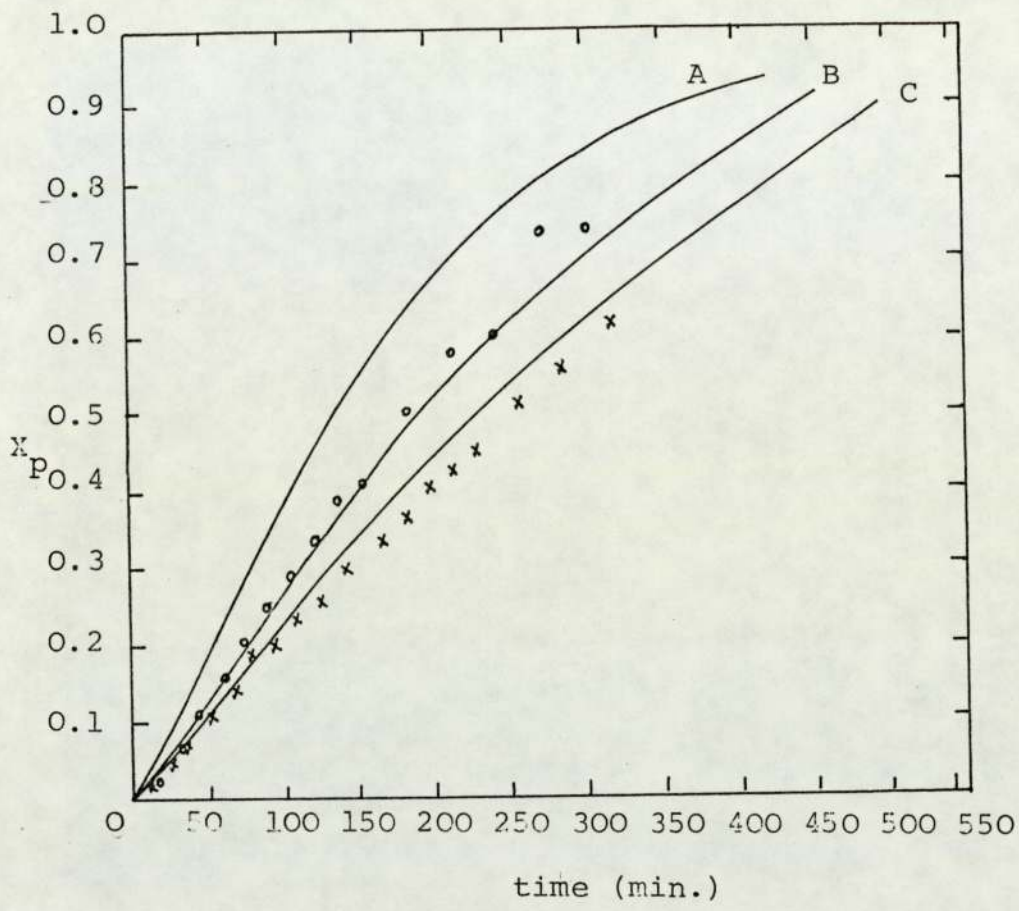


Figure 6.13 Comparison between theory and experimental results for baffled reactor $R_0=1.25 \text{ g/dm}^3$ water, $M_0=0.5 \text{ g/g water}$, "A" Smith-Ewart model, "B" present model, $S_0=2 \text{ g/dm}^3$ water, $N=600 \text{ r.p.m.}$, "C" present model, $N=800 \text{ r.p.m.}$, $S_0=2 \text{ g/dm}^3$ water, Reaction temperature 50°C .

SECTION VII

CONCLUSIONS

1) The classical models for emulsion polymerization as presented by Smith and Ewart and by Gardon do not present satisfactory predictions for stages I and II of the reaction for the case of low soap concentrations and for the case of high impeller speeds at intermediate and low soap concentrations. This is recognised in this project to be due to the fact that these two models fail to take into account the adsorption of a proportion of the emulsifying soap onto the surface of the dispersed monomer droplets. This adsorption clearly reduces the number of micelles available for polymer particle nucleation. Not surprisingly, therefore, the classical models predict more, though smaller, polymer particles and higher reaction rates than are observed in practice and this deviation becomes increasingly severe as the initial soap concentration is reduced.

2) The increase in viscosity within the polymer particles during Stage III of the emulsion polymerization reaction gives rise to a reduction in the translational mobility of the radicals within the particles. This is suggested to progressively reduce the effective termination constant of the reaction as the polymer concentration increases through Stage III. The classical models do not take this 'gel-effect' into account and thus they predict a declining reaction rate during Stage III whereas in practice the reaction rate is often observed to increase.

(3) The field of study of this project has been the effects upon the behaviour of the emulsion polymerization reaction of the adsorption of emulsifier onto the surface of monomer droplets and of the gel-effect. A mathematical model for predicting these effects in both unbaffled and baffled stirred batch reactors has been established. It is summarized below.

Stage I

$$A_p(t) = \frac{B_1}{6} t^{5/3} \{B_4 - 2.52A_p\left(\frac{t}{2}\right) - 2.52(B_2 - B_3V_p\left(\frac{t}{2}\right))^{2/3}\}$$

$$V_p(t) = \frac{C_1}{6} t^2 \{C_2 - 2A_p\left(\frac{t}{2}\right) - 2(B_2 - B_3V_p\left(\frac{t}{2}\right))^{2/3}\}$$

$$X_p(t) = D_1 t^2 \{C_2 - 2A_p\left(\frac{t}{2}\right) - 2(B_2 - B_3V_p\left(\frac{t}{2}\right))^{2/3}\}$$

$$N_p(t) = Z_1 t \{Z_2 - A_p(t) - (B_2 - B_3V_p(t))^{2/3} - 4A_p\left(\frac{t}{2}\right) - 4(B_2 - B_3V_p\left(\frac{t}{2}\right))^{2/3}\}$$

where

$$B_1 = 4\pi K^{2/3} (R/s)$$

$$B_2 = 3(4\pi N_d)^{1/2} V_d^0$$

$$B_3 = 3(4\pi N_d)^{1/2} (d_{sw}/d_m)$$

$$B_4 = 3.52S - A_d^0$$

$$C_1 = (4\pi/3)K(R/S)$$

$$C_2 = 3S - A_d^0$$

$$D_1 = C_1 d_p (1 - \phi_m) / 6M_0$$

$$Z_1 = R / 6S$$

$$Z_2 = 6S - A_d^0$$

$$K = (3/4\pi) (K_p / N_A) (d_m / d_p) \phi_m / (1 - \phi_m)$$

$$R = 2K_i f \{I\} N_A$$

$$S = (\{S\} - \{S\}_{cmc}) N_A A_S$$

$$N_d = (6/\pi) \{V_d^0 / (D_d^0)^3\}$$

$$A_d^0 = 6V_d^0 / D_d^0$$

$$D_d^0 = D_d^j \left\{ \frac{N}{N_i} \right\}^{-1.08} \left\{ \frac{H}{H_i} \right\}^{-0.185}$$

Stage II

$$\frac{df_i}{dx_p} = \frac{G_1}{I} (f_{i-1} - f_i) + \frac{G_2}{x_p^{1/3} I} \{f_{i+1}^{(i+1)} - f_i^{(i)}\} + \frac{G_3}{x_p I}$$

$$\{f_{i+2}^{(i+2)} - f_i^{(i-1)}\}$$

$$\sum f_i = 1$$

$$\sum f_i i = I$$

where

$$G_1 = \frac{R M_0 N_A}{(K_p N_p d_m \phi_m)^2}$$

$$G_2 = (K_O/K_P) (\pi^{1/3} N_A) (6M_O/N_P)^{2/3} (d^{1/3}/d_m) (1-\phi_m)/\phi_m$$

$$G_3 = (K_t/K_P) (d_p/d_m) (1-\phi_m)/\phi_m$$

$$K_t = \exp(A_1 + A_2 X_{p, II-III} + A_3 X_{p, II-III}^2 + A_4 X_{p, II-III}^3 + A_5 X_{p, II-III}^4)$$

$$\frac{dX_p}{dt} = \frac{K_p}{N_A} \cdot \frac{d_m}{M_O} \cdot N_p \phi_m^I$$

Stage III

$$I \frac{df_i}{dx} = H_1 J_1(X_p) (f_{i-1} - f_i) + H_2 J_2(X_p) \{f_{i+1}(i+1) - f_i i\} +$$

$$H_3 J_3(X_p) \{f_{i+2}(i+2)(i+1) - f_i i(i-1)\}$$

$$\sum f_i = 1$$

$$\sum f_i i = I$$

where

$$H_1 = R N_A M_O / (K_p N_p^2 d_m)$$

$$H_2 = (K_O/K_P) (\pi^{1/3} N_A) (6M_O/N_P)^{2/3} (d_p^{1/3}/d_m)$$

$$H_3 = 1/K_p$$

$$J_1(X_p) = 1 - d_m X_p / d_p (1 - X_p)$$

$$J_2(X_p) = (d_m/d_p)^{1/3} \{ (1 - X_p) + d_m X_p / d_p \}^{2/3} / (1 - X_p)$$

$$J_3(X_p) = \frac{1}{1 - X_p} \exp(A_1 + A_2 X_p + A_3 X_p^2 + A_4 X_p^3 + A_5 X_p^4)$$

$$\frac{dx_p}{dt} = \frac{K_p d_m}{N_A M_O} N_p I \phi(X_p)$$

$$\phi(X_p) = \frac{1-X_p}{(1-X_p) + (d_m/d_p) X_p}$$

4) The model for Stage I of the reaction demands a knowledge of the specific surface area of the monomer dispersion. A relationship relating Sauter mean droplet diameter, impeller speed and impeller diameter has been presented by Merry (17) for styrene in an aqueous solution of emulsifying soap in an unbaffled reactor. This has been incorporated into the model for Stage I of the reaction for emulsion polymerization of styrene in an unbaffled reactor. A relationship between Sauter mean droplet diameter, soap concentration and impeller speed for the dispersion of styrene in an aqueous solution of sodium lauryl sulphate in a baffled reactor has been determined during the current study. This relationship is presented below. It has been incorporated into the model for Stage I of emulsion polymerization of styrene in a baffled reactor.

$$D_d^O = 2.42 S_O^{0.013} N^{-1.86}$$

Internal dia. of the vessel = 152 mm, impeller combination diameter 75 mm.

5) The model for Stage III of the reaction demands a knowledge of the termination rate constant of the polymerization and its dependence on polymer concentration.

An empirical formula which relates radical termination constant, K_t , to monomer conversion, X_p , has been formulated from conversion against time data of suspension polymerization of styrene at 50°C. It is shown as follows:

$$K_t = \exp(A_1 + A_2 X_p + A_3 X_p^2 + A_4 X_p^3 + A_5 X_p^4)$$

where $A_1 = -9.5873$

$A_2 = -7.4332$

$A_3 = 45.8577$

$A_4 = -95.9184$

$A_5 = 47.4095$

This relationship is incorporated into the model for emulsion polymerization.

6) Emulsion polymerization of styrene at 50°C has been successfully carried out under a range of initial sodium lauryl sulphate concentrations from 1.5 → 7.5 gms dm⁻³ and for impeller speeds in the range 410-850 r.p.m. The progress of the reaction has been monitored gravimetrically and the final particle size has also been determined.

7) A technique for the measurement of particle size using a light transmission method has been developed based on Mie's light scattering theory. This technique is valid for measuring particle diameters down to 0.09 micron. The following set of equations relating particle radius to the Mie light scattering coefficient for various wavelengths have been

formulated and used in the current work.

$$\gamma_{3700} = 0.04387 + 0.1751X + 0.9485X^2 - 1.3463X^3$$

$$\gamma_{4300} = 0.04294 + 0.4171X - 1.2214X^2 + 11.1013X^3$$

$$\gamma_{5000} = 0.04254 + 0.7329X - 5.6351X^2 + 45.2569X^3$$

$$\gamma_{5600} = 0.04211 + 1.0947X - 13.7433X^2 + 122.572X^3$$

$$\gamma_{6500} = 0.04218 + 1.6546X - 29.9384X^2 + 336.231X^3$$

where X stands for k/α

The data determined with this technique have been shown to be in good agreement with that obtained measured using an electron microphotographic method.

8) Predictions of the computer model for stages I, II and III of emulsion polymerization of styrene at 50°C are in excellent agreement with experimental results. The model is clearly able to represent the dependence of the reaction on impeller speed, a facility that was not available in the use of the Smith and Ewart or Gardon models. The model also allows the progress of Stage III of the reaction to be successfully predicted in that it takes into account the

gel-effect. Particle size, particle number, reaction rate and the mean number of radicals per particle are predicted with good accuracy across the whole of the conversion, or at least up to the point at which the glass transition point falls above the temperature of the reaction (in this case this was 97.4% conversion). This excellent agreement is found both for unbaffled and baffled reactor operation.

Suggestions for Future Work

i) The validity of the present model is demonstrated only for the case of styrene as monomer under rather limited conditions, for instance it is a very simple recipe with no transfer agent, no electrolytes, no incremental soap and it has been tested only at one temperature. Future work should focus on testing different kinds and combinations of monomers under different phase ratios, initiator concentrations, emulsifier concentrations, impeller speeds, temperature and different sized reactors with or without baffles to further test the capabilities of the model and to expand its applications.

ii) In the present model, it has been assumed that the heat transfer in the system is perfect so that the reactor remains isothermal. For the real system however especially for large reactors, this will not be achieved in practice. To model the emulsion polymerization reactor more effectively, heat transfer in the reactor must be investigated and incorporated into the model.

iii) Molecular weight and its distribution directly affect the properties and application of the polymer. For the emulsion polymerization processes, these characteristics in turn relate to the number of particles, the initiator concentration, the purity of the contents in the reactor, environmental conditions and so on. A successful mathematical model of emulsion polymerization reactors should

correctly predict the molecular weight and its distribution of polymer.

(iv) In fact, the molecular weight of products produced by emulsion polymerization can be too high for some practical applications. For this reason, it is sometimes necessary to include within the recipe a chain transfer agent in order deliberately to reduce the molecular weight. In a further investigation this factor should be taken into account.

(v) Gel-effect is a very important phenomenon for emulsion polymerization. Although in the present work the model has given good results, this has only been possible using an empirical formula which clearly is only applicable to this single case. Future work starting from the study of the morphology of the polymer molecules, the structure of the polymer itself and the structure of the polymer solution could be directed towards determination of the dependence of the radical termination rate constant upon the monomer conversion which would be applicable to all polymers under different conditions.

(vi) Although the light transmission technique for measuring the particle size developed in the present work can determine the particle diameter down to 0.09 micron, it is still not adequate for the investigation at the whole course of the emulsion polymerization. Thus, it is necessary to further extend the technique down to an even smaller size range.

NOMENCLATURE.

a	Average surface area of one particle at a given time, cm^2
A_1	Constant
A_2	Constant
A_3	Constant
A_4	Constant
A_5	Constant
A_d^0	Initial surface area of monomer droplets, cm^2/cc water
A_p	Surface area of particles, cm^2/cc water
A_s	Surface area provided by one soap molecule, cm^2
B_1	Constant, $B_1 = 4\pi k^{2/3}(R/S)$
B_2	Constant, $B_2 = 3(4\pi N_d)^{1/2} V_d^0$
B_3	Constant, $B_3 = 3(4\pi N_d)^{1/2} (d_{sw}/d_m)$
B_4	Constant, $B_4 = 3.52S - A_d^0$
C_1	Constant, $C_1 = (4/3)k(R/S)$
C_2	Constant, $C_2 = 3S - A_d^0$
d_m	Density of monomer, g/cm^3
d_p	Density of polymer, g/cm^3
d_{sw}	Density of monomer swollen particles, g/cm^3
D_1	Constant, $D_1 = C_1 d_p (1 - \phi_m) / 6M_0$
D_d^0	Initial Sauter diameter of monomer droplets, cm
D_d^i	Reference Sauter diameter of monomer droplets, cm
f	Efficiency of initiator decomposition, fraction
f_i	Number fraction of the particles each of which contain i radicals
$f_{i, II-III}$	Number fraction of the particles each of which contains i radicals by the end of Stage II.

G_1	Constant, $G_1 = RM_O N_A / (K_p N_p^2 d_m \phi_m)$
G_2	Constant, $G_2 = (K_O / K_p) (\pi^{1/3} N_A) (6M_O / N_p)^{2/3} (d_p^{1/3} / d_m)$ $(1 - \phi_m)^{1/3} / \phi_m$
G_3	Constant, $(K_t / K_p) (d_p / d_m) (1 - \phi_m) / \phi_m$
H	Impeller diameter, cm.
H_1	Constant, $H_1 = RN_A M_O / (K_p N_p^2 d_m)$
H_2	Constant, $H_2 = (K_O / K_p) (\pi^{1/3} N_A) (6M_O / N_p)^{2/3} (d_p^{1/3} / d_m)$
H_3	Constant, $H_3 = 1 / K_p$
H_i	Reference impeller diameter, cm.
i	Number of radicals in one particle
$[I]$	Initial initiator concentration, mole/dm ³ water
I_{II-III}	Average number of radicals in one particle by the end of Stage II
$J_1(X_p)$	Function of X_p
$J_2(X_p)$	Function of X_p
$J_3(X_p)$	Function of X_p
K	Constant, $K = (3/4\pi \chi K_p / N_A) (d_m / d_p) \phi_m / (1 - \phi_m)$
K_i	Rate constant of initiator decomposition, 1/min
K_p	Rate constant of polymer propagation cm ³ /mole.min
K_{pO}	Rate constant of polymer propagation in pure monomer cm ³ /mole.min
K_t	Termination rate constant, cm ³ /mole.min
K_{tO}	Termination constant in pure monomer, cm ³ /mole.min
K_O	Radical desorption rate constant, cm/min
M_O	Ratio of monomer to water in initial charge, g/g
N	Impeller speed, rpm
N_A	Avogadro number
N_d	Number of monomer droplets, 1/cc water

N_i	Reference impeller speed, rpm
N_p	Number of particles, 1/cc water
r_d	Radius of monomer droplets, cm
r_p	Radius of polymer particles, cm
R	Rate of radical generation, 1/cc water
R_0	Initial initiator charged, g/dm ³ water
S	Total area provided by soap, cm ² /cc water
S	Initial soap charged, mole/cc water
$[S]_{cmc}$	Critical micelle concentration, mole/cc water
S_0	Initial soap charged, g/dm ³ water
t	Time, min
t_{I-II}	Time passed by the end of Stage I.
T_g	Glass transition temperature of the polymer, °C.
V_d^0	Initial volume of monomer droplets, cm ³ /cc water
V_p	Volume of particles, cm ³ /cc water
\bar{v}	Average volume of one particle, cm ³
X_p	Fractional monomer conversion.
$X_{p,I-II}$	Fractional monomer conversion by the end of Stage I.
$X_{p,II-III}$	Fractional monomer conversion by the end of Stage II.
Z_1	Constant, $Z_1 = R/6S$
Z_2	Constant, $Z_2 = 6S - A_d^0$
ϕ_m	Volume fraction of monomer in particles during the Stage I and Stage II.
$\phi(X_p)$	Volume fraction of monomer in particles during Stage III

REFERENCES

1. W.V. Smith and R.H. Ewart, *J.Chem. Phys.* 16, 592 (1948)
2. S.R. Shunmukham, V.L. Halenbeck and R.L. Guile, *J.Polym.Sci.*, 6, 691 (1951).
3. C.J. Schoot, J. Baker and K.H. Klasseus, *J. Plym. Sci.*, 7, 657 (1951)
4. C.P. Evans, P.M. Hay, L. Marker, R.W. Murry and O.J. Sweeting, *J. Appl. Polym. Sci.*, 5, 39, (1961)
5. S. Omi, Y. Shiraishi, H. Sato and H. Kubota, *J. Chem. Eng. Japan*, 2, 64 (1969)
6. M. Nomura, M. Harada, W. Eguchi and S. Nagata, *J. Appl. Polym. Sci.*, 16, 835 (1972)
7. N. Friis and A.E. Hamielec, Gel-effect in Emulsion Polymerization of vinyl monomer, *ACS Symp. Ser.* (1976)
8. N. Friis and A.E. Hamielec, *J. Polym. Sci.*, 11, 3321 (1973)
9. N. Friis and A.E. Hamielec, *Ibid*, 12, 251 (1974)
10. N. Friis and L.J. Nyhagen, *J. Appl. Polym. Sci.*, 17, 2311 (1973)
11. M.R. Grancio and D.J. Williams, *J. Polym. Sci. A-1*, 8, 2617 (1970)
12. A.W. Hui and A.E. Hamielec, *J. Appl. Polym. Sci.*, 16, 749 (1972)
13. J.L. Gardon, *J. Polym. Sci. A-1*, 6, 665 (1968)
14. J.L. Gardon, *Ibid*, A-1, 6, 687 (1968)
15. S. Nagata, *Mixing*, John Wiley and Sons (1975)
16. T. Vermeulen, G.M. Williams and G.E. Langlois, *Chem. Eng. Progr.* 47, 85 (1955)
17. A.J. Merry, PhD Dissertation, 1980, Dept. of Chem.Eng., University of Aston in Birmingham, U.K.
18. M. Harada, M. Nomura, H. Cojima, W. Eguchi and S. Nagata, *J. Appl. Polym. Sci.*, 16, 811 (1972)

19. G. Mie,
Ann. Physik., 25, 377 (1908)
20. J.B. Bateman, E.J. Weneck and D.C. Eshler,
J. Colloid. Sci., 14, 308 (1959)
21. W.D. Harkins
J.Chem.Phys. 13, 831 (1945)
22. W.D. Harkins
J.Chem.Phys. 14, 47 (1946)
23. W.D. Harkins
J. Am. Chem.Soc., 69, 1428 (1947)
24. W.D. Harkins
J. Polym. Sci., 5, 217 (1950)
25. K.W. Min and W.E. Ray,
Reviews in Macromolecular Chemistry,
12, 177 (1975)
26. W.V. Smith,
J.Amer.Chem.Soc., 69, 1428 (1947)
27. W.V. Smith
Ibid. 71, 4077 (1949)
28. J.L. Gardon,
J. Polym. Sci., A-1, 6, 623 (1968)
29. J.L. Gardon
J. Polym. Sci., A-1, 6, 643, (1968)
30. J.L. Gardon
J. Polym. Sci., A-1, 6, 2853 (1968)
31. J.L. Gardon
J. Polym. Sci., A-1, 6, 2859 (1968)
32. M. Harada, M. Nomura, H. Cojima, W. Eguchi
and S. Nagata,
J. Appl. Polym. Sci., 16, 811 (1972)
33. K.W. Min and W.H. Ray,
J. Macro-Sci. - Rew. Macromol. Chem.,
C11, 177(1974)
34. K.W. Min and W.H. Ray,
ACS Symposium Series, 24, 369 (1976)
35. K.W. Min and W.H. Ray
J. Appl. Polym.Sci., 22, 89 (1978)
36. K.W. Min and H.I. Gostin,
Ind. Eng. Chem.Prod.Dev. Vo. 18, No. 4 (1979)
37. E. Trommsdorff, H. Kohle and P. Legally,
Makromol Chem., 1, 169 (1947)

38. F.L. Marten and A.E. Hamielec,
High Conversion Diffusion Controlled Polymer-
ization Reactor Processes, ACS Sym. (1979)
39. J.W. Breatenbach and A. Schindler,
Monatsh. Chem., 83, 724 (1952)
40. D.B.V. Parker,
Polymer Chemistry, Applied Science Publishers,
London, 28 (1978)
41. N. Friis and A.E. Hamielec
J. Appl. Polym. Sci., 19, 97 (1975)
42. G.H. Olive and S. Olive,
Makromol.Chem., 37, 71 (1960)
43. T. Vermeulen, G.M. Williams and G.E. Langlois,
Chem. Eng. Progr., 51, 85 (1955)
44. P.H. Carldebank
Trans. Inst.Chem.Eng., 36, 443 (1958)
45. D.B. Scully,
J. Appl. Polym. Sci., 20, 2299 (1976)
46. D.E. Brown and K. Pitt,
Drop break-up in a stirred liquid-liquid
contactor,
Checa. 70 Melbourn, Sydney, 83 (1970)
47. Y. Mylnek and W. Resnick
A.I.Ch.E.J., 18, 122 (1972)
48. C.A. Coulaloglou and L.L. Tanlarides,
A.I.Ch.E.J., 22, 289 (1976)
49. F.A. Bovey, I.M. Kolthoff, A.I. Medalia and
E.J. Meehan,
Emulsion Polymerization, John Wiley and Sons (1954)
50. S.H. Maron, M.E. Elder and C. Moore,
J. Colloid Sci., 9, 104 (1954)
51. S.H. Maron, M.E. Elder and I.N. Ulevitch
Ibid., 9, 89 (1954)
52. S.H. Maron and M.E. Elder
Ibid, 9, 353, (1954)
53. H.B. Klevens,
J. Colloid Sci., 2, 365 (1947)
54. W.B. Dandliker,
J. Am. Chem. Soc., 72, 5110 (1950)
55. A. Nisonoff, W.E. Messer and U.H. Howland,
Anal. Chem. 26, 856 (1954)

56. M.D. Barnes and V.K. La Mer,
J. Colloid. Sci., 1, 79 (1946)
57. V.K. La Mer,
J. Phys. and Colloid Chem., 52, 65 (1948)
58. M.D. Barnes, A.S. Kenyon, E.M. Zaiser and
V.K. LaMer,
J. Colloid Sci., 2, 349 (1947)
59. G.W.C. Kaye and T.H. Laby,
Physical and Chemical Constants, 11th ed.
Longman's Green, London (1950)
60. T.L. Pugh and W.J. Heller,
J. Colloid Sci., 12, 173 (1957)
61. I.M. Kolthoff and I.K. Miller,
J. Am. Chem. Soc., 73, 305 (1951)

APPENDICES

APPENDIX I

COMPUTER PROGRAM FOR DETERMINATION OF PARTICLE SIZE USING
EXTINCTION METHOD.

WA

```
50 REM THIS PROGRAMME CALCULATES THE DIAMETER OF POLYMER PARTICLES
60 REM USING LIGHT TRANSMISSION TECHNIQUE.
100 READ I
110 FOR I=1 TO 5
120 READ UC(I)
130 NEXT I
140 FOR I=1 TO 5
150 FOR J=1 TO 5
160 READ AC(I,J)
170 NEXT J
180 NEXT I
190 FOR I=1 TO 5
200 READ BC(I)
210 NEXT I
220 FOR I=1 TO 5
230 READ EC(I)
240 NEXT I
250 READ T,P,G
260 FOR I=1 TO 2
270 READ WC(I),IC(I)
280 NEXT I
290 PRINT "BATCH: PS-12; JD: 12; C0=50G/ML WATER; J=4177; UNDIFFERED"

295 PRINT "*****"
300 PRINT
310 PRINT "THE DATA"
320 PRINT "*****"
330 PRINT "AMACT=",T
340 PRINT "AMATP=",P
350 PRINT "TSC=",G
360 PRINT "C1=",IC(1)
370 PRINT "C1=",IC(1)
380 PRINT "C2=",IC(2)
390 PRINT "C2=",IC(2)

400 PRINT
410 PRINT "WAVE LENGTH: 6700 4322 5000 5500 6500"
420 PRINT " E : 4.915 2.53 2.3 2.196 2.1135"

430 K1=T-C
440 I2=T-I1
450 K3=I-T
460 K4=I2/P
470 FOR I=1 TO 2
480 S9=S
490 S=S*IC(I)/WC(I)
500 P=P*G/S9
510 T=T*G/S9
520 IF I>1 THEN 470
530 IF K4>.43 THEN 470
540 P5=IC(I)*K2
550 C6=IC(I)*K1
560 P6=P5*.43
570 S6=P6-P5
580 S7=S6-S6
590 P=P-T*G/IC(I)
600 T=T-G/IC(I)
610 NEXT I
620 S8=T-(T-S)
630 S1=(T-S)*IC(1)
640 I2=(I-T)*IC(2)
650 C2=I-I2*IC(1)/(IC(1)+I*I2)
660 S3=S1-S2
670 C=C*(P1+S3)/WC(1)
680 PRINT
690 PRINT "THE RESULT"
700 PRINT "*****"
710 PRINT "C=";C
720 DS=1.5949*33*.957/(30+P10)+.1-1.5949*(13/(30-T10)+1.257
730 FOR I=1 TO 5
740 "C(I)=1.5553-1.7157E-10/(UC(I)+1.3-15) ** 2
750 "C(I)=1.384+2.145E-11/(UC(I)+1.2-15) ** 2
760 "C(I)=.99995*UC(I)+.00005*UC(I)
```

```

603 L1=1
610 K(1)=.4337*D5*(E11*(L11)*I+.L-33/(N11)*C*L1)
612 FOR J=1 TO 5
614 PC(J)=A(1,J)
616 NEXT J
618 Y6=K(1)
620 GOOS 1500
622 R(1)=Y6
630 NEXT 1
640 I1=8
650 FOR I=1 TO 5
660 J1=I1+R(1)
670 NEXT 1
680 R1=J1/5
690 D1=2*R1
700 IF I4>.43 THEN 730
710 L=D1*(D5*(1-33/(33+P1)))/.4176) ** (1/3)
720 GOTO 770
730 D6=(4*(1+.257*(1-14))*285
740 D=D1*(1+.52/(P1+33))*D5/D6) ** (1/3)
750 J=6*(1+I2)/(3.14159*(3*D6*(L*.2221) ** 3)
760 GOTO 730
770 J=4.5977*(32/(32/D*.2221) ** 3
780 PRINT "C3700=";K(11),"C3700=";R(1)
790 PRINT "C4300=";K(21),"C4300=";R(2)
800 PRINT "C5000=";K(31),"C5000=";R(3)
810 PRINT "C5600=";K(41),"C5600=";R(4)
820 PRINT "C6500=";K(51),"C6500=";R(5)
830 PRINT "R1=";R1
840 PRINT "D1=";D1
850 PRINT "DP=";D
860 PRINT "JP=";J
870 PRINT "CP=";C4
880 DATA 2.2393E-04
890 DATA 3700,4300,5000,5600,6500
900 DATA .2155,.2567,.1269,.2653,.334
910 DATA .2092,.2362,.3700,.2034,.3113
920 DATA .2053,.2227,.2663,.1502,.2434
930 DATA .2044,.2147,.2513,.1175,.2125
940 DATA .2029,.2107,.2350,.2901,.1665
950 DATA .2046,.2550,.2370,.1320,.174
960 DATA .2150,.5300,.1176,.1135
970 DATA .3414,.3306,.3263
980 DATA 100,.4540,100.45,10
990 END
1500 J6=5
1505 J7=J6
1507 J6=J6-1
1510 FOR J=1 TO J6
1520 O6=(J6-PC(J))*((J6-PC(J)+1)
1530 IF O6>0 THEN 1560
1540 I6=J
1550 GOTO 1620
1560 NEXT J
1570 J7=ABS(J6-PC(1))-ABS(J6-PC(J6))
1580 IF J7 >= J THEN 1610
1590 I6=1
1600 GOTO 1620
1610 I6=J6-1
1620 IF (I6-J6+1) <> J THEN 1650
1630 I6=I6-1
1640 GOTO 1690
1650 IF I6-1=0 THEN 1690
1660 O3=ABS(J6-PC(I6))-ABS(J6-PC(I6+1))
1670 IF O3 >= J THEN 1690
1680 I6=I6-1
1690 V6=0
1700 IF I6-I6+2 THEN 1720
1710 I6=I6-1
1720 L6=I6+2
1730 FOR K=I6 TO L6
1740 V6=O(1)
1750 FOR J=I6 TO L6
1760 IF J-I6=4 THEN 1790
1770 V6=(J6-PC(J))/PC(I6)-PC(J)+V6
1780 NEXT J

```

1774 V6=V6+J6
1322 NEXT K6
1312 V6=V6
1320 J6=J7
1330 RETURN
1343 END

END
UA

DATCH: PG-12; NO: 12; DD=53RAM/0; WATER; N=41270; UNBAPLED

THE DATA

=====
A.IAKT= .3414
A.IAKP= .3306
TSC= .3263
J1= 100
J1= .454
J2= 100.45
J2= 10

TAKE LENGTH: 3700 4300 5200 5600 6500
E : 2.915 3.53 4.3 2.176 3.1135

THE RESULTS

=====
C= 1.45251E-04
K3700= 3.91957E-02 R3700= 6.50530E-02
K4300= 6.80922E-02 R4300= 6.47400E-02
K5200= 3.93170E-02 R5200= 6.45730E-02
K5600= 2.91397E-02 R5600= 6.62702E-02
K6500= 1.96567E-02 R6500= .26475
R1= 6.50515E-02
D1= .130123
DP= .131529
JP= 4.21420E+14
KP= .954326

DOVE

APPENDIX II

COMPUTER PROGRAMS FOR THE COMPUTATION OF THE DEPENDENCE OF
TERMINATION RATE CONSTANT ON MONOMER CONVERSION

- 1) DEFFI The Computation of dx_p/dt from $t-x_p$ data using
- differentiation method.
- 2) REG 3 The Formulation of K_t and X_p using multiple
regression method.
- 3) XKT The Evaluation of K_t against X_p

LIS
DEFF1

```

1  REM THIS PROGRAMME IS AN NUMERICAL DIFFERENTIAL METHOD TO
2  REM CALCULATE THE CONVERSION RATE FROM THE DATA OF
3  REM SUSPENSION POLYMERIZATION.
5  DIM K(27),Y(27),F(27)
10  N1=15
20  FOR I=1 TO N1
30  READ K(I)
31  NEXT I
39  FOR I=1 TO N1
40  READ Y(I)
50  NEXT I
62  H=60
65  PRINT " NO","TIME(MIN)","CONVERSION","  D1/DT"
72  FOR I=1 TO N1
82  IF I=1 THEN 140
90  IF I=2 THEN 160
100  IF I=N1 THEN 200
110  IF I=N1-1 THEN 130
120  LET F(I)=(-2*Y(I-2)-Y(I-1)+Y(I+1)+2*Y(I+2))/(10*H)
130  GOTO 210
140  LET F(I)=(-21*Y(I)+13*Y(I+1)+17*Y(I+2)-9*Y(I+3))/(20*H)
150  GOTO 210
160  LET F(I)=(-11*Y(I-1)+3*Y(I)+7*Y(I+1)+Y(I+2))/(20*H)
170  GOTO 210
180  LET F(I)=-1*(-11*Y(I+1)+3*Y(I)+7*Y(I-1)+Y(I-2))/(20*H)
190  GOTO 210
200  LET F(I)=-1*(-21*Y(I)+13*Y(I-1)+17*Y(I-2)-9*Y(I-3))/(20*H)
210  PRINT I,K(I),Y(I),F(I)
220  NEXT I
430  DATA 0, 60, 120, 180, 240, 300, 360, 420, 480, 540, 600
490  DATA 660, 720, 780, 840
510  DATA 0,.2613,.1195,.1399,.2367,.2774,.3243
520  DATA .336,.4264,.4533,.5207,.5449,.6313
530  DATA .7502,.9655
550  END

```

RUN
DEFF1

NO	TIME(MIN)	CONVERSION	D1/DT
1	0	0	9.35167E-24
2	60	.2613	1.40933E-23
3	120	.1195	1.00250E-23
4	180	.1399	.000914
5	240	.2367	3.23500E-24
6	300	.2774	7.99667E-24
7	360	.3243	3.13333E-24
8	420	.336	7.73167E-24
9	480	.4264	7.23500E-24
10	540	.4533	6.53500E-24
11	600	.5207	.000329
12	660	.5449	1.19150E-23
13	720	.6313	1.39150E-23
14	780	.7502	2.30533E-23
15	840	.9655	3.92533E-23

DOVE

RE33

```
1  REI THIS PROGRAM IS FOR ESTABLISHING THE DEPENDENCE OF
2  REI TERMINATION RATE CONSTANT FROM MONOMER CONCENTRATION
3  REI POLYMERIZATION OF STYRENE BY VC113 MULTIPLE PRESSION
4  REI METHOD.
100  I=4
110  N=15
119  DIM X(30,10),Y(30),Z(30),B(10),C(10),D(10),E(30),F(30),G(30)
130  FOR I=1 TO J
140  READ Z(I)
150  NEXT I
160  DATA 0,.0613,.1195,.1399,.2367,.2774,.3243,.336
170  DATA .4264,.4533,.5207,.5449,.6313,.7542,.9655
200  FOR I=1 TO J
210  READ Y(I)
220  NEXT I
230  DATA 9.33167E-04,1.00933E-03,1.7025E-03,.002914,3.035E-04
240  DATA 7.99657E-04,3.13030E-04,7.73167E-04,7.035E-04,6.503E-04
250  DATA .000329,1.1915E-03,1.3915E-03,2.33500E-03,3.97500E-03
290  READ K1,K2,I1
300  DATA 1.27E+07,1.032E-04,2.159E-04
310  J=11 ** 2*(I2+1)
320  FOR I=1 TO J
330  Y(I)=1*(X(I-10)/Y(I)) ** 2
340  Y(I)=LOG(Y(I))
350  NEXT I
360  FOR I=1 TO J
370  FOR J=1 TO I
380  K(I,J)=Z(I) ** J
390  NEXT J
400  NEXT I
410  IOSUB 1000
420  IOSUB 2000
430  B=72
440  FOR I=1 TO I
450  B=B-C(I)*Y(I)
460  NEXT I
465  PRINT "      B=";B
470  PRINT
480  PRINT " I=";I " B"
490  FOR I=1 TO I
500  PRINT I,C(I)
510  NEXT I
520  END
1000  Y1=2
1050  FOR I=1 TO J
1060  Y1=Y1+Y(I)
1070  NEXT I
1080  Y2=Y1/J
1090  FOR I=1 TO J
1100  Y(I)=0
1110  FOR J=1 TO J
1120  Y(I)=Y(I)+C(J,I)
1130  NEXT J
1140  Y(I)=Y(I)/J
1150  NEXT I
1160  FOR I=1 TO J
1170  FOR J=1 TO I
1200  K1=2
1210  K2=0
1220  K3=0
1230  FOR R=1 TO J
1240  K1=K1+C(R,I)+C(R,J)
1250  K2=K2+C(R,I)
1260  K3=K3+C(R,J)
1270  NEXT R
1280  C(I,J)=K1-K2-K3/J
1290  NEXT J
1300  NEXT I
1310  FOR I=1 TO I
1320  K4=0
1340  FOR J=1 TO J
1350  K4=K4+C(I,J)*Y(I)
1360  NEXT J
1370  K5=Y(I)*K4
1380  C(I)=K4-K5/J
1390  NEXT I
```

```

1400 RETURN
2000 N2=N-1
2010 FOR K6=1 TO N2
2020 FOR L=K6 TO N
2030 IF LCL(K6)=0 THEN 2060
2040 L2=L
2050 GOTO 2030
2060 IF L-1=0 THEN 2410
2070 NEXT L
2080 IF L2-K6=0 THEN 2170
2090 FOR J=K6 TO N
2100 T6=L1(K6,J)
2110 LCK(K6,J)=LCL(J,J)
2120 LCL(J,J)=T6
2130 NEXT J
2140 T6=CK(K6)
2150 CK(K6)=CCL(J)
2160 CCL(K6)=T6
2170 A1=K6+1
2180 FOR J=A1 TO N
2190 LCK(K6,J)=LCK(K6,J)/LCK(K6,K6)
2195 NEXT J
2200 CCK(K6)=CCK(K6)/LCK(K6,K6)
2210 L=L2+1
2220 FOR I=L TO N
2230 FOR J=A1 TO N
2240 LCI(J)=LCI(J)-LCI(K6)*LCK(K6,J)
2250 NEXT J
2260 CCI=CCK(CCI)-CCK(K6)*LCK(K6,K6)
2270 NEXT I
2280 NEXT K6
2290 K7=N
2300 IF LCK(K7,K7)=0 THEN 2410
2310 CCK(K7)=CCK(K7)/LCK(K7,K7)
2320 A1=A-1
2330 FOR K6=1 TO A1
2340 I=A-K6
2350 L=I+1
2360 FOR J=L TO N
2370 CCI=CCK(CCI)-LCCI(J)*CCK(J)
2380 NEXT J
2390 NEXT K6
2400 RETURN
2410 PRINT "K6=",K6
2500 END

```

```

RUN
RES13

```

```

      B0=      29.841
      1      3
      1      -7.43325
      2      45.8335
      3      -95.9334
      4      47.419

```

```

DONE

```

L15
KKT

```
100 DIM X(30),Y(30)
110 LET N=20
120 FOR I=1 TO N
130 READ X(I)
140 NEXT I
150 READ A1,A2,A3,A4,A5
160 FOR I=1 TO N
170 S=A1+A2*X(I)+A3*X(I)**2+A4*X(I)**3+A5*X(I)**4
180 Y(I)=EXP(S)
190 NEXT I
200 PRINT " X(Y) " AT"
210 FOR I=1 TO N
220 PRINT X(I),Y(I)
230 NEXT I
240 DATA .1,.05,.1,.15,.2,.25,.3,.35,.4,.45,.5
250 DATA .55,.6,.65,.7,.75,.8,.85,.9,.95
260 DATA 29.5373,-7.4332,45.3577,-95.9134,47.4395
300 END
```

RUN
KKT

X(X)	Y
0	7.87293E+12
.05	5.43634E+12
.1	4.35673E+12
.15	4.32291E+12
.2	3.41512E+12
.25	5.29937E+12
.3	5.19515E+12
.35	4.31224E+12
.4	4.33552E+12
.45	3.42733E+12
.5	1.96376E+12
.55	1.12729E+12
.6	5.56109E+11
.65	2.51300E+11
.7	1.33395E+11
.75	3.73270E+10
.8	1.31323E+10
.85	4.57300E+09
.9	1.64330E+09
.95	5.43153E+08

DONE

L15

APPENDIX III

COMPUTER PROGRAM FOR FORMULATION OF THE DISPERSION DATA IN
BAFFLED REACTOR

- 1) DISPER The Evaluation of the average diameter of monomer droplets for the various sample from the dispersion data.
- 2) D Formulation of D_d^0 , S_0 and N using regression method.

DISPER

```

100 K1=15
110 K2=42
120 D1=D(42),K(42)
130 PRINT "I","D","K"
140 FOR I=1 TO K2
150 READ D(I)
160 NEXT I
165 FOR I1=1 TO K1
170 FOR I=1 TO K2
180 READ K(I)
190 NEXT I
200 N1=0
210 A1=4
220 V1=2
230 FOR I=1 TO K2
240 D=1.6129E-06*D(I)
250 A=3.1416*D ** 2*K(I)
260 V=(3.1416/6)*D ** 3*K(I)
270 N1=N1+K(I)
280 A1=A1+A
290 V1=V1+V
300 NEXT I
310 D1=V1*6/A1
320 PRINT I1, D1, N1
330 NEXT I1
340 DATA 2, 3, 4, 5, 6, 7, 8, 9, 10, 11, 12, 13, 14, 15, 16, 17, 18, 19, 22, 21
350 DATA 22, 23, 24, 25, 26, 27, 28, 29, 30, 31, 32, 33, 34, 35, 36, 37, 33
360 DATA 39, 42, 41
365 DATA 50, 56
370 DATA 99, 111, 103, 112, 64, 52, 43, 19, 24, 15, 16, 9, 6, 3, 4
380 DATA 3, 3, 4, 3, 1, 1, 2, 3, 3, 1, 1, 3, 3, 2, 1
390 DATA 3, 3, 3, 3, 3, 2, 1, 3, 1, 1, 3, 1
400 DATA 93, 114, 91, 72, 42, 23, 26, 17, 7, 11, 11, 3, 2, 3, 4
410 DATA 2, 3, 2, 3, 3, 3, 3, 3, 3, 3, 3, 1, 3, 3, 2
420 DATA 3, 1, 2, 3, 3, 3, 3, 3, 3, 3, 3
430 DATA 51, 37, 33, 22, 25, 23, 9, 7, 11, 5, 5, 3, 1, 2, 2
440 DATA 3, 3, 3, 3, 2, 3, 3, 3, 3, 3, 3, 3, 3, 3, 3
450 DATA 1, 3, 3, 3, 3, 3, 3, 3, 3, 3, 3, 3, 3, 3
460 DATA 2, 73, 27, 22, 16, 12, 7, 2, 2, 3, 3, 1, 3, 3, 3
470 DATA 2, 3, 3, 3, 3, 3, 3, 3, 3, 3, 3, 3, 3, 3, 3
480 DATA 3, 3, 3, 3, 3, 3, 3, 3, 3, 3, 3, 3, 3, 3, 3
490 DATA 66, 45, 21, 23, 13, 6, 5, 3, 3, 3, 3, 3, 3, 3, 3
500 DATA 3, 3, 3, 3, 3, 3, 3, 3, 3, 3, 3, 3, 3, 3, 3
510 DATA 3, 3, 3, 3, 3, 3, 3, 3, 3, 3, 3, 3, 3, 3, 3
520 DATA 29, 23, 11, 7, 7, 9, 6, 2, 2, 3, 3, 1, 1, 1, 2
530 DATA 2, 3, 2, 2, 2, 1, 1, 1, 2, 3, 1, 3, 3, 2, 3
540 DATA 3, 3, 3, 3, 3, 3, 3, 3, 3, 3, 3, 3, 3, 3, 3
550 DATA 61, 53, 27, 27, 16, 13, 5, 5, 7, 5, 2, 2, 1, 2
560 DATA 2, 3, 3, 1, 3, 3, 3, 3, 3, 3, 3, 3, 3, 3, 3
570 DATA 3, 3, 3, 3, 3, 3, 3, 3, 3, 3, 3, 3, 3, 3, 3
580 DATA 25, 37, 21, 23, 11, 3, 9, 5, 4, 2, 2, 3, 1, 2
590 DATA 3, 3, 3, 3, 3, 3, 3, 3, 3, 3, 3, 3, 3, 3, 3
600 DATA 3, 3, 3, 3, 3, 3, 3, 3, 3, 3, 3, 3, 3, 3, 3
610 DATA 42, 52, 13, 23, 11, 12, 15, 3, 3, 1, 3, 3, 2, 3, 3
620 DATA 3, 3, 3, 3, 3, 3, 3, 3, 3, 3, 3, 3, 3, 3, 3
630 DATA 3, 3, 3, 3, 3, 3, 3, 3, 3, 3, 3, 3, 3, 3, 3
640 DATA 14, 53, 22, 26, 17, 17, 9, 4, 3, 3, 3, 3, 2, 3, 2
650 DATA 3, 3, 3, 3, 3, 3, 3, 3, 3, 3, 3, 3, 3, 3, 3
660 DATA 3, 3, 3, 3, 3, 3, 3, 3, 3, 3, 3, 3, 3, 3, 3
670 DATA 125, 91, 26, 19, 17, 13, 5, 3, 6, 5, 3, 3, 1, 1, 3
680 DATA 1, 3, 3, 2, 3, 3, 1, 1, 3, 1, 3, 1, 3, 1, 3
690 DATA 3, 3, 2, 3, 3, 3, 3, 3, 3, 3, 3, 3, 3, 1, 2
700 DATA 22, 36, 9, 5, 13, 3, 4, 4, 1, 3, 3, 3, 3, 2, 1
710 DATA 1, 2, 3, 3, 3, 3, 2, 1, 3, 3, 3, 3, 3, 3, 3
720 DATA 3, 3, 3, 3, 3, 3, 3, 3, 3, 3, 3, 3, 3, 3, 3
730 DATA 62, 61, 77, 29, 24, 16, 12, 3, 4, 3, 3, 3, 2, 2, 2
740 DATA 3, 3, 3, 3, 3, 3, 3, 3, 3, 3, 3, 3, 3, 3, 3
750 DATA 3, 3, 3, 3, 3, 3, 3, 3, 3, 3, 3, 3, 3, 3, 3
760 DATA 41, 33, 24, 12, 23, 11, 5, 7, 1, 1, 1, 1, 3, 3, 2
770 DATA 3, 3, 3, 3, 3, 3, 3, 3, 3, 3, 3, 3, 3, 3, 3
780 DATA 3, 3, 3, 3, 3, 3, 3, 3, 3, 3, 3, 3, 3, 3, 3
790 DATA 56, 39, 33, 39, 15, 14, 6, 2, 7, 3, 3, 1, 3, 3, 3
800 DATA 3, 3, 3, 3, 3, 3, 3, 3, 3, 3, 3, 3, 3, 3, 3
810 DATA 3, 3, 3, 3, 3, 3, 3, 3, 3, 3, 3, 3, 3, 3, 3
820 END

```

D

```
1  REM THIS PROGRAM IS FOR SETTING UP THE INTERDEPENDENCE OF
2  REM AVERAGE DROPLET DIAMETER, ENVELOPER CONCENTRATION AND
3  REM IMPELLER SPEED BY USE OF MULTIPLE REGRESSION.
110  N=15
120  DIM X(29)
130  DIM Y(11)
140  DIM Z(29)
150  FOR I=1 TO N
160  READ X(I)
165  X(I)=LOG(X(I))
170  NEXT I
180  FOR I=1 TO N
190  READ Y(I)
195  Y(I)=LOG(Y(I))
200  NEXT I
210  FOR I=1 TO N
220  READ Z(I)
225  Z(I)=LOG(Z(I))
230  NEXT I
240  LET T1=0
250  LET T2=0
260  LET T3=0
270  LET J1=0
280  LET J2=0
290  LET J3=0
300  LET F1=0
310  LET F2=0
320  LET F3=0
330  FOR I=1 TO N
340  LET T1=T1+X(I)
350  LET T2=T2+Y(I)
360  LET T3=T3+Z(I)
370  LET J1=J1+X(I)*Z(I)
380  LET J2=J2+Y(I)*X(I)
390  LET J3=J3+Y(I)*Z(I)
400  LET F1=F1+X(I) ** 2
410  LET F2=F2+Z(I) ** 2
420  LET F3=F3+Y(I) ** 2
430  NEXT I
440  LET Y1=T2/I
450  LET X1=T1/I
460  LET X2=T3/I
470  LET L1=F1-(X1 ** 2)/I
480  LET L2=J1-(X1*X2)/I
490  LET L3=F3-(X2 ** 2)/I
500  LET L4=J2-(X1*X2)/I
510  LET L5=J3-(X2*X3)/I
520  LET B1=(L4*L3-L5*L2)/(L1*L3-L2 ** 2)
530  LET B2=(L5*L1-L4*L2)/(L1*L3-L2 ** 2)
540  LET B3=Y1-B1*X1-B2*X2
545  B3=EXP(B3)
550  PRINT "B2=",B2
560  PRINT "B1=",B1
570  PRINT "B3=",B3
580  DATA 0.75,0.75,0.75,0.75,0.75
590  DATA 2.75,2.75,2.75,2.75,2.75
600  DATA 1.75,1.75,1.75,1.75,1.75
610  DATA 2.96234E-25,1.33543E-25,1.77412E-25,1.45373E-25,9.32693E-26
620  DATA 2.73025E-25,1.47247E-25,1.22302E-25,1.24324E-25,1.54256E-25
630  DATA 3.46353E-25,2.12693E-25,1.19414E-25,1.14077E-25,3.37543E-26
640  DATA 450,550,650,750,850
650  DATA 450,550,650,750,850
700  END
```

END

```
B2=
B1=
B3=
```

END

APPENDIX IV

COMPUTER PROGRAM FOR SMITH-EWART MODEL

```

C012          -TRACE 1
C000          TRACE 0
C001          MASTER SWMODEL
C002          C THIS PROGRAMME RECALCULATES THE SMITH-EWART MODEL FOR EMULSION
C003          C POLYMERIZATION OF STYRENE
C004          C
C005          DIMENSION T1(8)
C006          COMMON /A/KP,KD,DM,DP,FI,NA,AS,SCMC
C007          REAL KP,KD,NA,K,MO,N10,MI
C008          C
C009          C INPUT DATA . KP(CC/MOLE.MIN),FI(%),NA(MOLECULES/CCW),DM(GRAM/CC),
C010          C DP(GRAM/CC),AS(SQCM/MOLECLES),KD(1/S),SCMC(GRAM/LW),T(MIN),SO(GRAM
C011          C /LW),MO(GRAM/CCW),RO(GRAM/LW)
C012          C
C013          DO 9999 I1=1,3
C014          READ(1,1) SO,MO,RO
C015          1 FORMAT(3F0.0)
C016          WRITE(2,391)
C017          391 FORMAT(////2X,'INITIAL DATA: AMOUNT OF SOAP SO; AMOUNT OF MONOMER
C018          * MO;AMOUNT OF INITIATOR RO'/2X,77(1H*)///10X,'SO(G/LW)',6X,
C019          *'MO(G/CCW)',7X,'RO(G/LW)')
C020          WRITE(2,392) SO,MO,RO
C021          392 FORMAT(/,3F15.2//2X,77(1H*)//)
C022          IF(SO.LT.2.5) GOTO 2
C023          T9=0.025
C024          DO 3 L=1,8
C025          T1(L)=2.0*T9
C026          T9=T1(L)
C027          3 CONTINUE
C028          GOTO 8
C029          2 T9=0.01
C030          DO 9 L=1,8
C031          T1(L)=2.0*T9
C032          T9=T1(L)
C033          9 CONTINUE
C034          8 CALL STAGE1(SO,MO,RO,R,T1,V10,N10,TB)
C035          CALL STAGE2(V10,N10,TB,MO,DM,DP,FI,KP,NA,R,T2,VP)
C036          CALL STAGE3(T2,VP,FI,KP,NA,N10,DM,DP,MO,MI,C.5)
C037          9999 CONTINUE
C038          STOP
C039          END

```

END OF SEGMENT, LENGTH 115, NAME SWMODEL

```

C040          BLOCK DATA
C041          COMMON /A/KP,KD,DM,DP,FI,NA,AS,SCMC
C042          REAL KP,KD,NA
C043          DATA KP,KD,DM,DP,FI,NA,AS,SCMC/1.27E7,5.7E-5,0.906,1.057,0.605,
C044          16.023E23,3.5E-15,0.5/
C045          END

```

```

C046          SUBROUTINE STAG1(SO,MO,RO,R,T1,V10,N10,TB)
C047          DIMENSION T1(8),A1(8),T(10),A(10),V(10),N(10),D(10),SM(10),X(10)
C048          COMMON /A/KP,KD,DM,DP,FI,NA,AS,SCMC
C049          REAL KP,KD,NA,K,MO,N,MI,N10
C050          C
C051          C FIX CONSTANTS
C052          C
C053          S=NA*AS*SO/(272.0*1000.0)
C054          R=2.0*KD*NA*RO/(270.0*1000.0)
C055          K=(3.0/(4.0*3.14159))*(KP/NA)*(DM/DP)*(FI/(1.0-FI))
C056          B=4.0*3.14159*K**((2.0/3.0)*R/S)
C057          C=(4.0*3.14159/3.0)*K+R/S
C058          C
C059          C FIND THE RELATIONSHIP BETWEEN TIME T1 AND THE AREA OF PARTICLES IN ONE
C060          C CC WATER A1
C061          DO 400 I=1,8
C062          IF(.NOT.I.EQ.1) GOTO300
C063          A1(I)=0.587*B*S*T1(I)**(5.0/3.0)
C064          GOTO400
C065          300 A1(I)=B*T1(I)**(5.0/3.0)*(0.587*S-0.42*A1(I-1))
C066          400 CONTINUE
C067          C
C068          C FIND THE TIME TB WHEN PARTICLENUCLEATION IS JUST COMPLETE
C069          C
C070          CALL CHAZHI(A1,T1,S,S,TB)

```

```

C071      C
C072      C  CALCULATE A SERIES OF VALUES OF PARAMETERS ALONG THE HISTORY OF
C073      C  POLYMERIZATION DURING THE STAGE ONE
C074          WRITE(2,450)
C075      450 FORMAT(//2X,'THE RESULTS CALCULATED ALONG THE REACTION HISTORY OF
C076          1STAGE ONE'/2X,62(1H=)//)
C077          WRITE(2,500)
C078      500 FORMAT(//8X,'TIME(MIN)',4X,'CONVERSION(Z)',3X,'S(MIC)(G/LW)',2X,
C079          2'AP(SQCM/CCW)',3X,'VP(CC/CCW)',4X,'DP(MICRON)',5X,'N(PARS/CCW)')
C080          DO 600 I=1,10
C081          T(I)=(TB/10.0)*FLOAT(I)
C082      600 CONTINUE
C083          DO 800 J=1,10
C084          CALL CHAZHI(T1,A1,S,T(J),A(J))
C085          TH=T(J)/2.0
C086          CALL CHAZHI(T1,A1,S,TH,AH)
C087          N(J)=(R/S)*T(J)+(S-A(J))/6.0-(2.0/3.0)*AH)
C088          V(J)=(T(J)**2/6.0)*(3.0*C*S-2.0*C*AH)
C089          D(J)=(V(J)/A(J))*60000.0
C090          X(J)=V(J)*(1.0-FI)+DP/MO*100.0
C091          SM(J)=(S-A(J))/AS/NA*272.0*1000.0
C092          WRITE(2,700) T(J),X(J),SM(J),A(J),V(J),D(J),N(J)
C093      700 FORMAT(/5X,DPF10.3,2F15.3,1P4E15.3)
C094      800 CONTINUE
C095          MI=1.44*KP*FI*DM*N(10)/R
C096          WRITE(2,190)
C097      190 FORMAT(//2X,'THE VALUES OF PARAMETERS AT THE END OF STAGE ONE',
C098          3//8X,'TIME(MIN)',4X,'CONVERSION(Z)',3X,'S(MIC)(G/LM)',2X,'AP(SQCM/
C099          4CCW)',2X,'VP(CC/CCW)',4X,'DP(MICRON)',5X,'MLEC.WT.',4X,'N(PARS/CC
C100          5W)')//)
C101          WRITE(2,191) T(10),X(10),SM(10),A(10),V(10),D(10),MI,N(10)
C102      191 FORMAT(/5X,F10.3,2F15.3,1P3E15.3,DPF15.0,1PE15.3)
C103          N10=N(10)
C104          V10=V(10)
C105          RETURN
C106          END

```

END OF SEGMENT, LENGTH 395, NAME STAGE1

```

C107      SUBROUTINE STAG=2(VI,NI,TB,MO,DM,DP,FI,KP,NA,R,T2,VP)
C108      REAL NI,NP,NT,NA,MO,KP,MI
C109          VDO=MO/DM
C110          VP=VI
C111          VD1=VDO-VP*(FI+(1.0-FI)*DP/DM)
C112          NT=NI
C113          T2=TB
C114          DELTAT=1.0
C115          WRITE(2,210)
C116      210 FORMAT(//2X,'THE RESULTS CALCULATED ALONG THE REACTION HISTORY OF
C117          2STAGE TWO'/2X,62(1H=)//8X,'TIME(MIN)',4X,'CONVERSION(Z)',3X,
C118          3'AP(SQCM/CCW)',3X,'VP(CC/CCW)',4X,'DP(MICRON)',4X,'VD(CC/CCW)')//)
C119          B=0.5*(KP/NA)*(DM/DP)*FI*NT
C120      C
C121      C  CALCULATE A SERIES OF VALUES OF PARAMETERS ALONG THE HISTORY OF POLYMERIZATI
C122      C  DURING THE STAGE TWO
C123      C
C124          DO 240 I=1,10000
C125          DO 220 J=1,2
C126          IF(VD1.LE.0.0) GO TO 250
C127          DELTAV=B*DELTAT/(1.0-FI)
C128          VP=VP+DELTAV
C129          DPA=(6.0*VP/(3.14159*NT))**((1.0/3.0)*10000.0
C130          AP=(VP/DPA)*60000.0
C131          VD1=VD1-DELTAV*(FI+(1.0-FI)*DP/DM)
C132          T2=T2+DELTAT
C133          X2=VP*(1.0-FI)*DP/MO*100.0
C134      220 CONTINUE
C135          WRITE(2,230) T2,X2,AP,VP,DPA,VD1
C136      230 FORMAT(/5X,DPF10.3,F15.3,1P4E15.3)
C137      240 CONTINUE
C138      250 MI=2.0*B*NA*DP/A
C139          WRITE(2,260)
C140      260 FORMAT(//2X,'THE VALUES OF PARAMETERS AT THE END OF STAGE TWO',
C141          5//8X,'TIME(MIN)',4X,'CONVERSION(Z)',2X,'AP(SQCM/CCW)',2X,'VP(CC/
C142          6CCW)',4X,'DP(MICRON)',4X,'VD(CC/CCW)',5X,'MLEC.WT.',//)
C143          WRITE(2,270) T2,X2,AP,VP,DPA,VD1,MI
C144      270 FORMAT(/5X,F10.3,F15.3,1P4E15.3,DPF15.0)
C145          RETURN
C146          END

```

END OF SEGMENT, LENGTH 219, NAME STAGE2

```
0147          SUBROUTINE STAGE3(T2,VP,FI,KP,NA,NT,DM,DP,MO,MI,Q)
0148          REAL MO,NI,KP,NA,NT,MI
0149          WRITE(2,310)
0150          310 FORMAT(/2X,'THE RESULTS CALCULATED ALONG THE REACTION HISTORY OF
0151          6STAGE THREE'/2X,64(1H=)//8X,'TIME(MIN)',4X,'CONVERSION(X)',2X,
0152          5*AP(SQCM/CCW)',3X,'VP(CCC/CCW)',4X,'DP(MICRON)',4X,'VMP(CCC/CCW)'/)
0153          VMP=VP*FI
0154          T3=T2
0155          DELTAT=1.0
0156          X3=0.0
0157          DO 360 I=1,100
0158          DO 340 J=1,5
0159          IF(X3.GE.95.0) GOTO370
0160          RATE=(KP/NA)*(VMP/VP)*(NT*Q)
0161          VMP=VMP-RATE*DELTAT
0162          VP=VP-RATE*DELTAT*(1.0-DM/DP)
0163          AP=(NT*3.14159)**(1.0/3.0)*(6.0*VP)**(2.0/3.0)
0164          DP3=(VP/AP)*60000.0
0165          X3=(1.0-VMP*DM/MO)*100.0
0166          T3=T3+DELTAT
0167          340 CONTINUE
0168          WRITE(2,350) T3,X3,AP,VP,DP3,VMP
0169          350 FORMAT(/5X,DPF10.3,F15.3,1P4E15.3)
0170          360 CONTINUE
0171          370 WRITE(2,380)
0172          380 FORMAT(/2X,'THE FINAL RESULTS OF THE CALCULATION',/2X,36(1H=)//
0173          87X,'TIME(MIN)',4X,'CONVERSION(%)',2X,'N(PARTICLES)',3X,'DP3(MICRON)',
0174          9)*,4X,'MOLECULE.WT.)/)
0175          WRITE(2,390) T3,X3,NT,DP3,MI
0176          390 FORMAT(/5X,F10.3,F15.3,1P2E15.3,DPF15.1)
0177          RETURN
0178          END
```

END OF SEGMENT, LENGTH 192, NAME STAGE3

```
0179          SUBROUTINE CHAZHI(A,B,N,X,Y)
0180          DIMENSION A(N),B(N)
0181          NC=N
0182          N=N-1
0183          DO 1 J=1,N
0184          IF((X-A(J))*(X-A(J+1))) 10,10,1
0185          10 I=J
0186          GOTO 22
0187          1 CONTINUE
0188          IF(ABS(X-A(1))-ABS(X-A(N))) 20,21,21
0189          20 I=1
0190          GOTO 22
0191          21 I=N-1
0192          22 IF(I-N+1) 24,23,24
0193          23 I=I-1
0194          GOTO 27
0195          24 IF(I-1) 25,27,25
0196          25 IF(ABS(X-A(I))-ABS(X-A(I+1))) 26,27,27
0197          26 I=I-1
0198          27 V=0.0
0199          IF(I-N) 29,28,28
0200          28 I=I-1
0201          29 L=I+2
0202          DO 2 K=I,L
0203          W=B(K)
0204          DO 3 J=I,L
0205          IF(J-K) 30,3,30
0206          30 W=(X-A(J))/(A(K)-A(J))*W
0207          3 CONTINUE
0208          V=V+W
0209          2 CONTINUE
0210          Y=V
0211          N=NC
0212          RETURN
0213          END
```

END OF SEGMENT, LENGTH 179, NAME CHAZHI

C214 FINISH

APPENDIX V

COMPUTER PROGRAM FOR STAGE I AND STAGE II IN UNBAFFLED REACTOR

```

C012          TRACE 1
C000          TRACE 0
C001          MASTER UNSTABLE MODEL
C002          C
C003          C THIS PROGRAMME SIMULATES THE EMULSION POLYMERIZATION . THE MODEL
C004          C PROPOSED TAKES INTO ACCOUNT THE SOAP ADSORBED ONTO THE SURFACE OF
C005          C MONOMER DROPLETS. THE REACTOR USED IS UNGAFFLED. AND THE PROGRESS OF
C006          C OF STAGE TWO IS CONSIDERED AS UNSTABLE
C007          C
C008          C
C009          C DIMENSION T1(8)
C010          C COMMON /A/KP,KD,DM,DP,FI,NA,AS,SCMC
C011          C REAL KP,KD,NA,K,MO,N10,MI
C012          C
C013          C INPUT DATA . KP(CC/MOLE.MIN),FI(X),NA(MOLECULES/CCW),DM(GRAM/CC),
C014          C DP(GRAM/CC),AS(SQCM/MOLECLES),KD(1/S),SCMC(GRAM/LW),T(MIN),SO(GRAM
C015          C /LW),MO(GRAM/CCW),RO(GRAM/LW)
C016          C
C017          C SO=5.0
C018          C MO=0.5
C019          C RO=1.25
C020          C H=7.5
C021          C REV=410
C022          C WRITE(2,391)
C023          C 391 FORMAT(//////2X,'INITIAL DATA: AMOUNT OF SOAP SO;AMOUNT OF MONOME
C024          C * MO; AMOUNT OF INITIATOR RO; DIAMETER OF IMPELLER H; IMPELLER SPE
C025          C *ED REV',/2X,118(1H*)//1CX,'SO(G/LW)',6X,'MO(G/CCW)',7X,'RO(G/LW)
C026          C *,8X,'H(CM)',8X,'REV(RPM)')
C027          C WRITE(2,392) SO,MO,RO,H,REV
C028          C 392 FORMAT(/,5F15.2///2X,118(1H*)//)
C029          C IF(SO.LE.2.5) GOTO 2
C030          C T9=0.025
C031          C DO 3 L=1,8
C032          C T1(L)=2.0*T9
C033          C T9=T1(L)
C034          C 3 CONTINUE
C035          C GOTO 8
C036          C 2 T9=0.01
C037          C DO 9 L=1,8
C038          C T1(L)=2.0*T9
C039          C T9=T1(L)
C040          C 9 CONTINUE
C041          C 8 CALL STAGE1(SO,MO,RO,S,R,K,T1,V10,N10,T10,TB,REV,H,X10)
C042          C CALL UNSTA(N10,T10,MO,RO,X10)
C043          C STOP
C044          C END

```

END OF SEGMENT, LENGTH 101, NAME UNSTABLEMODEL

```

C044          BLOCK DATA
C045          C COMMON /A/KP,KD,DM,DP,FI,NA,AS,SCMC
C046          C REAL KP,KD,NA
C047          C DATA KP,KD,DM,DP,FI,NA,AS,SCMC/1.27E7,5.7E-5,0.906,1.057,0.605,
C048          C 36.023E23,3.5E-15,0.5/
C049          C END

```

```

C050          SUBROUTINE STAG=1(SO,MO,RO,S,R,K,T1,V10,N10,T10,TB,REV,H,X10)
C051          C DIMENSION T1(8),A1(8),T(10),A(10),V(10),N(10),D(10),SM(10),X(10)
C052          C DIMENSION V1(8),VD(10),DD(10),AD(10),VD1(8),DD1(8),AD1(8),AM1(8)
C053          C COMMON /A/KP,KD,DM,DP,FI,NA,AS,SCMC
C054          C REAL KP,KD,NA,K,MO,N,MI,NDO,N10
C055          C XX=-1.03
C056          C Y=-0.185
C057          C REVI=845.0
C058          C HI=7.5
C059          C DDI=13.07
C060          C S=NA*AS*(SO-SCMC)/(272.0+1000.0)
C061          C R=2.0*KD*NA*RO/(270.0+1000.0)
C062          C K=(3.0/(4.0+3.14159))*(KP/NA)*(DM/DP)*(FI/(1.0-FI))
C063          C
C064          C CALCULATE DEGREE OF DISPERSION BEFORE REACTION
C065          C

```

```

0066          VDO=MO/DM
0067          DDO=DDI*(REV/REVI)**XX*(H/HI)**Y
0068          NDO=6.0*VDO/(3.14159*DDO**3)*1.0E 12
0069          ADO=(VDO/DDO)*60000.0
0070          C
0071          C   FIX THE CONSTANTS
0072          C
0073          B1=4.0*3.14159*K*(2.0/3.0)*R/S
0074          B2=3.0*(4.0*3.14159*NDO)**(1.0/2.0)*VDO
0075          DSW=0.966
0076          B3=3.0*(4.0*3.14159*NDO)**(1.0/2.0)*(DSW/DM)
0077          B4=3.52*S-ADO
0078          C1=(4.0*3.14159/3.0)*(K*R/S)
0079          C2=3.0*S-ADO
0080          Z1=R/(6.0*S)
0081          Z2=6.0*S-ADO
0082          C
0083          C   FIND THE RELATIONSHIP BETWEEN TIME T1 AND THE AREA OF PARTICLES IN ONE CC WAT
0084          C
0085          DO 420 I=1,8
0086          IF(.NOT.I.EQ.1) GOTO410
0087          A1(I)=0.587*B1*(S-ADO)*T1(I)**(5.0/3.0)
0088          V1(I)=(C1/2.0)*(S-ADO)*T1(I)**2
0089          GOTO 481
0090          410 A1(I)=(B1/6.0)*(B4-2.52*A1(I-1)-2.52*(B2-B3*V1(I-1))**(2.0/3.0))
0091             *T1(I)**(5.0/3.0)
0092          V1(I)=(C1/6.0)*(C2-2.0*A1(I-1)-2.0*(B2-B3*V1(I-1))**(2.0/3.0)
0093             3*T1(I)**2
0094          481 AD1(I)=(B2-B3*V1(I))**(2.0/3.0)
0095          AM1(I)=S-A1(I)-AD1(I)
0096          420 CONTINUE
0097          C
0098          C   FIND THE TIME TB WHEN PARTICLE NUCLEATION IS JUST COMPLETE
0099          C
0100          H1=10.0
0101          TB=0.365*(S/R)**0.6/K**0.4
0102          CALL CHAZHI(T1,AM1,8,TB,AMB)
0103          471 IF(AMB.GT.H1) GOTO477
0104          IF(AMB.LT.(-H1)) GOTO475
0105          GOTO436
0106          476 DO 435 I=1,1000
0107          CALL CHAZHI(T1,AM1,8,TB,AM)
0108          IF(ABS(AM).LE.H1) GOTO436
0109          IF(AM.GT.H1) GOTO478
0110          TB=TB-0.01
0111          435 CONTINUE
0112          478 H1=H1+10.0
0113          GOTO471
0114          477 DO 441 I=1,1000
0115          CALL CHAZHI(T1,AM1,8,TB,AM)
0116          IF(ABS(AM).LT.H1) GOTO436
0117          IF(AM.LT.(-H1)) GOTO478
0118          TB=TB+0.01
0119          441 CONTINUE
0120          C
0121          C   CALCULATE A SERIES OF VALUES OF PARAMETERS ALONG THE HISTORY OF
0122          C   POLYMERIZATION DURINGTHE STAGE ONE
0123          C
0124          436 WRITE (2,440)
0125          440 FORMAT(/2X,'THE RESULTS CALCULATED ALONG THE REACTION HISTORY OF
0126          1STAGE ONE'/2X,62(1H=)/)
0127          WRITE(2,444)
0128          444 FORMAT(/8X,'TIME(MIN)',4X,'CONVERSION(%)',4X,'SM(G/LW)',3X,'AP(SG
0129          *CM/CCW)',4X,'VP(CC/CCW)',5X,'DP(MICRON)',4X,'N(PARS/CC*)',5X,'VD(CC/CCW)/)
0130          *C/CCW)/)
0131          DO 460 I=1,10
0132          T(I)=(TB/10.0)*FLOAT(I)
0133          460 CONTINUE
0134          DO 480 J=1,10
0135          CALL CHAZHI(T1,T(I),8,T(J),A(J))
0136          CALL CHAZHI(T1,V1,8,T(J),V(J))
0137          TH=T(J)/2.0
0138          CALL CHAZHI(T1,T(I),8,TH,AH)
0139          CALL CHAZHI(T1,V1,8,TH,VH)
0140          N(J)=Z1*T(J)*(2.0-A(J)-(B2-B3*V(J))**(2.0/3.0))-4.0*AH-4.0*(B2-B3*VH
0141          1)**(2.0/3.0))

```

```

0142      D(J)=(V(J)/A(J))*60000.0
0143      X(J)=V(J)*(1.0-FI)*DP/MO*100.0
0144      VD(J)=VDO-V(J)*PSW/DM
0145      DD(J)=(6.0/3.14159)*(VD(J)/NDO)**(1.0/3.0)
0146      AD(J)=(VD(J)/DD(J))*6.0
0147      SM(J)=(S-A(J)-AD(J))/AS/NA*272.0*1000.0
0148      WRITE(2,470) T(J),X(J),SM(J),A(J),V(J),D(J),N(J),VD(J)
0149 470 FORMAT(/5X,OPF10.3,2F15.3,1P5E15.3)
0150 480 CONTINUE
0151      MI=1.44*KP*FI*DM*N(10)/R
0152      WRITE(2,490)
0153 490 FORMAT(/2X,'THE VALUES OF PARAMETERS AT THE END OF STAGE ONE',
0154 3//8X,'TIME(MIN)',4X,'CONVERSION(Z)',3X,'S(MIC)(G/LM)',2X,'AP(SGC+
0155 4CCW)',3X,'VP(CC/CCW)',5X,'DP(MICRON)',5X,'MCLEC.WT.',5Y,'N(PARS/C
0156 5W)')//)
0157      WRITE(2,494) T(10),X(10),SM(10),A(10),V(10),D(10),MI,N(10)
0158 494 FORMAT(/5X,F10.3,2F15.3,1P3E15.3,OPF15.0,1PE15.3)
0159      V10=V(10)
0160      X10=X(10)
0161      T10=T(10)
0162      N10=N(10)
0163      RETURN
0164      END

```

END OF SEGMENT, LENGTH 770, NAME STAGE1

```

0165      SUBROUTINE CHAZHI(A,B,N,X,Y)
0166      DIMENSION A(N),E(N)
0167      NC=N
0168      N=N-1
0169      DO 1 J=1,N
0170      IF((X-A(J))*(X-A(J+1))) 10,10,1
0171 10 I=J
0172      GOTO 22
0173 1 CONTINUE
0174      IF(ABS(X-A(1))-ABS(X-A(N))) 20,21,21
0175 20 I=1
0176      GOTO 22
0177 21 I=N-1
0178 22 IF(I-N+1) 24,23,24
0179 23 I=I-1
0180      GOTO 27
0181 24 IF(I-1) 25,27,25
0182 25 IF(ABS(X-A(I))-ABS(X-A(I+1))) 26,27,27
0183 26 I=I-1
0184 27 V=0.0
0185      IF(I=N) 29,28,29
0186 28 I=I-1
0187 29 L=I+2
0188      DO 2 K=I,L
0189      W=B(K)
0190      DO 3 J=I,L
0191      IF(J-K) 30,3,30
0192 30 W=(X-A(J))/(A(K)-A(J))*W
0193 3 CONTINUE
0194      V=V+W
0195 2 CONTINUE
0196      Y=V
0197      N=NC
0198      RETURN
0199      END

```

END OF SEGMENT, LENGTH 179, NAME CHAZHI

```

0200      SUBROUTINE UNSTF(NP,TO,MC,RC,XO)
0201      DIMENSION F(25),AM(25),AK(25),C(25),YY(25),Y1(25),Y2(25),Y3(25)
0202      COMMON G
0203      COMMON /A/KP,KD,DM,DP,FI,NA
0204      REAL NP,MO,NA,KF,MI,KD
0205      DO 610 I=1,25
0206      F(I)=0.0
0207 610 CONTINUE

```



```

0208          F(1)=X0
0209          F(2)=0.5
0210          F(3)=0.5
0211          Q=0.5
0212          WRITE(2,888)
0213      888  FORMAT(//2X,'THE RESULTS CALCULATED ALONG THE REACTION HISTO
* OF STAGE TWO'/2X,62(1H=))
0214          WRITE(2,999)
0215      999  FORMAT(//6X,'II',3X,'T(MIN)',8X,'Q',10X,'X(X)',10X,
*'FO',13X,'F1',13X,'F2',13X,'F3'/)
0216          N=10
0217          H=0.000025
0218          C(1)=0.5
0219          C(2)=0.5
0220          C(5)=0.5
0221          C(3)=1.0
0222          C(4)=1.0
0223          EPS=1.0E-4
0224          CUSI=47691.0
0225          DO 657 I=3,N-5
0226          AK(I)=0.0
0227      657  CONTINUE
0228          AK(1)=1.0
0229          R=2.0*KD*NA*RO/(270.0*1000.0)
0230          B=0.5*(KP/NA)*(DM/DP)*FI*NP
0231          G=R*MO/(200.0*NP*B*DP)
0232          D=200.0*B*DP/MO
0233          T=T0
0234          DO 50 II=1,200000
0235      50  DO 670 KK=1,100
0236          Q0=Q
0237          X0=F(1)
0238          CALL RUKB(N,H,C,EPS,F,AM,AK,G,YY,Y1,Y2,Y3,CUSI)
0239      420  SIGMAF=0.0
0240          DO 666 M=2,N-5
0241          SIGMAF=SIGMAF+F(M)
0242      666  CONTINUE
0243          DO 660 L=2,N-5
0244          F(L)=F(L)/SIGMAF
0245      660  CONTINUE
0246          Q=0.0
0247          DO 651 M=3,N-5
0248          Q=Q+FLOAT(M-2)*F(M)
0249      651  CONTINUE
0250          T=T+(F(1)-X0)/(D*Q0)
0251      670  CONTINUE
0252          WRITE(2,1000) II,T,Q,F(1),F(2),F(3),F(4),F(5)
0253      1000  FORMAT(/2X,I6,3F12.7,1P4E15.6)
0254          IF(F(1).GE.43.0) GOTO 705
0255          50  CONTINUE
0256          705  RETURN
0257          END
0258
0259

```

END OF SEGMENT, LENGTH 277, NAME UNSTA

```

0260          SUBROUTINE RUKB(N,H,C,EPS,Y,AM,AK,G,YY,Y1,Y2,Y3,CUSI)
0261          DIMENSION Y(N),M(N),AK(N),C(N),YY(N),Y1(N),Y2(N),Y3(N)
0262          COMMON G
0263          CALL RUKU(N,Y,Y1,AM,AK,H,G,CUSI,C)
0264      500  H=H/2.0
0265          CALL RUKU(N,Y,Y2,AM,AK,H,G,CUSI,C)
0266          CALL RUKU(N,Y2,Y3,AM,AK,H,G,CUSU,C)
0267          DO 197 I=2,N-5
0268          IF(Y3(I).LT.0.0.OR.Y2(I).LT.0.0) GOTO 72
0269          D=ABS(Y3(I)-Y1(I))
0270          IF(D.GT.EPS) GOTO 72
0271      197  CONTINUE
0272          GOTO 73
0273          72  DO 194 I=2,N-5
0274          Y1(I)=Y2(I)
0275      194  CONTINUE

```

```

0276          GOTO 500
0277          73 IF(D-EPS/32.0) 22,23,23
0278          22 H=4.0*H
0279          GOTO 292
0280          23 H=2.0*H
0281          292 DO 193 I=1,N-5
0282          Y(I)=Y3(I)
0283          193 CONTINUE
0284          RETURN
0285          END

```

END OF SEGMENT, LENGTH 187, NAME RUKB

```

0286          SUBROUTINE RUKU(N,Y,YY,AM,AK,H,Q,CUSI,C)
0287          DIMENSION Y(N),YY(N),C(N),AM(N),AK(N)
0288          COMMON G
0289          DO 30 I=1,N-5
0290          AM(I)=Y(I)
0291          YY(I)=Y(I)
0292          30 CONTINUE
0293          DO 22 J=1,4
0294          CALL RKFF(N,AM,AK,Q,CUSI)
0295          DO 201 I=1,N-5
0296          W=H*AK(I)
0297          IF(J.EQ.4) GOTO 31
0298          AM(I)=W+C(J)+Y(I)
0299          31 YY(I)=W+C(J+1)/3.0+YY(I)
0300          201 CONTINUE
0301          22 CONTINUE
0302          RETURN
0303          END

```

END OF SEGMENT, LENGTH 138, NAME RUKU

```

0304          SUBROUTINE RKFF(N,AM,AK,Q,CUSI)
0305          DIMENSION AM(N),AK(N)
0306          COMMON G
0307          A=G/Q
0308          B=CUSI/(AM(1)*Q)
0309          AK(2)=A+(-AM(2))+B*(2.0*AM(4))
0310          DO 650 L=3,N-5
0311          AK(L)=A*(AM(L-1)-AM(L))+B*(FLOAT(L*(L-1))
0312          #*AM(L+2)-FLOAT((L-2)*(L-3))*AM(L))
0313          650 CONTINUE
0314          RETURN
0315          END

```

END OF SEGMENT, LENGTH 115, NAME RKFF

0316 FINISH

END OF COMPILATION - NO ERRORS

APPENDIX VI

COMPUTER PROGRAM FOR GEL-EFFECT

```

0012          TRACE 1
0000          TRACE 0
0001          MASTER GELEFF1
0002          DIMENSION F(25),AM(25),AK(25),C(25),YY(25),Y1(25),Y2(25),Y3(25)
0003          DIMENSION AFO(500),AF1(500),AF2(500),AF3(500),AF4(500),AF5(500),
0004          AAG(500),AZ(500),AT(500)
0005          COMMON /G1/A1,A2,A3,A4,A5,KP
0006          COMMON /B2/G,DP,DM,GT
0007          REAL NP,MO,NA,KF,KD
0008          DO 610 I=4,25
0009          F(I)=0.0
0010          610 CONTINUE
0011          F(1)=0.4857612
0012          F(2)=0.4999665
0013          F(3)=0.4999933
0014          F(4)=3.34648E-5
0015          F(5)=6.739512E-6
0016          Q=0.5000804
0017          TO=51.2626822
0018          N=10
0019          NP=8.08E14
0020          RO=2.5
0021          MO=0.5
0022          A1=29.5873
0023          A2=-7.43322
0024          A3=45.3577
0025          A4=-95.9184
0026          A5=47.4095
0027          KP=1.27E7
0028          NA=6.023E23
0029          FI=0.605
0030          DP=1.057
0031          DM=0.905
0032          KD=5.7E-5
0033          H=0.000025
0034          C(1)=0.5
0035          C(2)=0.5
0036          C(5)=0.5
0037          C(3)=1.0
0038          C(4)=1.0
0039          EPS=1.0E-4
0040          DO 657 I=3,N-5
0041          AK(I)=0.0
0042          657 CONTINUE
0043          AK(1)=1.0
0044          R=2.0*KD*NA*RO/(270.0*1000.0)
0045          B=.5*(KP/NA)*(D*/DP)*FI*NP
0046          G=R*(NA/NP**2)*(MO/(DM*KP))
0047          GT=G*(DM/DP-1.0)
0048          D=2.0*B*DP/MO
0049          T=TO
0050          DO 50 I1=751,200000
0051          IF(F(N-5).LT.1.0E-4) GOTG 703
0052          N=N+1
0053          703 DO 670 KK=1,100
0054          Q=Q
0055          XQ=F(1)
0056          CALL RUKB(N,H,C,EPS,F,AM,AK,Q,YY,Y1,Y2,Y3)
0057          420 SIGMAF=0.0
0058          DO 666 M=2,N-5
0059          SIGMAF=SIGMAF+F(M)
0060          666 CONTINUE
0061          DO 660 L=2,N-5
0062          F(L)=F(L)/SIGMAF
0063          660 CONTINUE
0064          Q=0.0
0065          DO 651 M=3,N-5
0066          Q=Q+FLOAT(M-2)*F(M)
0067          651 CONTINUE
0068          D10=(D/FI)+F10(F(1))
0069          T=T+(F(1)-XQ)/(D10+Q)
0070          670 CONTINUE
0071          WRITE(2,1000) I1,T,Q,F(1),F(2),F(3),F(4),F(5),F(6)
0072          1000 FORMAT(/2X,I6,3F12.7,1P5E15.6)
0073          IF(F(1).GE.0.98) GOTG 705
0074          50 CONTINUE

```

0075 705 STOP
0076 END

END OF SEGMENT, LENGTH 306, NAME GLEFF1

```

0077 SUBROUTINE RUKB(N,H,C,EPS,Y,AM,AK,Q,YY,Y1,Y2,Y3)
0078 DIMENSION Y(N),H(N),AK(N),C(N),YY(N),Y1(N),Y2(N),Y3(N)
0079 CALL RUKU(N,Y,Y1,AM,AK,H,Q,C)
0080 CALL RUKU(N,Y,Y2,AM,AK,H,Q,C)
0081 CALL RUKU(N,Y,Y3,AM,AK,H,Q,C)
0082 DO 197 I=2,N-5
0083 IF(Y3(I).LT.0.0.OR.Y2(I).LT.0.0) GOTO 72
0084 D=ABS(Y3(I)-Y1(I))
0085 IF(D.GT.EPS) GOTO 72
0086 197 CONTINUE
0087 GOTO 73
0088 72 DO 194 I=2,N-5
0089 Y1(I)=Y2(I)
0090 194 CONTINUE
0091 GOTO 500
0092 500 IF(D-EPS/32.0) 22,23,23
0093 22 H=4.0*H
0094 GOTO 292
0095 23 H=2.0*H
0096 292 DO 193 I=1,N-5
0097 Y(I)=Y3(I)
0098 193 CONTINUE
0099 RETURN
0100 END
0101
0102

```

END OF SEGMENT, LENGTH 173, NAME RUKB

```

0103 SUBROUTINE RUKU(N,Y,YY,AM,AK,H,2,C)
0104 DIMENSION Y(N),YY(N),C(N),AM(N),AK(N)
0105 DO 30 I=1,N-5
0106 AM(I)=Y(I)
0107 YY(I)=Y(I)
0108 30 CONTINUE
0109 DO 22 J=1,4
0110 CALL RKFF(N,AM,AK,Q)
0111 DO 201 I=1,N-5
0112 W=H*AK(I)
0113 IF(J.EQ.4) GOTO 31
0114 AM(I)=W*C(J)+Y(I)
0115 31 YY(I)=W*C(J+1)/3.0+YY(I)
0116 201 CONTINUE
0117 22 CONTINUE
0118 RETURN
0119 END
0120

```

END OF SEGMENT, LENGTH 131, NAME RUKU

```

0121 SUBROUTINE RKFF(N,AM,AK,4)
0122 DIMENSION AM(N),AK(N)
0123 P1=FU(AM(1))/Q
0124 P2=TK(AM(1))/Q
0125 AK(2)=P1*(-AM(2))+P2*(2.0*AM(4))
0126 DO 650 L=3,N-5
0127 AK(L)=P1*(AM(L-1)-AM(L))+P2*(FLOAT(L*(L-1))*AM(L+2)
0128 -FLOAT((L-2)*(L-3))*AM(L))
0129 650 CONTINUE
0130 RETURN
0131 END
0132

```

END OF SEGMENT, LENGTH 114, NAME RKFF

```

0133
0134          FUNCTION TK(X)
0135          COMMON /G1/A1,A2,A3,A4,A5,KP
0136          REAL KP
0137          Y=A1+A2*X+A3*X**2+A4*X**3+A5*X**4
0138          TK=EXP(Y)/(KP*(1.0-X))
0139          RETURN
0140          END

```

END OF SEGMENT, LENGTH 46, NAME TK

```

0141
0142          FUNCTION FU(X)
0143          COMMON /B2/G,DP,DM,GT
0144          FU=(G+GT*X)/(1.0-X)
0145          RETURN
0146          END

```

END OF SEGMENT, LENGTH 19, NAME FU

```

0147          FUNCTION F10(X)
0148          COMMON /B2/G,DP,DM
0149          F10=(1.0-X)/((X+DM/DP)+(1.0-X))
0150          RETURN
0151          END

```

END OF SEGMENT, LENGTH 20, NAME F10

```

0152          FINISH
END OF COMPILATION - NO ERRORS

```

APPENDIX VII

COMPUTER PROGRAM FOR BAFFLED REACTOR

```

0012          TRACE 1
0000          MASTER BAFFLE
0001          C
0002          C THIS PROGRAM SIMULATES EMULSION POLYMERIZATION OF STYRENE .IT PASED ON FAST
0003          C TERMINATION RATE WITHIN LATEX PATICLES
0004          C
0005          DIMENSION T1(8)
0006          COMMON /A/KP,KD,DM,DP,FI,NA,AS,SCMC
0007          REAL KP,KD,NA,K,MO,N10,MI
0008          C
0009          C INPUT DATA . KP(C/MOLE.MIN),FI(,),NA(MOLECULES/CCW),DM(GRAM/CC),
0010          C DP(GRAM/CC),AS(SCCM/MOLECLES),KD(1/S),SCMC(HGRAM/LW),T(MIN)SO(GRAM
0011          C /LW),MO(GRAM/CCW),PO(GRAM/LW)
0012          C
0013          READ(1,100) (T1(I),I=1,8)
0014          100 FORMAT(8F0.0)
0015          READ(1,200) SO,MO,RO,REV,H
0016          200 FORMAT(5F0.0)
0017          WRITE(2,391)
0018          391 FORMAT(///2X,'INITIAL DATA : AMOUNT OF SAOP SO;AMOUNT OF MONOMER MO;
0019          *O;AMOUNT OF INITIATOR RO;DIAMRTER OF IMPELLER H;IMPELLER SPEED REV
0020          **/2X,118(1H=)///2X,'SO(G/LW)',6X,'MO(G/CCW)',7X,'RO(G/LW)',8X,'H(CM
0021          *)',8X,'REV(RMP)')
0022          WRITE(2,392) SO,MO,RO,H,REV
0023          392 FORMAT(//,5F15.2)
0024          C
0025          C THE CASE OF FAST T-RMINATION AND NOT CONSIDERING THE SOAP ON MONOMER DROPLET
0026          C *****
0027          C
0028          C
0029          C STAGE ONE
0030          C =====
0031          C
0032          CALL ST1A(SO,MO,RO,R,K,T1,V10,N10,TB)
0033          C
0034          C STAGE TWO
0035          C =====
0036          C
0037          CALL STAGE2(V10,N10,TB,MO,DM,DP,FI,KP,NA,R,T2,VP)
0038          C
0039          C STAGE THREE
0040          C =====
0041          C
0042          CALL STAGES3(T2,VP,FI,KP,NA,N10,DM,DP,MO,MI,0.5)
0043          C
0044          C THE CASE OF FAST TERMINATION AND CONSIDERING THE SOAP ON MONOMER DROPLETS
0045          C *****
0046          C
0047          C
0048          C STAGE ONE
0049          C =====
0050          C
0051          CALL ST1B(SO,MO,RO,R,K,T1,V10,N10,T10,TB,REV,H,X10)
0052          C
0053          C STAGE TWO
0054          C =====
0055          C
0056          CALL STAGE2(V10,N10,TB,MO,DM,DP,FI,KP,NA,R,T2,VP)
0057          C
0058          C STAGE THREE
0059          C =====
0060          C
0061          CALL STAGES3(T2,VP,FI,KP,NA,N10,DM,DP,MO,MI,0.5)
0062          C
0063          STOP
0064          END

```

END OF SEGMENT, LENGTH 127, NAME B-FFLE

```

0065          BLOCK DATA
0066          COMMON /A/KP,KD,DM,DP,FI,NA,AS,SCMC
0067          REAL KP,KD,NA
0068          DATA KP,KD,DM,DP,FI,NA,AS,SCMC/1.27E7,5.7E-5,0.906,1.007,0.605,
0069          36.023E23,3.5E-11,0.5/
0070          END

```



```

C071      SUBROUTINE ST1A(SO,MO,RO,R,K,T1,V10,N10,TB)
C072      DIMENSION T1(8),A1(8),T(10),A(10),V(10),N(10),D(10),SM(10),X(10)
C073      COMMON /A/KP,KD,DM,DP,FI,NA,AS,SCMC
C074      REAL KP,KD,NA,K,MO,N,MI,N10
C075      WRITE(2,201)
C076      201 FORMAT(//2X,'THE CASE OF FAST TERMINATION AND NOT CONSIDERING
C077      *SOAP ON MONOMER DROPLETS'/2X,7?(1H*)//)
C078
C079      C
C080      C   FIX CONSTANTS
C081      C
C082      S=NA*AS*SO/(270.0*1000.0)
C083      R=2.0*KD*NA*RO/(270.0*1000.0)
C084      K=(3.0/(4.0+3.14159))*(KP/NA)*(DM/DP)*(FI/(1.0-FI))
C085      B=4.0*3.14159*K*(2.0/3.0)*R/S
C086      C=(4.0*3.14159/3.0)*K*R/S
C087
C088      C   FIND THE RELATIONSHIP BETWEEN TIME T1 AND THE AREA OF PARTICLES IN ONE
C089      C   CC WATER A1
C090      DO 400 I=1,8
C091      IF(.NOT.I.EQ.1) GOTO300
C092      A1(I)=0.587*B*S*AT1(I)**(5.0/3.0)
C093      GOTO400
C094      300 A1(I)=B*T1(I)**(5.0/3.0)*(0.587*S-0.42*A1(I-1))
C095      400 CONTINUE
C096
C097      C   FIND THE TIME TB WHEN PARTICLENUCLEATION IS JUST COMPLETE
C098      C
C099      CALL CHAZHI(A1,T1,8,S,TB)
C100
C101      C   CALCULATE A SERIES OF VALUES OF PARAMETERS ALONG THE HISTORY OF
C102      C   POLYMERIZATION DURINGTHE STAGE ONE
C103      WRITE(2,450)
C104      450 FORMAT(//2X,'THE RESULTS CALCULATED ALONG THE REACTION HISTORY OF
C105      1STAGE ONE'/2X,6?(1H=)//)
C106      WRITE(2,500)
C107      500 FORMAT(//8X,'TIME(MIN)',4X,'CONVERSION(X)',3X,'S(MIC)(G/LW)',2X,
C108      2'AP(SGCM/CCW)',2X,'VP(CC/CCW)',4X,'DP(MICRON)',5X,'N(PARS/CCW)')
C109      DO 600 I=1,10
C110      T(I)=(TB/10.0)*FLOAT(I)
C111      600 CONTINUE
C112      DO 800 J=1,10
C113      CALL CHAZHI(T1,A1,8,T(J),A(J))
C114      TH=T(J)/2.0
C115      CALL CHAZHI(T1,A1,8,TH,AH)
C116      H(J)=(R/S)*T(J)+(S-A(J))/6.0-(2.0/3.0)*AH)
C117      V(J)=(T(J)**2/6.0)*(3.0*C*S-2.0*C*AH)
C118      D(J)=(V(J)/A(J))*60000.0
C119      X(J)=V(J)*(1.0-FI)*DP/MC+100.0
C120      SM(J)=(S-A(J))/S/NA*272.0*1000.0
C121      WRITE(2,700) T(J),X(J),SM(J),A(J),V(J),D(J),N(J)
C122      700 FORMAT(/5X,0PF10.3,2F15.3,1P4E15.3)
C123      800 CONTINUE
C124      MI=1.44*KP*FI*DM*N(10)/P
C125      WRITE(2,190)
C126      190 FORMAT(//2X,'THE VALUES OF PARAMETERS AT THE END OF STAGE ONE',
C127      3//8X,'TIME(MIN)',4X,'CONVERSION(X)',3X,'S(MIC)(G/LM)',2X,'AP(SGCM/
C128      4CCW)',2X,'VP(CC/CCW)',4X,'DP(MICRON)',5X,'MOLEC.WT.',4X,'N(PARS/CC
C129      5W)')//)
C130      WRITE(2,191) T(10),X(10),SM(10),A(10),V(10),D(10),MI,N(10)
C131      191 FORMAT(//5X,F10.3,2F15.3,1P3E15.3,0PF15.0,1PE15.3)
C132      N10=N(10)
C133      V10=V(10)
C134      RETURN
      END

```

END OF SEGMENT, LENGTH 407, NAME ST1A

```

0135      SUBROUTINE ST1B(SO,MO,RO,R,K,T1,V10,N10,T10,TB,REV,H,X10)
0136      DIMENSION T1(8),A1(8),T(10),A(10),V(10),N(10),D(10),SM(10),X(10)
0137      DIMENSION V1(8),VD(10),DD(10),AD(10),VD1(8),DD1(8),AD1(8),AM1(8)
0138      COMMON /A/KP,KD,DM,DP,FI,NA,AS,SCMC
0139      REAL KP,KD,NA,K,MO,N,MI,NDO,N10
0140      READ(1,250) XX,Y,REVI,HI,DDI
0141      250 FORMAT(6F0.0)
0142      WRITE(2,251)
0143      251 FORMAT(///2X,'THE CASE OF FAST TERMINATION AND CONSIDERING THE
0144      *SOAP ON MONOMER DROPLETS'/2X,73(1H*)//)
0145      C
0146      C CALCULATE DEGREE OF DISPERSION BEFORE REACTION
0147      C
0148      S=NA*AS*(SO-SCMC)/(270.0*1000.0)
0149      VDO=MO/DM
0150      DDO=2.42303*SO**(.0129)*REV**(-1.861)
0151      WRITE(2,3000) SO,REV,H,DDO
0152      3000 FORMAT(2X,'SO=',F4.2,2X,'REV=',F6.2,2X,'H=',F4.2,2X,'DDO=',E15.5
0153      1////)
0154      DDO=DDO*1.0E6
0155      NDO=6.0*VDO/(3.14159*DDO**3)*1.0E12
0156      ADO=(VDO/DDO)*6.0000.0
0157      WRITE(2,2000) DDO,ADO,REV
0158      2000 FORMAT(////,10X,'DDO=',E15.5,10X,'ADO=',E15.5,10X,'REV=',F6.2/)
0159      C
0160      C FIX THE CONSTANTS
0161      C
0162      B1=4.0*3.14159***(.20/3.0)*R/S
0163      B2=3.0*(4.0*3.14159*NDO)**(1.0/2.0)+VDO
0164      DSW=0.966
0165      B3=3.0*(4.0*3.14159*NDO)**(1.0/2.0)*(DSW/DM)
0166      B4=3.52*S-ADO
0167      C1=(4.0*3.14159/3.0)*(K*F/S)
0168      C2=3.0*S-ADO
0169      Z1=R/(6.0*S)
0170      Z2=6.0*S-ADO
0171      C
0172      C FIND THE RELATIONSHIP BETWEEN TIME T1 AND THE AREA OF PARTICLES IN ONE CC WA
0173      C
0174      DO 420 I=1,8
0175      IF(.NOT.I.EQ.1) GOTO410
0176      A1(I)=0.587*B1*(S-ADO)*T1(I)**(5.0/3.0)
0177      V1(I)=(C1/2.0)*(S-ADO)*T1(I)**2
0178      GOTO 481
0179      410 A1(I)=(B1/6.0)*(B4-2.52*A1(I-1)-2.52*(B2-B3*V1(I-1))**(.20/3.0))*
0180      *T1(I)**(5.0/3.0)
0181      V1(I)=(C1/6.0)*(C2-2.0*A1(I-1)-2.0*(B2-B3*V1(I-1))**(.20/3.0))
0182      3*T1(I)**2
0183      481 AD1(I)=(B2-B3*V1(I))**(.20/3.0)
0184      AM1(I)=S-A1(I)-4D1(I)
0185      420 CONTINUE
0186      C
0187      C FIND THE TIME TB WHEN PARTICLE NUCLEATION IS JUST COMPLETE
0188      C
0189      H1=10.0
0190      TB=0.365*(S/R)**0.6/K**0.4
0191      CALL CHAZHI(T1,AM1,8,TB,AMB)
0192      471 IF(AMB.GT.H1) GOTO477
0193      IF(AMB.LT.(-H1)) GOTO476
0194      GOTO436
0195      476 DO 435 I=1,1000
0196      CALL CHAZHI(T1,AM1,8,TB,AM)
0197      IF(ABS(AM).LE.H1) GOTO436
0198      IF(AM.GT.H1) GOTO478
0199      TB=TB-0.01
0200      435 CONTINUE
0201      478 H1=H1+10.0
0202      GOTO471
0203      477 DO 441 I=1,1000
0204      CALL CHAZHI(T1,AM1,8,TB,AM)
0205      IF(ABS(AM).LT.H1) GOTO436
0206      IF(AM.LT.(-H1)) GOTO478
0207      TB=TB+0.01
0208      441 CONTINUE

```

```

C209 C
C210 C CALCULATE A SERIES OF VALUES OF PARAMETERS ALONG THE HISTORY OF
C211 C POLYMERIZATION DURING THE STAGE ONE
C212 C
C213 436 WRITE (2,440)
C214 440 FORMAT(/2X,'THE RESULTS CALCULATED ALONG THE REACTION HISTORY OF
C215 1STAGE ONE'/2X,6Z(1H=)//)
C216 WRITE(2,444)
C217 444 FORMAT(8X,'TIME(MIN)',4X,'CONVERSION(%)',4X,'SM(G/L)',3X,'AP(SQ
C218 *CM/CCW)',4X,'VP(CC/CCW)',3X,'DP(MICRON)',6X,'N(PARS/CC)',5X,'VD(CC/CCW)/
C219 *C/CCW')//)
C220 DO 460 I=1,10
C221 T(I)=(TB/10.0)*FLOAT(I)
C222 460 CONTINUE
C223 DO 480 J=1,10
C224 CALL CHAZHI(T1,A1,S,T(J),A(J))
C225 CALL CHAZHI(T1,V1,S,T(J),V(J))
C226 TH=T(J)/2.0
C227 CALL CHAZHI(T1,A1,S,TH,AH)
C228 CALL CHAZHI(T1,V1,S,TH,VH)
C229 N(J)=Z1+T(J)*(Z2-A(J))-(B2-B3*V(J))*(2.0/3.0)-4.0*AH-4.0*(B2-B3*VH
C230 1)*(2.0/3.0)
C231 D(J)=(V(J)/A(J))*60000.0
C232 X(J)=V(J)*(1.0-FI)*DP/MO*100.0
C233 VD(J)=VDO-V(J)*DSW/DM
C234 DD(J)=(6.0/3.14159)*(VD(J)/NDO))*(1.0/3.0)
C235 AD(J)=(VD(J)/DD(J))*6.0
C236 SM(J)=(S-A(J)-AD(J))/AS/NA*272.0+1000.0
C237 WRITE(2,470) T(J),X(J),SM(J),A(J),V(J),D(J),N(J),VD(J)
C238 470 FORMAT(5X,DPF10.3,2F15.3,1P5E15.3)
C239 480 CONTINUE
C240 MI=1.44*KP*FI*DM*N(10)/R
C241 WRITE(2,490)
C242 490 FORMAT(/2X,'THE VALUES OF PARAMETERS AT THE END OF STAGE ONE',
C243 3//8X,'TIME(MIN)',4X,'CONVERSION(%)',3X,'S(MIC)(G/LM)',2X,'AP(SQCM/
C244 4CCW)',2X,'VP(CC/CCW)',4X,'DP(MICRON)',5X,'MOLEC.WT.',4X,'N(PARS/CC
C245 5W')//)
C246 WRITE(2,494) T(10),X(10),SM(10),A(10),V(10),D(10),MI,N(10)
C247 494 FORMAT(/5X,F10.3,2F15.3,1P3E15.3,DPF15.0,1PE15.3)
C248 V10=V(10)
C249 X10=X(10)
C250 T10=T(10)
C251 N10=N(10)
C252 RETURN
C253 END

```

END OF SEGMENT, LENGTH 762, NAME ST1B

```

0254 SUBROUTINE STAGE2(VI,NI,TB,MO,DM,DP,FI,KP,NA,R,T2,VP)
0255 REAL NI,NP,NT,NA,MO,KP,MI
0256 VDO=MO/DM
0257 VP=VI
0258 VD1=VDO-VP*(FI+(1.0-FI)*DP/DM)
0259 NT=NI
0260 T2=TB
0261 DELTAT=1.0
0262 WRITE(2,210)
0263 210 FORMAT(/2X,'THE RESULTS CALCULATED ALONG THE REACTION HISTORY OF
0264 2STAGE TWO'/2X,6Z(1H=)//2X,'TIME(MIN)',4X,'CONVERSION(%)',3X,
0265 3*AP(SQCM/CCW)',3X,'VP(CC/CCW)',4X,'DP(MICRON)',4X,'VD(CC/CCW)')//)
0266 E=0.5*(KP/NA)*(DM/DP)*FI*NT
C267 C
C268 C CALCULATE A SERIES OF VALUES OF PARAMETERS ALONG THE HISTORY OF POLYMERIZATIO
C269 C DURING THE STAGE TWO
C270 C
C271 DO 240 I=1,10000
C272 DO 220 J=1,2
C273 IF(VD1.LE.0.0) GOTO250
C274 DELTAV=B*DELTAT/(1.0-FI)
C275 VP=VP+DELTAV
C276 DPA=(6.0*VP/(3.14159*NT))*(1.0/3.0)+10000.0
C277 AP=(VP/DPA)*60000.0
C278 VD1=VD1-DELTAV*(FI+(1.0-FI)*DP/DM)
C279 T2=T2+DELTAT
C280 X2=VP*(1.0-FI)*DP/MO*100.0
C281 220 CONTINUE
C282 WRITE(2,230) T2,X2,AP,VP,DPA,VD1
C283 230 FORMAT(5X,DPF10.3,F15.3,1P4E15.3)
C284 240 CONTINUE
C285 250 MI=2.0*E*NA*DP/R
C286 WRITE(2,260)
C287 260 FORMAT(/2X,'THE VALUES OF PARAMETERS AT THE END OF STAGE TWO',
C288 5//8X,'TIME(MIN)',4X,'CONVERSION(%)',2X,'AP(SQCM/CCW)',2X,'VP(CC/
C289 6CCW)',4X,'DP(MICRON)',4X,'VD(CC/CCW)',5X,'MOLEC.WT.',//)

```

```

0290 WRITE(2,270) T2,X2,AP,VP,DPA,VD1,MI
0291 270 FORMAT(/5X,F10.3,F15.3,1P4E15.3,CPF15.0)
0292 RETURN
0293 END

```

END OF SEGMENT, LENGTH 221, NAME STAGE2

```

0294 SUBROUTINE STAGE3(T2,VP,FI,KP,NA,NT,DM,DP,MO,MI,Q)
0295 REAL MO,NI,KP,NA,NT,MI
0296 WRITE(2,310)
0297 310 FORMAT(/12X,'THE RESULTS CALCULATED ALONG THE REACTION HISTORY OF
0298 6STAGE THREE'/2X,64(1H=)//8X,'TIME(MIN)',4X,'CONVERSION(X)',2X,
0299 5*AP(SGCM/CCW)',2X,'VP(CC/CCW)',4X,'DP(MICRON)',4X,'VMP(CC/CCW)'/)
0300 VMP=VP*FI
0301 T3=T2
0302 DELTAT=1.0
0303 X3=0.0
0304 DO 360 I=1,100
0305 DO 340 J=1,5
0306 IF(X3.GE.95.0) GOTO370
0307 RATE=(KP/NA)*(VMP/VP)*(NT*Q)
0308 VMP=VMP-RATE*DELTAT
0309 VP=VP-RATE*DELTAT*(1.0-DM/DP)
0310 AP=(NT*3.14159)**(1.0/3.0)*(6.0*VP)**(2.0/3.0)
0311 DP3=(VP/AP)*60000.0
0312 X3=(1.0-VMP*DM/MO)*100.0
0313 T3=T3+DELTAT
0314 340 CONTINUE
0315 WRITE(2,350) T3,X3,AP,VP,DP3,VMP
0316 350 FORMAT(/5X,DPF10.3,F15.3,1P4E15.3)
0317 360 CONTINUE
0318 370 WRITE(2,380)
0319 380 FORMAT(/12X,'THE FINAL RESULTS OF THE CALCULATION',/2X,36(1H=)//
0320 87X,'TIME(MIN)',4X,'CONVERSION(X)',2X,'N(PARTICLES)',3X,'DP3(MICRON)',
0321 9)',4X,'MOLECULE.T.//)
0322 WRITE(2,390) T3,X3,NT,DP3,MI
0323 390 FORMAT(/5X,F10.3,F15.3,1P2E15.3,CPF15.1)
0324 RETURN
0325 END

```

END OF SEGMENT, LENGTH 194, NAME STAGE3

```

0326 SUBROUTINE CHAZHI(A,B,N,X,Y)
0327 DIMENSION A(N),B(N)
0328 NC=N
0329 N=N-1
0330 DO 1 J=1,N
0331 IF((X-A(J))*(X-A(J+1))) 10,10,1
0332 10 I=J
0333 GOTO 22
0334 1 CONTINUE
0335 IF(ABS(X-A(1))-ABS(X-A(N))) 20,21,21
0336 20 I=1
0337 GOTO 22
0338 21 I=N-1
0339 22 IF(I-N+1) 24,23,24
0340 23 I=I-1
0341 GOTO 27
0342 24 IF(I-1) 25,27,25
0343 25 IF(ABS(X-A(I))-ABS(X-A(I+1))) 26,27,27
0344 26 I=I-1
0345 27 V=0.0
0346 IF(I-N) 29,28,28
0347 28 I=I-1
0348 29 L=I+2
0349 DO 2 K=I,L
0350 W=B(K)
0351 DO 3 J=1,L
0352 IF(J-K) 30,3,30
0353 30 W=(X-A(J))/(A(K)-A(J))*W
0354 3 CONTINUE
0355 V=V+W
0356 2 CONTINUE
0357 Y=V
0358 N=NC
0359 RETURN
0360 END

```

END OF SEGMENT, LENGTH 181, NAME CHAZHI

0361 FINISH

END OF COMPILATION - NO ERRORS